Technical Report HL-95-2
March 1995

US Army Corps
of Engineers
Waterways Experiment
Station

Albuquerque Arroyos Sedimentation Study

Numerical Model Investigation

by Ronald R. Copeland

Prepared for U.S. Army Engineer District, Albuquerque

PRINTED ON RECYCLED PAPER

Technical Report HL-95-2
March 1995

Albuquerque Arroyos Sedimentation Study

Numerical Model Investigation

by Ronald R. Copeland

U.S. Army Corps of Engineers
Waterways Experiment Station
3909 Halls Ferry Road
Vicksburg, MS 39180-6199

Final report

Approved for public release; distribution is unlimited

Prepared for U.S. Army Engineer District, Albuquerque
P.O. Box 1580
Albuquerque, NM 87103-1580

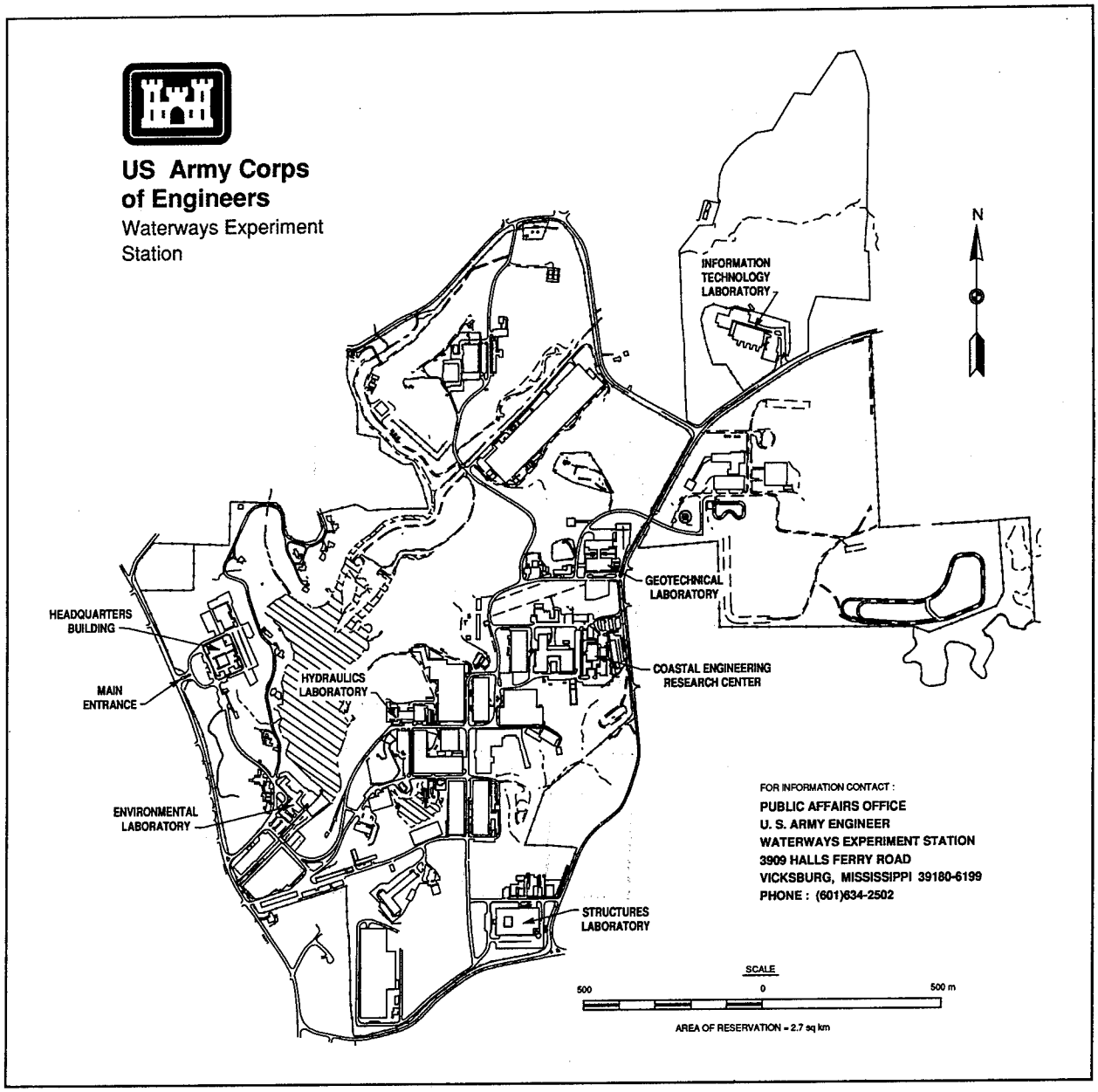

Waterways Experiment Station Cataloging-in-Publication Data

Copeland, Ronald R.
Albuquerque arroyos sedimentation study : numerical model investigation / by Ronald R. Copeland ; prepared for U.S. Army Engineer District, Albuquerque.
153 p. : ill. ; 28 cm. -- (Technical report ; HL-95-2)
Includes bibliographic references.
1. Arroyos -- New Mexico -- Albuquerque. 2. Sedimentation and deposition -- Mathematical models. 3. Sediment transport -- New Mexico -- Albuquerque. 4. Flood control -- New Mexico -- Albuquerque. I. United States. Army. Corps of Engineers. II. U.S. Army Engineer Waterways Experiment Station. III. Hydraulics Laboratory (U.S.) IV. Title. V. Series: Technical report (U.S. Army Engineer Waterways Experiment Station) ; HL-95-2.
TA7 W34 no.HL-95-2

Contents

List of Figures

List of Tables

Preface

The Albuquerque Arroyos Sedimentation Study, reported herein, was conducted at the U.S. Army Engineer Waterways Experiment Station (WES), at the request of the U.S. Army Engineer District, Albuquerque (SWA). The sedimentation study included a geomorphic study conducted by Resource Consultants and Engineers Inc. (RCE), of Fort Collins, CO, under contract to WES.

The sedimentation study was conducted during the period November 1992 to September 1993 in the Hydraulics Laboratory (HL) of WES, under the direction of Messrs. Frank A. Herrmann, Jr., Director, HL; Richard A. Sager, Assistant Director, HL; various acting Chiefs of the Waterways Division (WD), and Michael J. Trawle, Chief, Math Modeling Branch (MMB). Mr. William A. Thomas, WD, contributed guidance and review. The Project Engineer for this study was Dr. Ronald R. Copeland, MMB, who also prepared this report. The professional team at WES included Ms. Lisa Hubbard, MMB, and Mrs. Peggy Hoffman, MMB.

The project manager and principal engineer at RCE was Dr. Robert A. Mussetter; principal geomorphologist was Dr. Michael D. Harvey. Mr. B. Scott Queen and Mr. C. Gary Wolff performed significant roles in completing the study.

Mr. Bruce Beach served as the Hydraulic Project Engineer in SWA, and Ms. Bet Lotosky, SWA, provided valuable contributions and review during the course of the study.

At the time of publication of this report, Director of WES was Dr. Robert W. Whalin. Commander was COL Bruce K. Howard, EN.

Conversion Factors, Non-SI to SI Units of Measurement

Non-SI units of measurement used in this report can be converted to SI units as follows:

Multiply	By	To Obtain
acre	0.404686	hectares
acre-feet	1233.489	cubic metres
cubic feet	0.02831685	cubic metres
cubic yards	0.7645549	cubic metres
feet	0.3048	metres
inches	2.54	centimetres
miles (U.S. statute)	1.609347	kilometres
pounds per cubic foot	16.01846	kilograms per cubic metre
square miles	2.589998	square kilometres
tons (2,000 pounds, mass)	907.1847	kilograms

1 Introduction

The city of Albuquerque, located along the Rio Grande in north-central New Mexico, is the state's largest city. The city has experienced rapid growth since the 1950's and its 1990 population was about 385,000. Albuquerque is an industrial, trade, and transportation center for the southwestern United States. The rapid expansion of the city into areas where unstable arroyos formerly spread their water and sediment loads freely has introduced flooding problems.

The city of Albuquerque lies on three distinct geomorphic features. These are, in an easterly direction: (a) the floodplain of the Rio Grande, (b) a pediment, and (c) the foothills of the Sandia Mountains. The Sandia Mountains are composed primarily of granite and produce a relatively coarse, predominantly sand-sized sediment. The mountains are steep, rising to a peak elevation of 10,678[1,2]. The foothills and mesa consist of relatively thick deposits of highly erodible sandy material with relatively small amounts of clay and silt and in some locations coarse gravel and boulders.

The Albuquerque arroyos drain approximately 102 square miles of mountain and mesa in Albuquerque's northwest quadrant. About one-half of this drainage basin is urbanized. The arroyos drain into the North Diversion Channel, which is a concrete-lined channel constructed by the U.S. Army Corps of Engineers in 1965-67 to divert flow and to provide flood protection to the urban and suburban areas of the Rio Grande Valley in Albuquerque. The trapezoidal channel collects runoff from arroyos that have headwaters in the Sandia Mountains to the east and diverts it to the Rio Grande, north of Albuquerque. The significant arroyos that drain into the North Diversion Channel, starting with the southernmost and proceeding northward, are Campus Wash, Embudo Arroyo and Channel, Hahn Arroyo, Grantline Channel, Vineyard Arroyo, Bear Canyon Arroyo, South Pino Arroyo, North Pino Arroyo, Domingo Baca Arroyo, La Cueva Arroyo, and Camino Arroyo. Major tributaries to Embudo Arroyo include the I-40 Channel, Embudito Arroyo, and Piedra Lisa Arroyo. These are shown in Figure 1.

---

[1] A table of factors for converting non-SI units of measurement to SI units is found on page viii.

[2] Elevations are in feet referenced to National Geodetic Vertical Datum (NGVD).

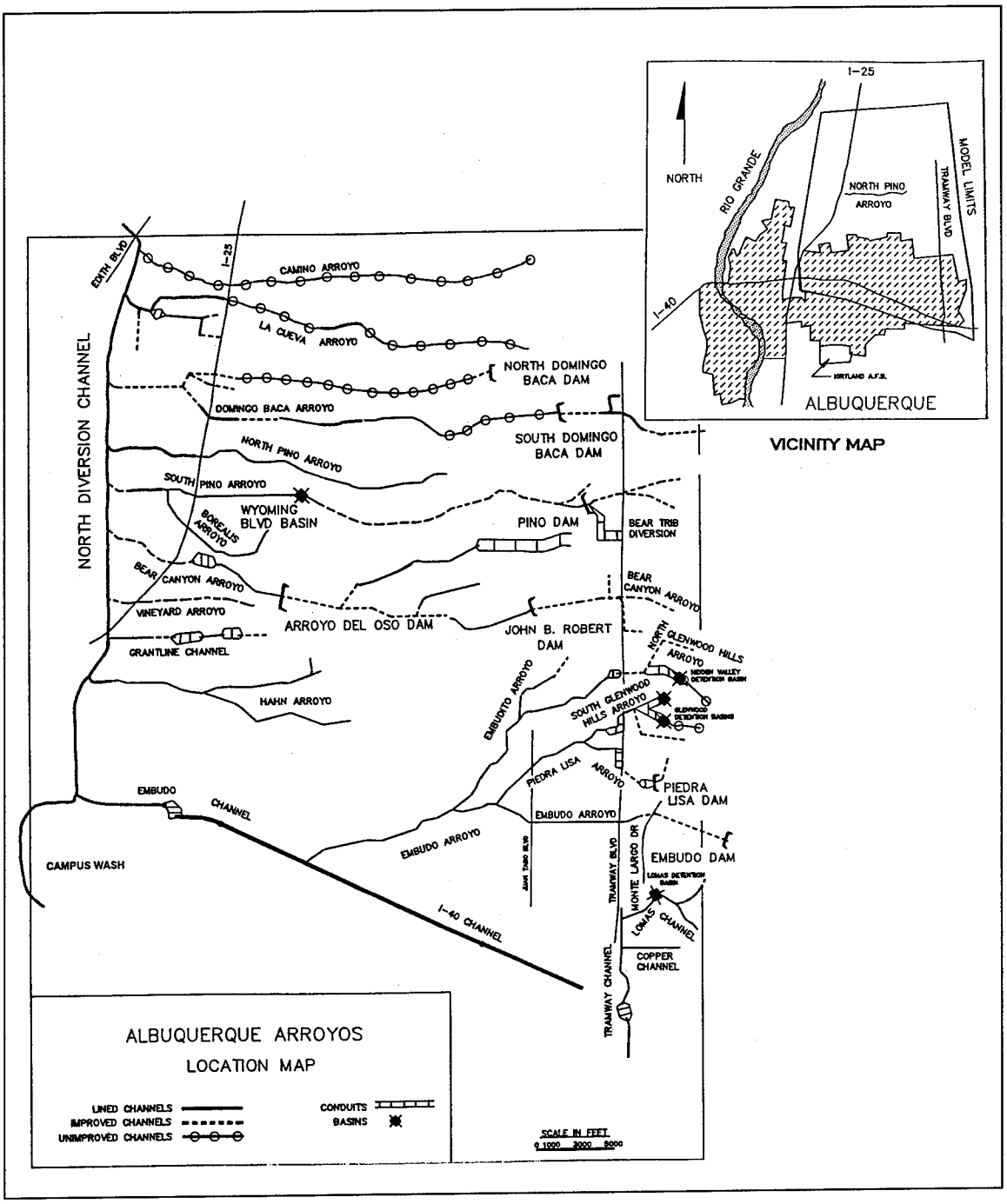

Figure 1. Location and vicinity maps

Four of these arroyos (Campus, Hahn, Grantline, and Vineyard) are almost entirely concrete-lined and drain fully urbanized watersheds. Reaches of Embudo, Bear Canyon, South Pino, North Pino, Domingo Baca, and La Cueva Arroyos are concrete-lined. Sediment traps have been constructed at the confluences of Bear Canyon, South Pino, North Pino, and Domingo Baca Arroyos with the North Diversion Channel. Flood detention dams have been constructed on several of the arroyos including Embudo and South Pino

Arroyos, North and South Domingo Baca Arroyos, and two on Bear Canyon Arroyo. A detention dam has also been constructed on Piedra Lisa Arroyo. The drainage area upstream from the detention dams is approximately 30 square miles, most of which is undeveloped and mountainous. Smaller detention basins have been constructed at the canyon mouths of some of the smaller arroyos in the Embudo watershed; these are the Hidden Valley Detention Basin and the Glenwood Detention Basins. A detention basin has been constructed on South Pino Arroyo at Wyoming Boulevard at the inlet to a concrete-lined channel.

The climate in Albuquerque is semiarid. There are some perennial flows in the upper canyons, but generally these flows disappear into the alluvial deposits at the canyon mouths. Runoff in the arroyos is primarily the result of intense rainfall of short duration. The average annual rainfall in Albuquerque is about 8 in. and increases to 22 in. at the peak of the Sandia Mountains.

Purpose of the Sedimentation Study

The numerous concrete-lined channels and detention dams constructed for flood control in Albuquerque were designed without accounting for the effects of sedimentation on flow conveyance or maintenance. Due to the steep slopes and erodible nature of the material in the unlined portions of the arroyos, runoff from intense thunderstorms has the potential to entrain and transport large quantities of sediment. Significant sediment sources include the watershed itself, channel beds and banks, and gullies that develop due to flow concentration or head-cutting.

During July 1988, Albuquerque experienced an extreme rainfall event in which deposition of sediment in the concrete-lined channels seriously affected flood-control capability. The July 1988 storm was centered over the Embudo Arroyo watershed downstream from the detention dam. The runoff frequency is uncertain, but based on HEC-1 (USAEHEC 1981) simulations, the peak flow on Embudo Arroyo was greater than the 100-year-frequency event. Structural failure of some of the concrete lining and extensive sediment deposition in the downstream reaches of the Embudo Arroyo occurred. Sediment deposited to within 6 in. of the soffit of the Tramway Boulevard bridge deck and completely filled the channel at Juan Tabo Boulevard. Numerous roads and intersections required cleaning due to sediment deposition as a result of the flood. The effects of sedimentation during this extreme event raised questions as to the anticipated effects of sedimentation for the 100-year-frequency flood, which had been designated as the design event.

The sedimentation study for the Albuquerque Arroyos Flood Control Project reported herein was conducted to evaluate the effect of sediment on the function of the North Diversion Channel during the 100-year-frequency flood. The primary design parameters required were the cross-sectional area remaining in the channel after sediment had deposited and the Manning's

roughness coefficient of the channel when sediment was present on the bed. In order to determine the effect of sedimentation in the concrete-lined channels, the sediment yield from the unlined arroyos and from the watershed had to be determined. To accomplish these purposes the study was organized into four primary tasks: (a) a geomorphic investigation of the arroyos was conducted to determine channel stability, (b) an engineering determination of the watershed's sediment yield was conducted, (c) the trap efficiencies of detention basins were determined, and (d) a numerical model of the North Diversion and Embudo Channels was developed and used to predict future sediment deposition.

Approach

The geomorphic analysis was conducted on the arroyos that have potential for supplying sediment to the North Diversion Channel. This analysis assessed the overall stability of existing channels to determine whether they are degrading or aggrading and whether they are subject to severe bank erosion during flood events. Evaluation of existing channel stabilization works was made relative to their potential for affecting downstream sediment yield. The effect of increased development on stability was evaluated. Potential for debris flows or hyper-concentrated flows was assessed. The purpose of the geomorphic analysis was to determine the primary sources of sediment within the system.

The sediment yield for each watershed was estimated. These estimates included an average annual sediment yield and sediment yields for several specified frequency curves up to the 100-year-frequency flood. Due to the uncertainty associated with any single method, more than one technique was used to calculate sediment yield. Sediment yield methods used to calculate fine sediment load included a simple sediment yield predictor based on soil type, the Modified Universal Soil Loss Equation (MUSLE), and rainfall simulator experiments. Sand loads were calculated using a sediment transport equation. Debris amounts from steep mountainous watersheds were estimated using the Tatum and Los Angeles District Methods. Calculated sediment yields were compared with measured data to assess reliability.

Trap efficiency of each detention dam and detention basin was determined. Reservoir or basin capacity was compared with sediment yield to determine its effects during flood events. The purpose of these calculations was to determine sediment delivery by size class to downstream channels.

The TABS-1 numerical sedimentation model was used to model deposition and scour in the concrete-lined North Diversion Channel and the downstream portion of Embudo Arroyo. TABS-1 is an enhanced research version of the well known U.S. Army Corps of Engineers HEC-6 program (USAEHEC 1993) and is described in Appendix B. Version 4.1 of HEC-6, dated October 1993, has incorporated all of the significant TABS-1 enhancements used in

this study. The effect of sediment deposits on boundary roughness was determined using analytical techniques. Calculated roughnesses were incorporated into the numerical model. Sediment inflow to the numerical model was determined by calculating sediment-transport capacity in the unlined channels, upstream from the inlets to concrete-lined channels. This assumes that these unlined arroyos are not supply limited. The reasonableness of this assumption was evaluated during the adjustment and circumstantiation phase of the numerical model study. Results from the geomorphic, sediment yield, and trap efficiency studies were also used to assess the reliability of the calculated sediment inflow. Considerable uncertainty exists relative to the quantity of sediment delivered by the 100-year-frequency flood. Sensitivity studies were conducted to assess the impact of different sediment loadings.

2 Geomorphic Study

The geomorphic phase for the Albuquerque Arroyos Sedimentation Study was conducted by Resource Consultants and Engineers Inc. (RCE) under contract to the U.S. Army Engineer Waterways Experiment Station (WES). RCE had conducted several geomorphic and sedimentation studies in the Albuquerque area and was very familiar with the physical processes unique to this area. Results of that study are summarized herein. Copies of the RCE report (RCE 1993) are on file at the Albuquerque District of the Corps of Engineers and at the Hydraulics Laboratory at WES. The purpose of the geomorphic study was to assess the overall stability of the arroyos that drain into the North Diversion Channel and to identify primary sources of sediment within the system.

Data sources for the geomorphic study included orthophoto-based topographic maps of the watershed and arroyos provided by the Albuquerque Metropolitan Arroyo and Flood Control Authority (AMAFCA), bed-material sediment gradations provided by WES and collected by RCE staff during a field reconnaissance, as-built plans for certain components of the improved channels within the study area, records of sediment deposits removed from the arroyo system by AMAFCA, field-surveyed cross sections and longitudinal profiles, and other general information derived from previous studies of the area.

Factors Affecting Sediment Yield

The North Diversion Channel system collects the sediment and water discharges from a pediment and Pleistocene-age alluvial fans. This area is locally referred to as the East Mesa and is located between the Sandia Mountains and the Rio Grande floodplain. The southern part of the drainage basin is the most urbanized, with development decreasing progressively in a northward direction. As a result, runoff is greater in the southern part of the drainage basin. However, potential for sediment yield is greater in the northern areas because more natural surface area is exposed and more of the channels are unlined.

The drainage basin of the North Diversion Channel can be divided into four geomorphic components: (a) the Sandia Mountains, (b) the modern alluvial fans, (c) the incised Pleistocene-age pediment surface and alluvial fans, and (d) the depositional zone:

a. The Sandia Mountains are composed of porphyritic granite that produces relatively coarse, predominantly sand-sized sediment.

b. The modern alluvial fans are located at the mountain front and tend to have relatively small contributing drainage basins. On an annual basis, these fans produce little sediment, but over a period of decades these fans may accumulate significant quantities of sediment that could produce a very significant quantity of sediment during large storm events.

c. The incised pediment surface and older alluvial fans tend to be armored with coarse sediments varying from gravel to boulders. These are lag deposits from the original pediment surface. Sedimentological evidence indicates that a significant portion of the coarser pediment was delivered by sediment gravity flows, including debris flows. The surfaces tend to be more heavily vegetated since they are located at a higher elevation where precipitation is somewhat greater. Consequently, this region of the mesa has a low sediment yield potential. The upper and middle reaches of the arroyos that traverse this landscape component are incised and the bed and banks are armored with boulder to cobble-sized sediments. The lower reaches of the channels tend to be confined, but less armored, and exhibit some tendency to migrate laterally.

d. The depositional zone, located primarily west of Tramway Boulevard, is characterized by temporally and spatially alternating reaches of local erosion and deposition. Sediments eroded from the upper watersheds and from channel erosion are deposited when sediment-transport capacity is locally diminished. The long-term effect is an increase in channel slope by aggradation followed by channel incision into the deposited sediments when the threshold slope is exceeded. Sediment transport through the system is, therefore, an episodic phenomenon that depends to a great extent on local topography and the duration and magnitude of sediment-transporting flood events. A typical aggrading condition is shown in Figure 2, and an incised condition is shown in Figure 3. Confinement of flows and armoring of the arroyos upstream have led to a westward displacement of the alluvial fans through time. The confinement of the valley floor fans by the roughly parallel drainage divides, that formed in response to base level lowering of the Rio Grande, prevents the individual fans from coalescing. Caliche accumulation tends to increase the erosion resistance of the divides. The net effect of the topographic controls is the development of a series of parallel fans that will be displaced downslope through time whether as a result of natural processes or by man-induced activity.

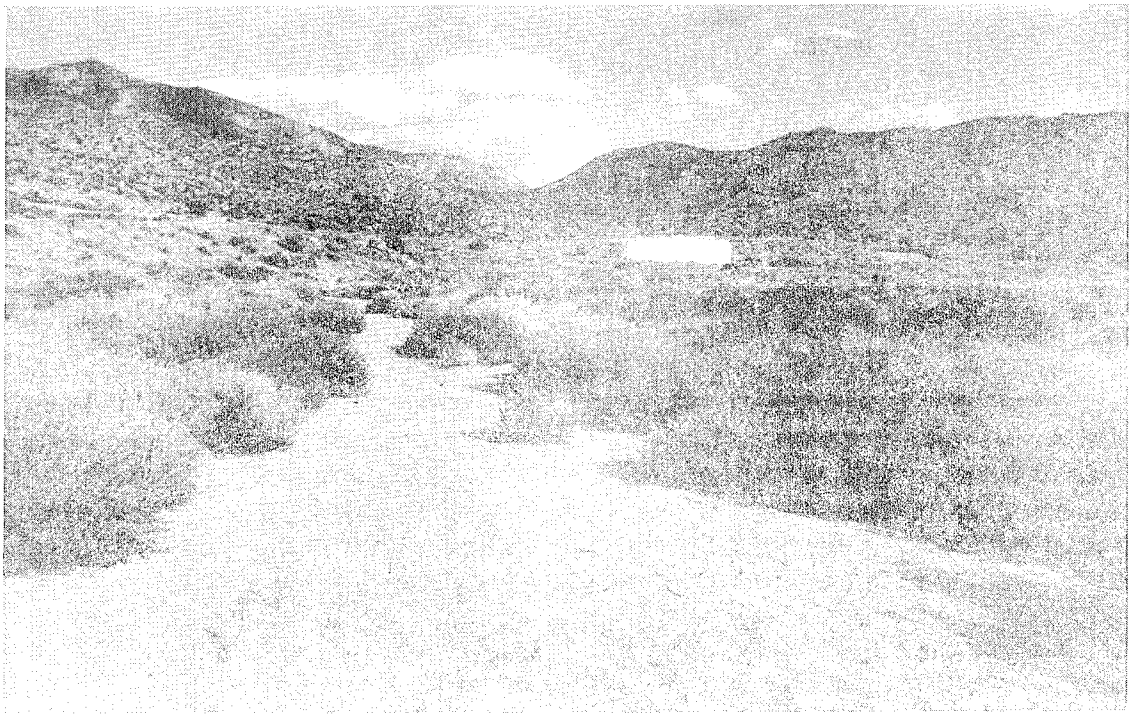

Figure 2. Embudo Arroyo downstream from Embudo Dam—aggrading arroyo without well defined banks

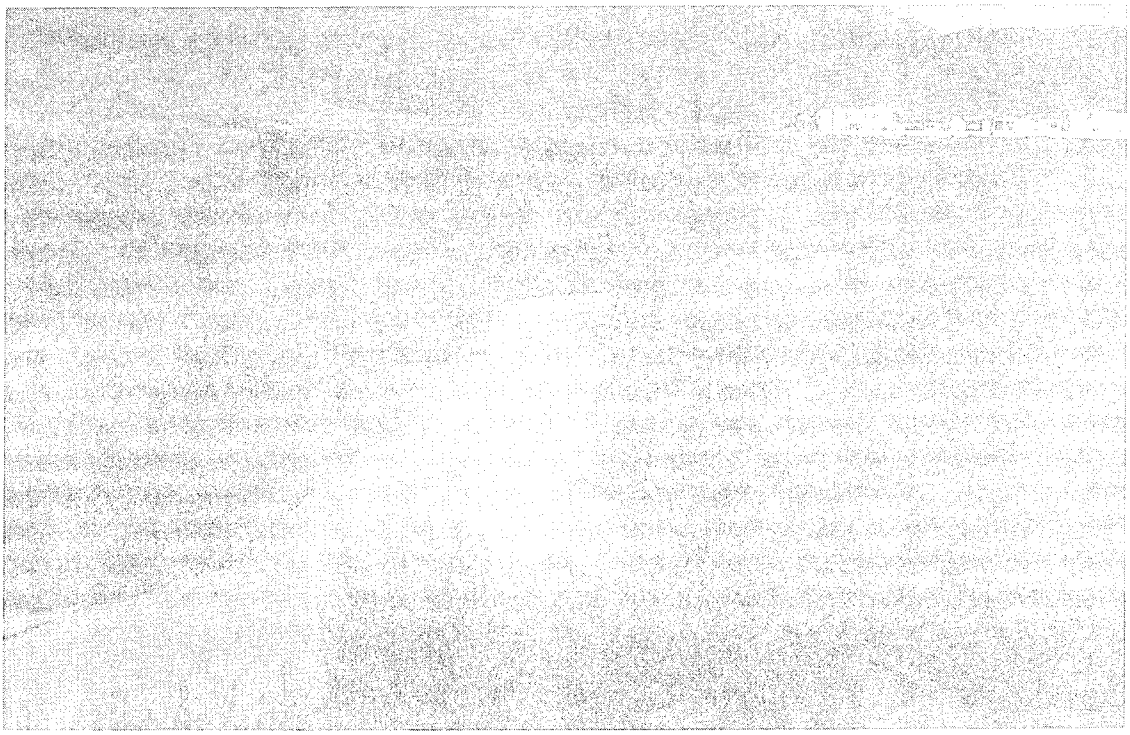

Figure 3. La Cueva Arroyo upstream from Interstate 25—incised arroyo

Effect of Urbanization on Sediment Yield

Sediment yield off of the East Mesa alluvial fans has generally decreased due to urbanization. Sediment yield has been reduced due to the construction of flood-control structures. Sediment is trapped in detention dams and basins, sediment traps, and upstream of culverts and road crossings. Channel erosion has been reduced by the construction of concrete-lined channels and channel stabilization structures. Watershed erosion is reduced by paving and landscaping. However, urbanization can also result in increases in sediment yield due to the increased volume of runoff caused by reduction of rainfall infiltration, and by confining and concentrating flows both on streets and within the channels. Increased concentration of flow leads to bank erosion and degradation of unlined channels.

Flood-control detention dams have high bed-material trap efficiencies and, as a result, where they discharge downstream to an unlined channel, there is significant scour and channel erosion. Both vertical and lateral channel erosion occur downstream of both North and South Domingo Baca Dams for a distance of approximately 1,000 ft (Figure 4). The base level lowering that accompanies the degradation results in gully development in the surrounding interfluves. Below this point the sediment-transport capacity has been replenished by gully and channel erosion so that downstream delivery of sediment is dependent on local hydraulic controls. The most significant effect of the

Figure 4. South Domingo Baca downstream from dam—incision due to clearwater releases from detention basin

flood-control detention dams is the dramatic change in flood hydrographs where a rapidly rising and falling peak flow is reduced to a much lower steady outflow.

Sediment traps are located at the downstream end of four of the arroyos where they confluence with the North Diversion Channel. These are Bear Canyon, South Pino, North Pino, and Domingo Baca Arroyos. Trap efficiencies of sand are relatively high at these structures for most discharges. Thus, even if sediment is delivered to the lined-channel segments upstream, where the sediment-transport capacity is very high, the delivery rate to the North Diversion Channel is much lower. The sediment trap at North Pino Arroyo is shown in Figure 5. A sediment trap has also been constructed on South Pino Arroyo at Wyoming Boulevard, at the upstream end of the concrete-lined portion of the arroyo. The slope of Bear Canyon Arroyo, upstream from its sediment trap, has been significantly reduced by a series of drop structures (Figure 6). This will reduce sediment-transport capacity and sediment delivery to the North Diversion Channel.

Culverts that create backwater and sediment deposition have a significant effect on sediment delivery at high flows. Unlined channels downstream from culverts typically are characterized by channel erosion. La Cueva Arroyo downstream from San Pedro Avenue is an example.

Paving and landscaping in the watershed decrease the sediment yield off of the watershed, but increase the volume and peak flow rate of the runoff. The net result is usually an increase in channel erosion. An example is a housing development adjacent to the Embudo Arroyo downstream from Embudo Dam where stormwater drainage has caused 6 to 7 ft of degradation in the arroyo downstream of the local drainage outlet. If sufficient runoff is generated upstream of the incision a headcut will migrate upstream and supply a significant quantity of sediment to the concrete-lined portion of Embudo Arroyo downstream. Another example of increased channel erosion is the upper reaches of Embudito Arroyo, a tributary of Embudo Arroyo, where grade control structures have been installed in an attempt to stabilize the channel (Figure 7).

In the natural arroyos that cross the mesa, the overall trend is for deposition of sediment. However, concentration of flows by urbanization interferes with the natural processes. Natural arroyos have localized reaches in which the channel is unconfined and deposition is induced. Arroyos confined by bank protection tend to degrade. In addition, runoff is frequently concentrated by roads that are oriented parallel to the natural slope of the mesa. Flow along the road margins causes roadside erosion and increased sediment delivery to the channels.

Channel relocation and straightening generally results in steeper slopes and greater erosion potential.

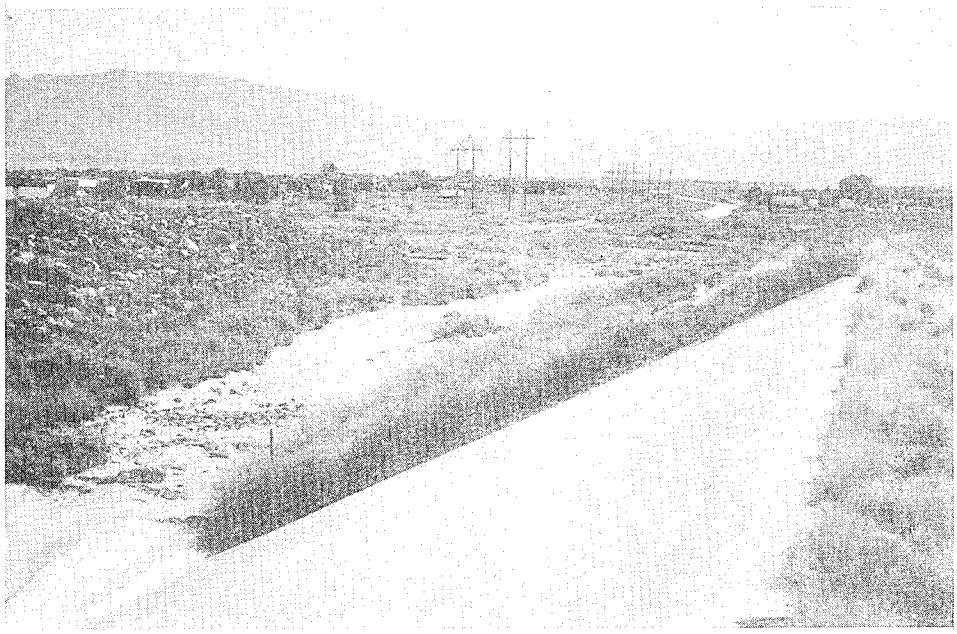

Figure 5. Sediment trap at North Pino Arroyo

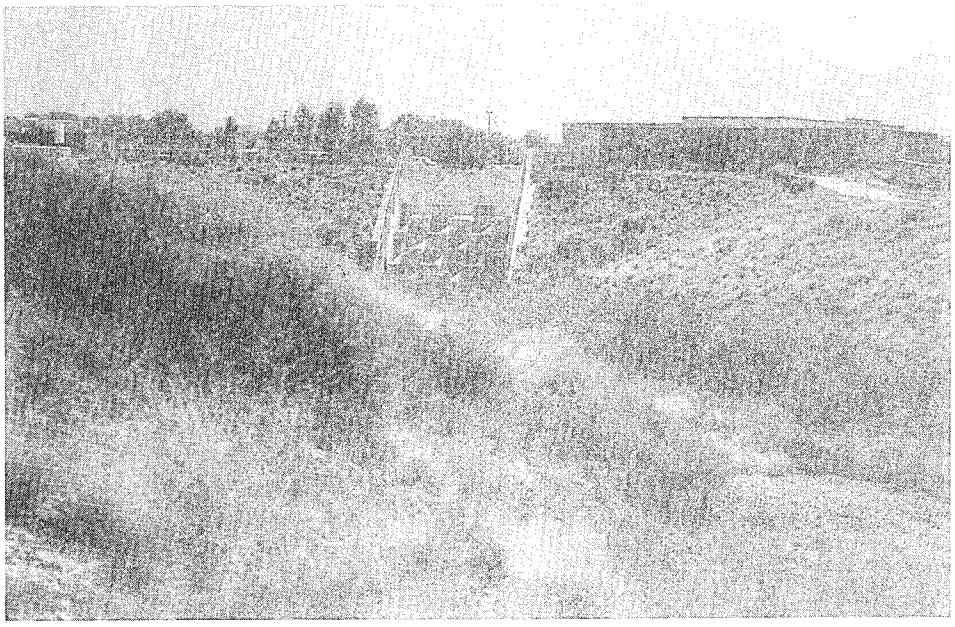

Figure 6. Bear Canyon Arroyo drop structures upstream from confluence with North Diversion Channel

Figure 7. Embudito Arroyo downstream from Montgomery Boulevard channel stabilization weir

Lining the channels that traverse the East Mesa probably has the greatest effect on potential sediment delivery to the North Diversion Channel. The channels are generally lined because the increased runoff related to development causes severe erosion of the unlined channels. Progressive lining of the channel of North Pino Arroyo in the last few years has reduced the delivery of sediment to the sediment trap.

Table A1 in Appendix A is a summary of geomorphological observations prepared by RCE. This table summarizes the channel stability and sediment yield potential of each arroyo in the North Diversion Channel drainage basin. The primary sources of sediment to the Embudo and North Diversion Channels were identified as bed and bank erosion in the unlined arroyos. Localized sources are created when developments significantly alter the natural sediment regime and induce the creation or expansion of gully erosion. The primary sediment sources are:

a. Embudo Arroyo upstream from Monte Largo Drive.

b. North Glenwood Hills Arroyo.

c. South Glenwood Hills Arroyo Tributary.

d. Embudito Arroyo.

e. Piedra Lisa Outlet Channel.

f. Bear Canyon Arroyo at the North Diversion Channel.

g. Domingo Baca Arroyo at the North Diversion Channel.

Dominant Discharge

The concept of a dominant discharge is a convenient simplification that suggests that a single uniform discharge can be the independent variable on which channel size, shape, and slope of a perennial stream are dependent. Two common definitions of dominant discharge exist in the literature:

a. The **effective discharge** is defined as the flow that transports the most sediment over a long period of time. The effective discharge is computed as the average discharge over a specified increment of flow in the flow duration curve that has the largest product of discharge and sediment concentration. If most of the transported sediment is coarse, then the effective discharge will occur less frequently and be larger than if the sediments are finer.

b. The **bankfull discharge** of the channel has been described as the formative discharge of the channel because it represents a maximum shear stress condition. The frequency of bankfull discharge typically varies between the less than the 1-year-frequency event and the greater than the 10-year-frequency event.

Even though Andrews (1980) showed that there is a good correlation between bankfull discharge and the effective discharge, other studies (Pickup and Warner 1975, Benson and Thomas 1966) have shown that the recurrence interval for the effective and bankfull discharges in perennial flow streams can vary significantly. In incised channels in the humid southeastern United States, Watson et al. (1988) determined that the effective channel discharge was equivalent to the bermfull discharge, that is the bankfull discharge for the dynamic equilibrium channel located within the incised valley floor. In Watson's streams the recurrence interval of the bermfull discharges was about 1.5 years. In contrast, the capacity of the incised channel was in many cases in excess of the 100-year-frequency event.

Ephemeral stream channels have been characterized hydrologically and hydraulically by nonuniform, unsteady flow behavior with major transmission losses. Ephemeral flow stream channels often have two sections. The upstream section has a concave-up longitudinal profile and a relatively low width-to-depth ratio, attributes that are similar to perennial flow channels in upland areas. The downstream section, which begins at the point of channel alluviation, has an almost linear longitudinal profile and a relatively high width-to-depth ratio that reflects the noncohesive nature of the alluvium and the high flow losses to infiltration. The changes in the channel profiles indicate that the two sections are controlled by different sets of hydraulic relations.

Unlike humid regions, sediment in semiarid and arid regions tends to be stored in valley floors rather than on hillslopes. Transport of the stored sediments is dependent on infrequent hydrological events of sufficient magnitude and duration to generate surface flow. These hydrologic conditions cause temporal and spatial episodes of aggradation and degradation and a significantly spatial and temporal variable sediment yield. Channel reaches under such flow conditions can be out of phase, and this episodic behavior of ephemeral stream channels suggests that they may be inherently unstable.

Due to these factors, RCE concluded that the concept of dominant discharge is not applicable since a fundamental assumption is channel equilibrium. Therefore, dominant discharge methods were not used in the Albuquerque Arroyos sediment study.

3 Sediment Yield

Introduction

Sediment yields were calculated for each watershed contributing sediment to the North Diversion Channel. These calculations were made to assess the adequacy of the sediment storage capacity of the detention reservoirs and to estimate the concentration of fine sediment load into the North Diversion Channel. Estimates of both the average annual and 100-year-frequency flood sediment yields were calculated.

The sediment yield is composed of both wash load and bed-material load. The wash load is the fine sediment that remains in suspension once it reaches a channel. Wash-load sources are the surface of the watershed, gullies, and the channel bed and banks. The bed-material load is the sediment load that actively exchanges with the channel bed as it is transported downstream. The bed-material load capacity is determined by the composition of the bed and the hydraulic properties of the channel.

There is no generally accepted method for calculating sediment yield. Available techniques require measured sediment deposition or transport data for adjustments or to establish coefficients. Because there are many factors that affect the sediment yield, it is generally necessary to have a significant sediment database to refine a technique to the point where it can be used to make reliable predictions. This database does not exist in the Albuquerque Arroyos study area. The approach taken herein, therefore, is to apply several different techniques, compare calculated results from these techniques with the limited available data, and then draw some general conclusions about the magnitude and uncertainty of the sediment yield.

The wash-load sediment yield was estimated using the Modified Universal Soil Loss Equation (MUSLE) (Williams and Berndt 1977), rainfall simulator experiments, and a simple sediment yield predictor based on soil type. These techniques account only for the sediment yield from the watershed surface, most of which is fine sediment.

Wash-load estimates were compared with measured sediment concentrations. Since the wash-load concentration is a function of watershed conditions

and not necessarily hydraulic conditions in the channel, there is usually a poor correlation between discharge and wash-load concentration. Therefore, a large number of measurements are required to obtain a statistically reliable comparison.

Sediment yields for bed-material load can be estimated using sediment-transport equations. Sediment yield is calculated by integrating a sediment-transport rating curve with a flow duration curve. These calculations depend on knowing the bed gradation of the channel, the hydraulic properties during each discharge event, and a reliable sediment-transport equation. It is generally assumed that bed gradation and geometry remain constant.

Sediment yields from steep mountainous watersheds during a storm event can be estimated using the Tatum Method (Tatum 1963) and the Los Angeles District Method (USAED Los Angeles 1992). These empirical methods were developed using data from watersheds in the Southern California Coastal Range. Sediment yields predicted by these methods represent sediment trapped in debris basins and consist primarily of coarser sediment sizes.

Measured Sediment Concentrations

Measured suspended-sediment concentrations for arroyos in the vicinity of Albuquerque were reported in the original Design Memorandum (DM No.1) for the North Diversion Channel (USAED Albuquerque 1956). The equipment and technique employed to collect these data were not reported, so the reported concentrations must be considered approximate.

During flash floods between 1937 and 1947, 26 suspended-sediment samples were collected from Tijeras Canyon, which is located just south of the North Diversion Channel drainage area. The average concentration was 58,000 mg/l and the average discharge was 300 cfs. Sediment concentrations ranged between 20,000 and 300,000 mg/l. Particle size analysis was conducted on 13 of these samples. The average size class breakdown was 19 percent clay, 69 percent silt, and 12 percent sand.

During flash floods in 1953, four suspended-sediment samples were collected from Embudo Arroyo. Discharges ranged between 8 and 350 cfs; suspended loads varied between 9,000 and 29,000 mg/l.

Thirteen suspended-sediment samples were taken from an arroyo headed in the Manzano Mountains, located 40 miles south of Albuquerque. These had an average sediment concentration of 16,000 mg/l for flows averaging 140 cfs.

Average-annual sediment yields for the North Diversion Channel drainage area were estimated for DM No. 1. A suspended-sediment-discharge rating curve was developed from all the available suspended-sediment data. These

data are summarized in Table A2 in Appendix A. The curve was increased by 20 percent to account for the unmeasured load. Peak flows and volumes between 1931 and 1952 were estimated for Embudo Arroyo. These were then integrated to obtain a total sediment yield for the period. Assuming a sediment-deposit density of 90 lb/ft^3, an average-annual sediment yield of 0.58 acre-ft/square mile was calculated. This sediment-yield rate was assumed to be applicable to the rest of the drainage basins in the North Diversion Channel study area.

Between 1957 and 1964, sediment concentrations were measured upstream from Bernalillo Reservoir, located on Piedra Lisa Arroyo (not the same arroyo as in the study area), which is about 17 miles north of Albuquerque (Funderburg 1977). These measurements were made with standard US DH-48 suspended sediment samplers. It was reported that sediment larger than 6.36 mm was not sampled because it exceeded the size of the sampler nozzle opening. It was also reported that sampling was difficult due to the flashy nature of the storm runoff. The largest reported discharge was only 30 cfs. The average of 12 sampled concentrations was 64,000 mg/l; and the average percentage of sediment finer than 0.0625 mm was 79 percent. Measured concentrations upstream from Bernalillo Reservoir are listed in Table A3 in Appendix A.

Between May 1982 and September 1983 and between October 1990 and July 1991, the U.S. Geological Survey (USGS) collected suspended-sediment data in the North Diversion Channel. These data were supplied by the Albuquerque office of the USGS. Data for 1982 and 1983 are also published in USGS annual water-data reports (USGS 1982,1983). The gage was located on the channel about 0.5 mile upstream from Edith Boulevard and is called North Floodway Channel near Alameda. Samples were collected with a pumping sampler having an intake located on the channel sidewall about 1 ft above the bottom of the channel. The sampler did not collect samples isokinetically, which means the measured concentrations at high flows may be too low. In addition, the measured samples may not be representative of average concentrations in the vertical water column, due to the sampler intake location. Because of these factors, the measured data have a relatively high degree of uncertainty. The largest discharge at which data were collected was 6,400 cfs. As is typical of measured suspended data, there was a poor correlation between discharge and sediment concentration. At discharges greater than 100 cfs, total sediment concentrations varied between 300 and 15,000 ppm. About 70 percent of this material was finer than 0.0625 mm.

Measured Sediment Deposition

Sediment yields have been measured in two New Mexico reservoirs with watersheds similar to those in Albuquerque. The drainage basins have steep mountainous headwaters and narrow alluvial mesas. Bernalillo Reservoir, located about 17 miles north of Albuquerque, was monitored between 1957 and 1967 (Funderburg 1977, USDA SCS 1987). Its headwaters are in the

Sandia Mountains. As a conservation measure, the Soil Conservation Service treated the alluvial mesa in 1956 to reduce erosion and gullying and to retard rainfall runoff. Due to these conservation practices a relatively low average-annual sediment yield of 0.16 acre-ft/square mile/year was determined. Tortugas Reservoir is located about 225 miles south of Albuquerque near Las Cruces (Funderburg and Roybal 1977). This watershed drains the Organ Mountains; its alluvial mesa has not been treated. Based on sediment surveys taken in 1963 and 1975 the average annual deposition rate in the reservoir was determined to be 0.28 acre-ft/square mile/year. It was also determined that both reservoirs had trap efficiencies of about 96 percent. More than 99 percent of the sand sizes were trapped.

Based on measured water and sediment outflow, sampled density of the deposits, and measured deposition in the reservoirs, an average concentration of inflowing sediment can be estimated from Bernalillo and Tortugas Reservoirs. The average sediment inflow concentration at Tortugas Reservoir was 57,800 mg/l and at Bernalillo it was 176,700 mg/l. These calculated concentrations are expected to be somewhat high because infiltration and evaporation are unaccounted for. Also, at Bernalillo Reservoir, measurements ceased in July 1974, and the reservoir survey was not taken until January 1976.

Sediment deposition in the North Diversion Channel, and its inlets, provides some additional insight into sediment yield. Available data consist of sediment removal records from various locations within the North Diversion Channel system maintained by AMAFCA. Records were available for the years 1976 through 1992 and are based on the number of reported truck loads hauled. Both sand and silt were removed from the North Diversion Channel outfall. Sediment removed from other locations was primarily sand.

Annual removal quantities from the North Diversion Channel including the inlets and outfall are shown in Figure 8. The figure indicates a general decline in sediment deposition. Factors that are primarily responsible for this reduction are detention dam construction and channel improvements. The effects of paving and landscaping are considered to be a minor influence in terms of reducing sediment yield and deposition. Urbanization may reduce some surface erosion, but the increased rainfall runoff volume, caused by increases in surface imperviousness and the resultant increase in flow concentration, leads to more gully and bank erosion. Therefore, unless lined channels are provided to convey the increased runoff, urbanization generally results in an increase in sediment yield and deposition. Average-annual runoff and average-annual rainfall are compared in Figure 9. Allowing for normal annual fluctuations, this figure indicates that the annual runoff has generally increased, even though the annual rainfall shows no signs of increasing. This further demonstrates the effectiveness of AMAFCA's flood-control improvements, in that even with an increase in annual runoff, there has been a decrease in sediment deposition in the North Diversion Channel.

Sediment deposition in the North Diversion Channel and its inlets and outfall, including Embudo Channel, over the 17-year period can be used to

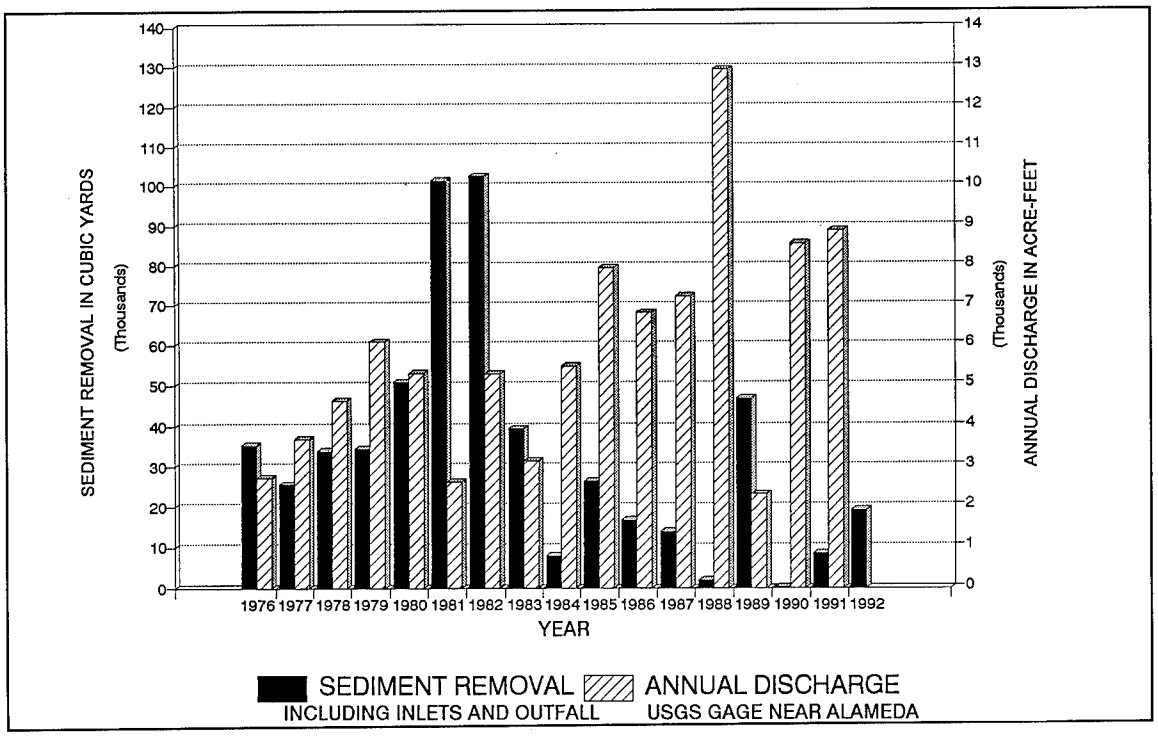

Figure 8. Annual sediment removal from North Diversion Channel

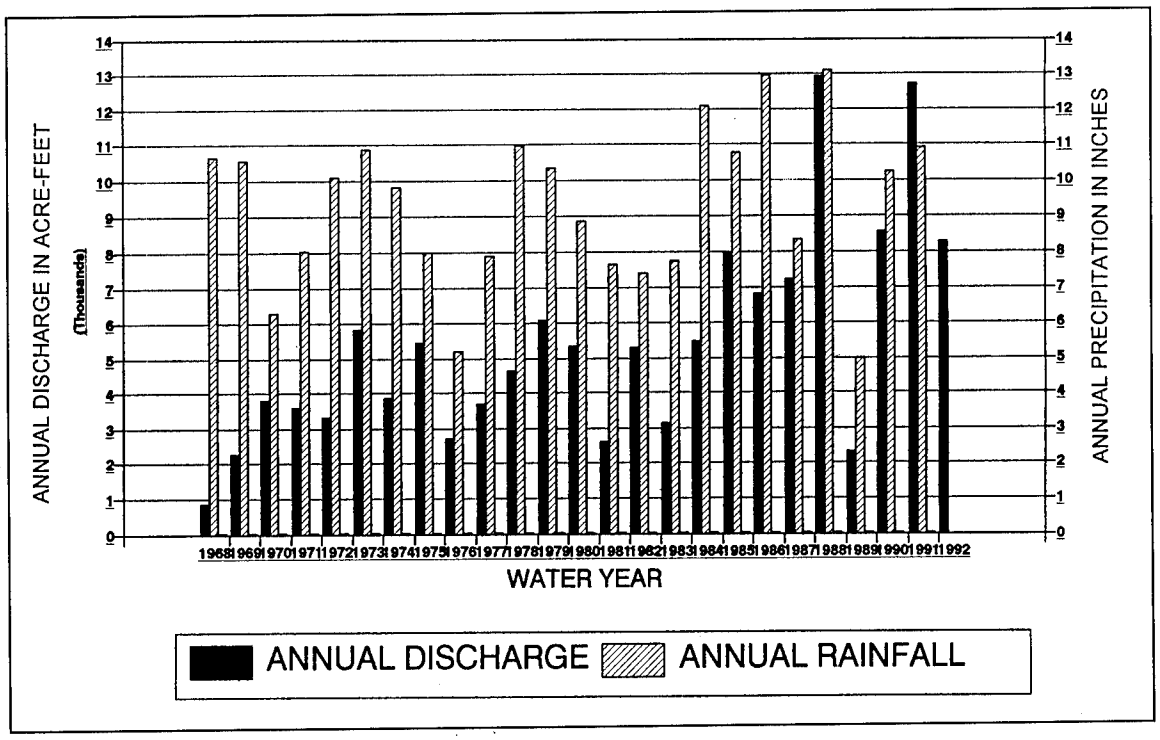

Figure 9. Average annual runoff and rainfall

estimate sediment yield. Using these data, and the entire 102-square-mile drainage area, an average-annual sediment deposition of 0.20 acre-ft/square mile/year was calculated. In considering the total sediment yield, this does not account for sediment trapped in the upstream detention reservoirs or for the sediment that passes through the outfall into the Rio Grande. This figure represents a low estimate for sediment yield and must be considered very approximate due to the uncertainty related to the haul records and the variable period of record for different locations in the system.

Summary of Measured Data

The measured suspended sediment and sediment deposition data demonstrate a high degree of variability in estimated sediment yield. Individual suspended-sediment measurements from actual arroyos ranged between 4,000 and 300,000 mg/l. An average concentration from 55 reported measurements was 47,000 mg/l. Limited size class analyses indicated that between 12 and 21 percent of this suspended sediment was sand. These measurements were made at relatively low discharges. Measured suspended-sediment data from the North Diversion Channel itself indicated significantly lower sediment concentrations—between 300 and 15,000 mg/l. This is attributed to the significant contribution of relatively sediment-free runoff from the urban areas delivered to the North Diversion Channel by lined channels and to the effective trapping of sediment in detention reservoirs and inlet sediment traps. Average-annual sediment yields calculated from measured data ranged between 0.16 and 0.58 acre-ft/square mile/year. The lowest yield was from Bernalillo Reservoir where the watershed had received conservation treatment. The highest, reported in DM No.1, was based on an integration of measured sediment from natural arroyos and estimated runoff. Data from haul records in the North Diversion Channel indicate a declining average-annual sediment yield.

Calculated Estimates Using SCS Soil Erosion Rates

As part of the sediment impact assessment conducted by WES for the U.S. Army Engineer Division, Albuquerque, average-annual sediment yield was estimated for the undeveloped portions of the North Diversion Channel watershed. The Bernalillo County Soil Survey (USDA SCS 1977) was used to determine soil types in each sub-basin. Approximate sediment yields for each soil type were provided by the Albuquerque Soil Conservation Service (SCS) office. These sediment yields, listed in Table A4 in Appendix A, are approximate and are considered "unofficial" by the SCS.

Several soil classifications in the soil survey did not have a sediment yield value. For such cases the description of the soil and those of similar soils for which yields were available were compared and an estimate of the yield was

obtained. The average calculated yield for watersheds upstream from detention basins was 0.23 acre-ft/square mile/year.

The sediment yields determined using the SCS soil erosion rates are less than half those determined in DM No.1. The SCS yield rates account only for surface erosion, while the integration method, employed in DM No.1, accounts for surface, gully, and bank erosion.

MUSLE Estimates

The MUSLE (Williams and Berndt 1977) was developed to predict soil losses from agricultural land for specific precipitation events. Coefficients were developed from rainfall simulator tests, where soil erosion occurred primarily in the form of rills. Reliable application of this method requires considerable data gathering and calibration effort.

The MUSLE method has not been specifically calibrated for the Albuquerque area, but it includes variables that account for the significant processes that cause erosion of sediment from overland areas. The MUSLE calculates sediment yield, Y_s, in tons:

$$Y_s = \alpha(Q_p V_w)^{\beta} \, K L_s C P \qquad (1)$$

where

Q_p = peak discharge for storm event, cfs
V_w = runoff volume for storm event, acre-ft
K = soil erodibility factor
L_s = topographic factor
C = cover and management factor
P = erosion control practice factor
α, β = calibration constants

Sediment yield was calculated by RCE using MUSLE. They calculated sediment yields for the 2-, 5-, 10-, 25-, 50-, and 100-year-frequency floods. The flood peaks and volumes were determined using the HEC-1 hydrologic computer program. Four separate storm centerings were used to maximize runoff for individual drainage basins. Values for the 10-, 50-, and 100-year frequency storm events were developed by the U.S. Army Engineer District Albuquerque (USAED Albuquerque 1992). RCE revised the HEC-1 input files using rainfall depth ratios from the city of Albuquerque's hydrology manual to obtain values for the 2-, 5-, and 25-year storm events.

The soil erodibility factor is a function of the percentage of silt and very-fine sand, sand, and organic matter in the soil; the soil structure; and the soil permeability. Nomographs are available (Wischmeier and Smith 1978) to

determine the soil erodibility factor. Soil types for each sub-basin were determined from SCS soil surveys (USDA SCS 1977). The erodibility factor K associated with various soil types was taken from studies conducted by the SCS (USDA SCS 1992). Weighted K values were calculated for each sub-basin based on the percentage of each soil type in the sub-basin.

The topographic factor is defined as the ratio of soil loss from any slope and length to the soil loss from a standard 72.6-ft plot with a 9 percent slope. Slope length is defined as the distance the overland flow travels from its origin until it enters a channel or forms a depositional delta. Wischmeier and Smith (1978) provided the following equation for the topographic factor:

$$L_s = \left[\frac{\lambda}{72.6}\right]^n (0.065 + 0.0454S + 0.00655S^2) \quad (2)$$

$n = 0.3$ *when* $S \leq 3$ *percent*
$n = 0.4$ *when* $S = 4$ *percent*
$n = 0.5$ *when* $S \geq 5$ *percent*

where

λ = slope length, ft
S = percent slope
n = an exponent that varies with slope

RCE determined the topographic factors, which ranged from 0.16 on the mesa to 5.2 in the steeper areas of the watershed, from topographic maps.

The cover and management factor C accounts for vegetative cover in the watershed. For relatively sparse vegetation, which includes most of the study area, a C of 0.4 was assigned. C values as low as 0.1 were assigned to highly urbanized areas where there is essentially no bare soil.

The erosion-control practice factor P accounts for the effect of conservation practices, such as terracing and strip cropping. This factor is not significant for the North Diversion Channel drainage area and was assigned a value of 1.0.

Coefficients α and β were taken to be 285 and 0.56, respectively. The beta coefficient is the same as that recommended by Williams and Berndt (1977) which was developed from data from experimental watersheds in Texas and Nebraska. Based on previous experience in the Albuquerque area, RCE used an alpha coefficient three times the value reported by Williams and Berndt.

In their determination of sediment yield, RCE reduced the computed total sediment yield from the MUSLE by the percentage of the watershed that was impermeable. The percentage of impermeable area was taken from the HEC-1 input files. The wash-load component of the sediment yield was then determined assuming it would be equal to the percentage of material finer than 0.074 mm in the watershed's soil type. RCE's computation tables for the 2-, 5-, 10-, 25-, 50-, and 100-year storms are provided as Tables A5-A14, in Appendix A. A summary of calculated concentrations for wash-load and total sediment yield concentrations for the 100-year storm are tabulated below.

Calculated Sediment Yield, MUSLE
100-year-frequency Flood

Location	Average Concentration, mg/l	
	Wash Load	Total Load
Camino Arroyo at NDC	11,600	28,700
La Cueva Arroyo at NDC	10,400	26,500
Domingo Baca Arroyo at NDC	11,000	26,400
North Pino Arroyo at NDC	20,400	50,400
Pino Arroyo at NDC	6,100	15,000
Bear Arroyo at NDC	4,800	11,800
Embudito Arroyo at Montgomery	1,600	4,000
North Glenwood Hills Channel	3,300	8,600
Hidden Valley Basin	6,700	17,800
Glenwood Hills Basins	4,600	12,300
South Glenwood Hills Tributary	2,900	7,500
Piedra Lisa Dam	900	2,300
Embudo Dam	2,900	7,800

Wash-load concentrations in this tabulation were taken from RCE's Table A14 in Appendix A. Total load was calculated using the average percentage of soils less than 0.074 mm from the same table.

Average-annual sediment yields were determined using RCE-calculated yields for various frequency floods and incrementally integrating them with the frequency curve using the following equation:

$$Y_m = 0.015(Y_{100} + Y_{50}) + 0.04Y_{25} + 0.08Y_{10} + 0.2Y_5 + 0.4Y_2 \quad (3)$$

where average-annual sediment yield is Y_m, and Y_i represents sediment yield for specific hyrographs where i is the frequency of the hydrograph. This equation is derived by incremental integration of the sediment-yield frequency curve, considering no yields greater than the 100-year-frequency yield and assuming no yield for flows less than the 2-year-frequency yield. Calculated average-annual sediment yields are tabulated below.

Calculated Average Annual Sediment Yield, MUSLE

Location	Tons	Acre-ft/mi^2
Camino Arroyo at NDC	1159	0.10
La Cueva Arroyo at NDC	1874	0.12
Domingo Baca Arroyo at NDC	3335	0.15
North Pino Arroyo at NDC	1868	0.34
Pino Arroyo at NDC	1910	0.10
Bear Arroyo at NDC	2523	0.08
Embudito Arroyo at Montgomery	94	0.06
North Glenwood Hills Channel	99	0.06
South Glenwood Hills Tributary	44	0.12
Piedra Lisa Dam	13	0.01
Embudo Dam	192	0.03

The average of the tabulated values is 0.11 acre-ft/square mile/year. Results from the MUSLE calculations produce average-annual yields considerably less than the measured data, and less than those calculated using the SCS soil-erosion rates. Calculated concentrations also appear to be too low.

Rainfall Simulator Experiments

An experimental rainfall simulator study was conducted to measure the sediment yield for actual experimental plots in the Albuquerque Arroyos study area (Ward 1992). Rainfall simulation was used to measure runoff and sediment yields from three sites. Three 1-m-wide by 3-m-long plots were tested at each site. Plot slopes varied between 7 and 24 percent. One plot was scraped bare at each of the three sites to simulate disturbance caused by clearing and construction activities. The other plots had the natural vegetation left intact. Cover, which included vegetation and rock, varied between 20 and

65 percent for the natural plots. Simulated rainfall was supplied by sprinklers and was applied to "dry" and "wet" antecedent soil moisture conditions. After the simulator was installed, the first test was conducted representing dry conditions. On the next morning, a second test was run on the same plot representing the wet condition. The tests were conducted 15-18 September 1992. There had been significant rainfall in the area on the evening of 14 September and the morning of 15 September, so that dry conditions had higher antecedent moisture content than would be expected for a typical dry situation. Soil water content at the beginning of the simulation varied between 4.8 and 8.2 percent for the dry runs, and between 8.6 and 12.8 percent for the wet runs. A total of 18 plot-runs were conducted.

Sediment yields from the experimental plots were collected in two ways. Suspended material was pumped with the runoff water into a collection tank. Coarser material that deposited in the water collection device at the end of the experimental plot was collected at the end of each run.

Rainfall was applied at the rate of 3 in./hr for 30 minutes. Steady-state infiltration rates ranged between 0.12 and 2.72 in./hr for the dry runs and between 0.71 and 1.65 in./hr for the wet runs.

Sediment yield per unit area of runoff can be used to estimate loading to a channel once runoff is modeled. Runoff is characterized as a depth distributed equally over the surface area. Results from this study indicate that 0.52 tons/acre/in. of runoff is reasonable for undisturbed plots and that 3.12 tons/acre/in. is reasonable for plots which are scraped bare of vegetation. Finer particles were preferentially eroded from the plots leaving a coarser surface at the conclusion of each run. On the average, 50 percent of the sediment yield was finer than 0.075 mm and 50 percent coarser. However, there were large variations in all the measured values demonstrating the natural spatial and temporal variability found in southwestern United States upland watersheds.

Ward (1992) concluded that more material came off the wet watershed, but that it was due to the greater runoff. When runoff from the dry and wet soil samples were normalized by runoff, then the sediment yield rate was about the same. This fact is demonstrated by the concentrations tabulated below:

Condition	Measured Sediment Yield from Rainfall Simulator Concentration, ppm
Covered	
Dry	611
Wet	769
Uncovered	
Dry	7,190
Wet	4,360

The very low sediment concentrations obtained from the rainfall simulator demonstrate the small role that surface erosion plays in the total sediment yield. It can be concluded that gully, bed, and bank erosion are much more significant contributors. These results help explain the low yield estimates obtained from MUSLE which used rainfall simulator data in its development.

Sediment-Transport Method

Sediment yield can be estimated by assuming that the natural unlined channels are transporting bed-material load at maximum capacity and then, using a reliable sediment-transport equation, integrating a sediment-transport rating curve with a discharge hydrograph. RCE combined this technique with the MUSLE method to obtain a total sediment yield for channels entering the North Diversion Channel. Wash load was calculated for the entire watershed using MUSLE. This sediment was assumed to pass through the detention reservoirs without settling out. Bed-material load was calculated for reaches upstream from the lined-channel inlets.

RCE developed a sediment-transport equation, herein referred to as the Mussetter equation, especially for streams with high sediment concentrations. The Mussetter equation computes bed load by size fraction using a form of the Meyer-Peter Müller equation (USBR 1960). The suspended load is computed for the median size of the bed material. The suspended-sediment-concentration vertical profile is calculated based on a form of the diffusion equation developed by Woo, Julien, and Richardson (1988) and a power function velocity profile developed by Karim and Kennedy (1983). RCE has determined from previous work with southwestern United States arroyos that reasonable sediment-transport rates can be predicted with this equation.

The hydraulic characteristics of unlined channels were determined at the critical concentration points. The U.S. Army Corps of Engineers HEC-2 water-surface profile numerical model (USAEHEC 1990) was used to compute hydraulic parameters. Cross-section geometry for the model was determined from a combination of field surveys and topographic mapping. Cross sections developed from topographic mapping were adjusted as necessary to reflect the observed shape of the arroyos; i.e. a rectangular shape with width-to-depth ratios of approximately 40. Manning's roughness coefficients of 0.03 and 0.04 were assigned to the main channel and overbank, respectively. Calculated hydraulic parameters were averaged for similar computational reaches.

The bed-material sediment yield, for each reach, was calculated for the 2-, 5-, 10-, 25-, 50-, and 100-year-frequency flood events by integrating a sediment-transport rating curve, calculated using the Mussetter equation, over the respective storm hydrographs. RCE used four separate storm centerings to maximize runoff for individual drainage basins. Summary tables for the average annual sediment yields and 100-year frequency flood sediment yields

are presented in Tables A15 and A16, respectively. The bed gradations for the sediment transport calculations were based on field samples.

The total sediment yield for each storm event was determined by adding the computed bed-material load to the wash load that had been computed using the MUSLE. The total sediment yields for each concentration point are tabulated below.

Calculated Total Sediment Yield Sediment Transport Method Combined with MUSLE

Location	100-year-flood		Average Annual	
	tons	average mg/l	tons	acre-ft/square mile
La Cueva at NDC	132,000	321,000	6,670	0.53
Domingo Baca at NDC	72,200	94,100	6,210	0.27
North Pino at NDC	14,000	59,600	960	0.17
Pino at Wyoming Basin	19,100	66,700	1,830	0.16
Pino at NDC	3,010	6,200	533	0.03
Bear at NDC	22,900	102,000	3,300	0.11
Embudito at Montgomery	16,900	174,000	2,400	1.50
North Glenwood Hills	20,800	271,000	1,800	1.02
South Glenwood Hills Trib	2,600	113,000	330	0.88
Piedra Lisa d/s from dam	785	18,100	88	0.07
Embudo at Monte Largo	76,300	310,000	7,150	0.98

The average-annual sediment yield computed using this method was 0.19 acre-ft/square mile/year. However, yields at mountain canyons and in unlined channels were much higher. The average-annual yield using this method is very close to that determined from the North Diversion Channel sediment removal records. Average concentrations for the 100-year-frequency flood are significantly higher than the average of the measured suspended-sediment data. However, they are within the range of individual measurements. Also it must be remembered that the 100-year-frequency discharges are much greater than any for which samples were collected.

Tatum Method

The Tatum method (1963) was developed to size debris basins in the San Gabriel Mountains, which are part of the Southern California Coastal Range. The method predicts the quantity of debris actually trapped by a debris

structure from a single hydrologic event. Debris includes silt, sand, clay, gravel, boulders, and organic material. All of the watersheds in the database used to develop the method had relatively high soil moisture content due to antecedent rainfall. The method can be used to account for increased debris yields from watersheds that have been denuded by wildfire. The method was developed using reported debris accumulation in existing debris basins. Since actual deposition in the basins was used to develop the Tatum method, trap efficiencies are inherently assumed to be equal. Calculations are made from nomographs using an equation with adjustment factors for size, shape, and slope of the drainage area, 3-hour precipitation, the portion of the drainage area burned, and the years occurring between the time of the burn and the time of the flood. In the Albuquerque Arroyos study, the effects of fire were not considered.

The parameters developed for application of the Tatum method are listed in Table A17 in Appendix A. The calculated debris yield from using this method in Albuquerque is an extrapolation of the method beyond its intended use. Therefore, results must be considered approximate and must be used in conjunction with results using other methods in order to make general conclusions regarding sediment yield.

Los Angeles District Method

The Los Angeles District Method (USAED Los Angeles 1992) is based on a statistical analysis of measured deposition in debris basins, hydrologic data, and watershed characteristics. The database for these equations includes that of Tatum (1963) plus additional data collected from debris basins located in the Southern California Coastal Range. The method is intended to be used for estimation of debris yield from coastal-draining, mountainous Southern California watersheds. Outside of the recommended application area, careful adjustment of the calculated yields may be required.

The variables determined to be significant for debris production are: relief ratio, *RR*, in ft/mile; drainage area, *A*, in acres; unit peak flow, *Q*, in cfs/square mile or maximum 1-hour precipitation *P* in inches times 100; and a nondimensional fire factor *FF*. In the Albuquerque Arroyos study, destruction of the watershed vegetation by fire was not considered. The parameters developed for application of the Los Angeles District method are listed in Table A18 in Appendix A. The following regression equation is used to calculate unit debris yield D_y, in cubic yards/square mile, for drainage areas up to 3 square miles, using maximum 1-hour precipitation:

$$\log D_y = 0.65(\log P) + 0.62(\log RR) + 0.18(\log A) + 0.36 \quad (4)$$

A total of 350 observations from 80 watersheds were used to develop this regression equation. The calculated debris yield from this equation, in statistical terms, is the "expected" value. Uncertainty associated with the calculated result can be measured using the standard deviation of the estimate of the expected value. The standard deviation for Equation 4 is 0.465 (log D_y). It can be stated with 67 percent confidence that the "true" value of debris yield is within one standard deviation of the expected value. It can also be stated with 95 percent confidence that the true debris yield will fall within two standard deviations of the expected value. These statistics are based on the data used to develop the regression equation and assume that any calculated value comes from a watershed with similar geomorphic and hydrologic conditions.

For drainage areas between 3 and 10 square miles, the following regression equation was developed:

$$\log D_y = 0.85(\log Q) + 0.53(\log RR) + 0.04(\log A) + 0.66 \quad (5)$$

The equation for drainage areas between 10 and 25 square miles is

$$\log D_y = 0.88(\log Q) + 0.48(\log RR) + 0.06(\log A) + 0.60 \quad (6)$$

A total of 187 observations from seven watersheds were used in the development of Equations 5 and 6. The standard deviation for Equations 5 and 6 was determined to be 0.242 log D_y.

Debris yields into the detention basins and reservoirs and at the upstream end of improved channels in the Embudo Arroyo watershed were calculated using the Tatum and Los Angeles District methods. The calculated yields are tabulated below and are compared with capacity. Capacities are significantly greater than the sediment yields. Average concentration was calculated as the total volume of debris divided by the total volume of runoff.

Reported depositions in two detention basins from the July 1988 thunderstorm were used to evaluate calculated results from the Tatum and Los Angeles District Methods. Debris yield was calculated for the two basins using the July 1988 rainfall. Total storm rainfall of 2.37 in. and 3.15 in. were determined for the Piedra Lisa and Lomas drainage basins, respectively, from isohyetal maps produced by Wright Water Engineers Inc. (1989). Reported deposition in the basins was based on estimates made by the city of Albuquerque to determine excavation costs after the storm event. Deposition of 2,800 cu yd was estimated for Piedra Lisa Basin and deposition of 45,000 cu yd was estimated for Lomas Basin. Lomas Basin is located just outside the North Diversion Channel drainage area, adjacent to the Embudo watershed. There was significant lateral erosion of a levee just upstream from

Calculated Sediment Yield
100-Year-Frequency Storm

Location	Sediment Volume cu yd			Average Concentration mg/l	
	Detention Basin Capacity	LA District Method	Tatum Method	LA District Method	Tatum Method
Embudo Dam	248,200	70,700	22,700	344,000	121,000
Piedra Lisa Dam	47,400	9,700	7,600	246,000	197,000
Glenwood Basins	5,500	3,400	1,800	273,000	152,000
Hidden Valley Basins	2,600	1,700	1,900	231,000	256,000
J. B. Robert Dam	748,100	116,500	40,400	266,000	99,000
Pino Dam	834,100	87,600	20,000	322,000	81,000
South Domingo Baca	563,500	78,800	12,000	327,000	55,600
North Domingo Baca	218,900	21,600	2,100	191,000	18,500
Downstream from Embudo Dam		9,300	5,800	307,000	200,000
South Glenwood Hills Tributary		2,300	1,400	123,000	76,000
North Glenwood Hills		12,100	11,900	196,000	194,000

Piedra Lisa Basin that contributed to the sediment deposition in 1988. Upstream from Lomas Basin there was considerable gully erosion through areas that had recently been graded for residential construction. The calculated and reported depositions are compared in the following tabulation. Deposition in Piedra Lisa Basin was overestimated by both methods. Deposition was underestimated in the Lomas Basin by both methods. Calculated results with the Los Angeles District method were within one standard deviation at the Lomas Basin, and almost within a standard deviation at the Piedra Lisa Basin.

The Los Angeles District Method provides several techniques to account for geomorphic differences between the subject watershed and the San Gabriel Mountain watersheds. Adjustment is achieved by multiplying calculated debris yields by an Adjustment-Transposition (AT) factor. Techniques for determining the AT factor require data from the subject or nearby watersheds. The required data include measured deposition in debris basins from storms with known runoff or rainfall, average-annual rainfall and sediment yield, or a detailed field analysis which identifies geomorphic characteristics of the watershed.

Comparison of Calculated and Reported Storm Yield, July 1988					
	Sediment Deposition, cu yd				
			LA District Method		
Location	Reported	Tatum Method	Expected Value	Plus One Standard Deviation	Minus One Standard Deviation
Piedra Lisa Dam	2,800	8,600	10,800	31,500	3,700
Lomas Basin	45,000	24,300	26,800	78,200	9,200

Insufficient data are available in the Albuquerque Arroyos watersheds to establish a reliable AT factor for the application of the Los Angeles District Method. Estimates ranged between 0.13 and 1.68. But the general indication is that the AT factors should be less than 1.00 and that the method overpredicts the debris yield in the Albuquerque Arroyos.

Calculated concentrations using the Los Angeles District method without an AT factor are generally higher than those calculated with the Tatum method. However, calculated results are similar to RCE's calculated results, using the sediment transport method, for the arroyos at canyon mouths. Differences become more apparent the further the concentration point is away from the canyon mouth. The Los Angeles District method does not appear to be appropriate for application to the mesa detention reservoirs.

Sediment Yield Summary

Sediment yield to the North Diversion Channel consists of fine-sediment wash load and coarser sand bed-material load. The two sediment loads are supplied by surface, gully, bed, and bank erosion. Surface erosion was found to be less important than gully, bed, and bank erosion in terms of the quantity of sediment load supplied. High concentrations of coarser bed-material load can be supplied by the unlined channels and the steep mountain watersheds. Average concentrations for the 100-year-frequency flood could be as high as 300,000 mg/l. The detention reservoirs have sufficient capacity to store the sediment supplied by the 100-year-frequency flood. The construction of detention dams and lined channels in the Albuquerque Arroyos study area has effectively decreased the supply of sediment to the North Diversion Channel.

It should be noted that the detention dams were designed without any specified sediment allowance. Reduced storage capacity in the detention reservoirs could result in an increase in downstream peak flows. It is recommended that hydrology studies be conducted to determine the effect of reduced storage due to sediments for design or analysis of the arroyos downstream from detention dams.

4 Trap Efficiency

Introduction

Trap efficiency is often defined as the percent of the inflowing sediment that is trapped. The trap efficiency of a reservoir is a measure of sediment removal from the inflowing water-sediment mixture. It is the ratio of the total weight of sediment deposited in a reservoir to the weight of sediment delivered to the reservoir. It can be given in terms of a long-term average or for a specific storm. Detention time in the reservoir and the size of the sediment entering the reservoir are the primary factors that determine trap efficiency.

Data needed to calculate trap efficiency include reservoir surveys to determine the volume of sediment deposited over a period of time, density of the sediment deposit, and measurements of sediment inflow or outflow. Total inflow or outflow can be predicted by integrating a reliable discharge-concentration rating curve, developed from the measured data, with a discharge hydrograph that covers the period between reservoir surveys. Typically, available data are insufficient to determine trap efficiency by this method.

Empirical relationships have been developed to estimate trap efficiency in cases where data are insufficient for direct calculations. Three such methods are presented in the U.S. Army Corps of Engineers, Engineer Manual, EM 1110-2-4000, "Sedimentation Investigations of Rivers and Reservoirs" (USAEHQ 1989). These are the Brown (1950), Brune (1953) - Dendy (1974), and Churchill (1948) methods. A fourth method is the Hazen (1904) method. As with all empirical methods, one must assess applicability to specific cases. The methods presented in EM 1110-2-4000 were all developed for normally ponded reservoirs and calculate trap efficiency based on average-annual conditions. They do not account for the variability in inflowing sediment sizes, nor do they account for the effect of reservoir outlet configuration; e.g. the elevation and size of the outlet ports above the reservoir bed. Outlet configuration is probably not as important in normally ponded reservoirs as it is in dry reservoirs. The Hazen method can be used to calculate trap efficiency by size class and was developed to design sediment basins in water and wastewater treatment plants.

Trap Efficiency Methods

A simple method for estimating trap efficiency is the capacity-watershed method proposed by Brown (1950). This method is useful if the drainage area and the reservoir capacity are the only known data. Brown plotted measured trap efficiency versus the ratio of storage capacity to drainage area and developed an equation to fit the data:

$$E = 1.0 - \frac{1.0}{1.0 + \frac{KC}{W}} \tag{7}$$

where

E = trap efficiency as a fraction

K = coefficient, ranging between 0.046 and 1.0, median value of 0.1

C = reservoir capacity, acre-ft

W = watershed area, square miles

This equation is not dimensionally homogeneous and requires use of designated units of measurement. Brown's curve with the supporting data are shown in Figure 10. Brown's method does not consider reservoir outlet size nor detention time and application of the method requires fore-knowledge of the K coefficient, or acceptance of the median value.

The capacity-inflow method proposed by Brune (1953) empirically relates trap efficiency and the ratio of reservoir capacity to mean annual inflow. Brune's data were from normally ponded reservoirs. Dendy (1974) collected more data, including data from dry reservoirs, and displayed them with Brune's data as shown in Figure 11. In general, Dendy's data indicated lower trap efficiencies than Brune's data. In addition, Dendy's data suggested an even lower trap efficiency for dry reservoirs. Using both his own and Brune's data, Dendy developed a dimensionally homogeneous empirical relationship for normally ponded reservoirs.

$$E = (0.97)^{0.19^{\log \frac{C}{I}}} \tag{8}$$

where C is reservoir capacity and I is annual inflow. The Brune-Dendy method is an improvement over the Brown method because the

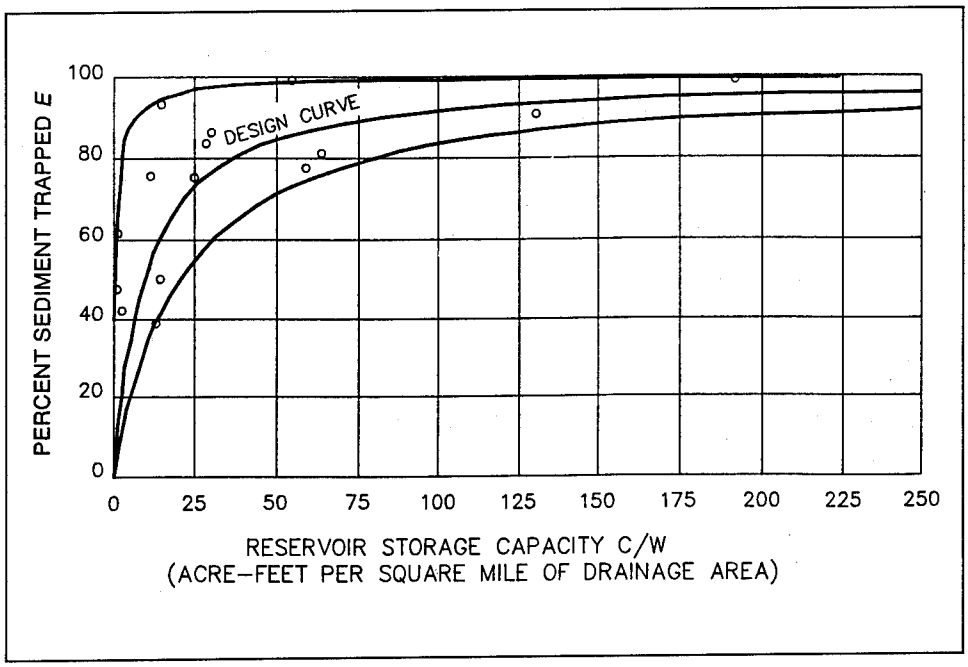

Figure 10. Trap efficiency curve by Brown

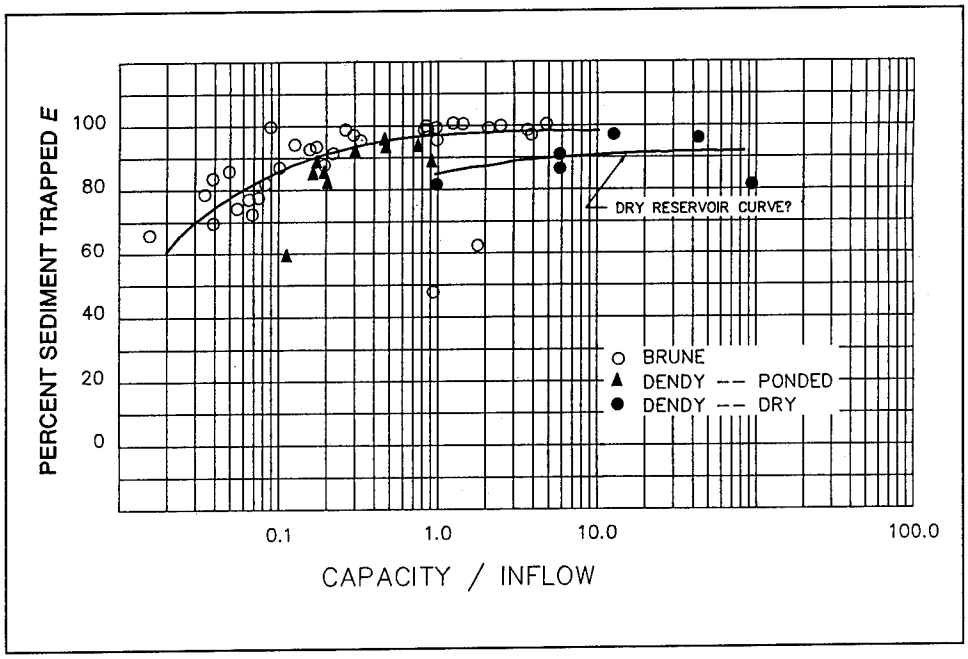

Figure 11. Trap efficiency curve by Brune-Dendy

capacity-inflow ratio is a better surrogate for detention time than the capacity-watershed ratio.

Churchill (1948) presented a relationship between trap efficiency and a sediment index (SI) where SI is the ratio of retention period to the mean reservoir velocity. Retention period can be estimated as the ratio of reservoir capacity to inflow. Velocity can be estimated as inflow divided by cross-sectional area. Algebraic manipulation leads to the following equation for sedimentation index:

$$SI = \frac{\left(\frac{C}{Q}\right)^2}{L} \tag{9}$$

where

C = reservoir capacity, cu ft

Q = mean annual discharge through reservoir, cfs

L = reservoir length, ft

Churchill's curve was developed using data from Tennessee Valley Authority reservoirs where the sediment load consists entirely of silts and clays.

Churchill's and Brune's curves are displayed in Figure 12 with additional data plotted by the U.S. Bureau of Reclamation (1987). The U.S. Bureau of Reclamation introduced a dimensionless parameter K which is obtained by multiplying SI times the acceleration of gravity.

Hazen (1904) derived an equation to determine trap efficiency for unhindered settling of discrete particles in a rectangular basin:

$$E = \frac{\omega_s A}{Q} \tag{10}$$

where

ω_s = particle fall velocity

A = surface area of the basin

Q = rate of flow through basin

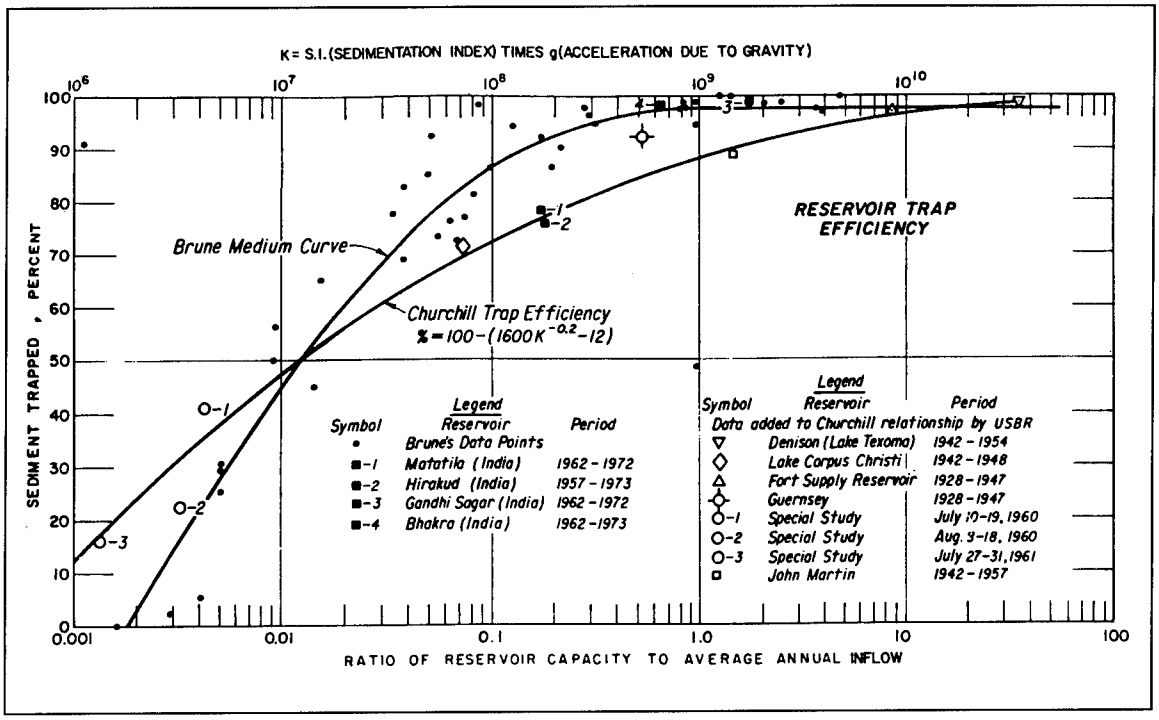

Figure 12. Trap efficiency curve by U.S. Bureau of Reclamation

Any set of consistent units may be used with this equation. Hazen's equation calculates trap efficiency independent of the flow depth or the detention time although the effects of these variables are inherent to the equation. The equation assumes that re-entrainment of deposited sediment does not occur. The reasonableness of this assumption can be determined by comparing calculated applied shear stress with the critical shear stress for each size class using the Shield's equation:

$$\tau = \gamma RS \tag{11}$$

$$\tau_c = \theta(\gamma_s - \gamma)d \tag{12}$$

where

τ = applied shear stress

τ_c = critical shear stress

γ = specific weight of water

γ_s = specific weight of sediment

R = hydraulic radius

S = energy slope

θ = Shield's parameter

d = grain size.

Settling basin efficiency is reduced by eddy currents set up at the basin inlet when flow expands, by wind-induced surface currents, by density currents caused by vertical variations in temperature or concentration, and by re-entrainment of sediment by turbulence. These conditions cause the flow to "short-circuit" the sediment basin. Hazen proposed accounting for short-circuiting using the following equation:

$$E = 1.0 - \left[1.0 + n\frac{\omega_s A}{Q}\right]^{-\frac{1}{n}} \qquad (13)$$

where n is a coefficient between 0 and 1.0 that qualitatively defines basin performance between "best" and "very poor." Settling curves for a range of n are shown in Figure 13. Total trap efficiency for a reservoir cannot be calculated using the Hazen method unless the gradation of the inflowing sediment load is known or can be reliably estimated.

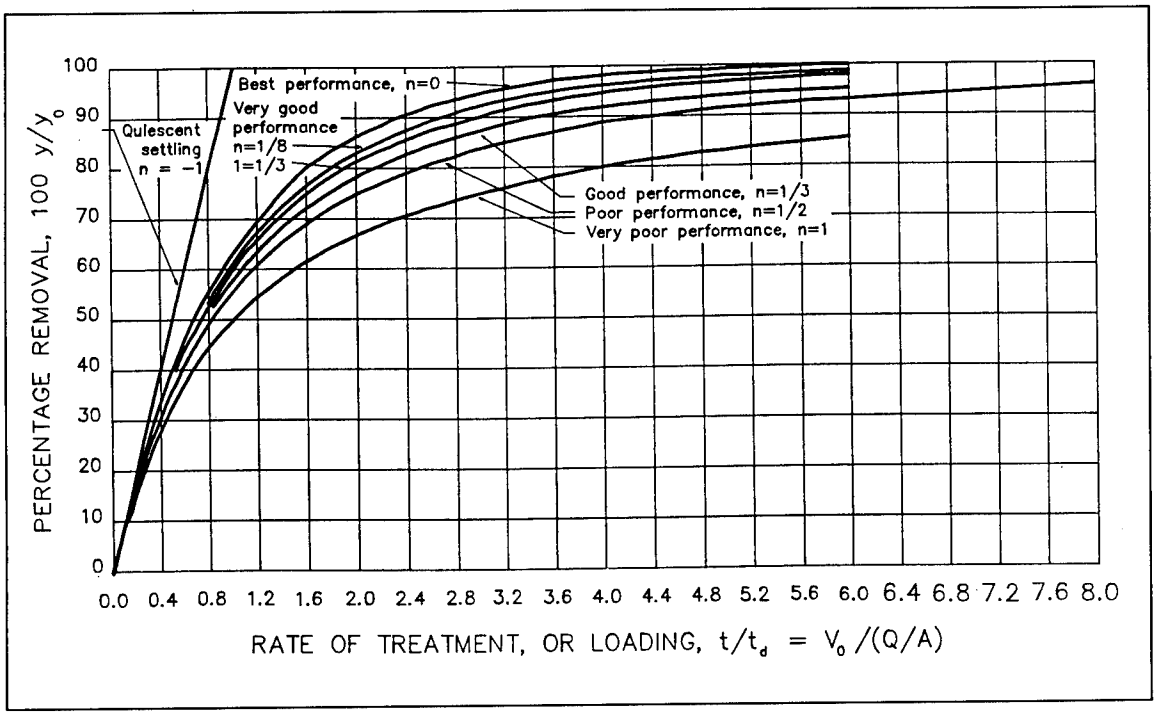

Figure 13. Performance curves for settling basins by Hazen

Prototype Reservoir Data

The applicability of the four trap efficiency methods to the detention reservoirs, detention basins, and sediment traps in the Albuquerque Arroyos study area was tested using data from two detention reservoirs in New Mexico where conditions are similar to those in Albuquerque. Bernalillo Reservoir, near Bernalillo, which is 17 miles north of Albuquerque, and Tortugas Arroyo Reservoir, near Las Cruces, which is 225 miles south of Albuquerque, were part of a nationwide investigation of trap efficiencies of detention reservoirs conducted by the U.S. Geological Survey (Funderburg 1977 and Funderburg and Roybal 1977). Both detention reservoirs are normally dry and runoff generally occurs from high intensity summer thunderstorms. Bernalillo and Tortugas detention reservoirs have drainage areas of 4.1 and 20.7 square miles, respectively. Both drainage basins have steep mountains in their headwaters and have alluvial mesa formations similar to those in Albuquerque. The alluvial mesa area upstream from Bernalillo had been treated in 1958 to reduce erosion and gullying and to retard the rapid runoff of rainfall. The land treatment consisted of pits, terraces, seeding, and restricted grazing. Hydrologic and deposition data covered a 30-year period at Bernalillo and an 11-year period at Tortugas. Average-annual inflow to Bernalillo was 7.4 acre-ft, and to Tortugas it was 158 acre-ft. Reservoir capacities are 311 and 1,324 acre-ft at Bernalillo and Tortugas, respectively. Trap efficiency at both detention dams was determined using measured sediment concentrations at the outlets and reservoir surveys. Reported trap efficiency at both detention dams was 96 percent; 99 percent of the sand and coarser size classes were trapped.

Evaluation of Trap Efficiency Methods

Four methods were used to predict trap efficiency at Bernalillo and Tortugas detention dams. The predictions were then compared with the reported trap efficiencies in order to establish a level of confidence for each method. Applications of the methods were modified to meet the available data and special circumstances of dry reservoirs.

The Brown method requires fore-knowledge of the K coefficient to determine trap efficiency or use of the median value of 0.1. Using a K of 0.1, trap efficiencies of 87 and 86 percent were calculated for Bernalillo and Tortugas, respectively. These values are considerably less than the reported trap efficiencies. Therefore, an appropriate K factor was determined using the reported trap efficiency of 96 percent. For Bernalillo, a K value of 0.32 was calculated, and for Tortugas, a value of 0.38 was calculated. Data points for the two reservoirs are compared with Brown's data in Figure 14. It can be seen that these detention reservoirs have high trap efficiencies compared with most of the reservoirs considered by Brown.

Application of the Brune-Dendy method to dry reservoirs is questionable because data from dry reservoirs were not included in the development of the

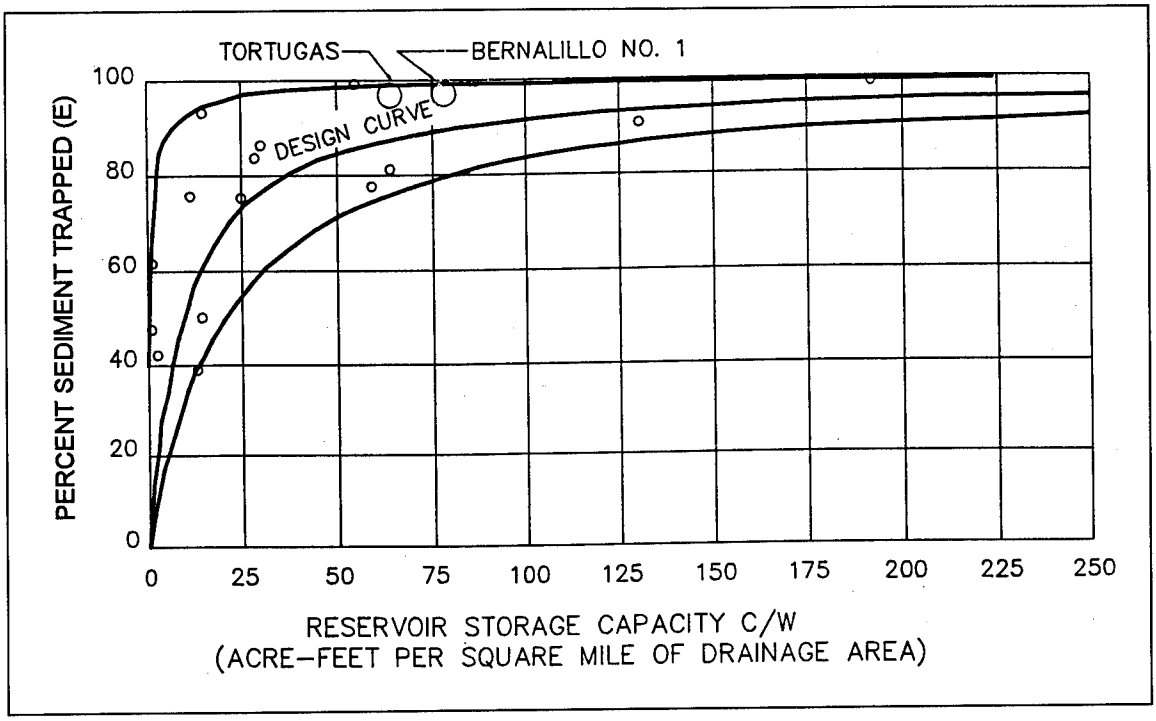

Figure 14. Trap efficiency for Tortugas and Bernalillo detention basins using Brown's curve

curve. In fact, Brune and Dendy both suggested that dry reservoirs should have considerably lower trap efficiencies than normally ponded reservoirs. The mean pool elevation in the reservoirs considered by Brune and Dendy was generally close to reservoir capacity. The ephemeral arroyos feeding the reservoirs in Albuquerque are significantly different from the rivers and streams considered by Brune and Dendy.

Due to questions related to the appropriate capacity and inflow to use with the Brune-Dendy method for dry reservoirs, the capacity-inflow ratio was calculated three different ways for Bernalillo and Tortugas detention dams. First, the detention reservoir capacity was divided by the average-annual inflow as suggested originally by Brune. Secondly, the detention reservoir capacity was divided by the annual inflow for the year with the largest recorded inflow. At Bernalillo, this was in 1956 when the annual inflow was 63.2 acre-ft. At Tortugas this was in 1967 when the annual inflow was 456 acre-ft. Finally, the largest storm event was evaluated using the actual maximum reservoir storage during the storm divided by the storm inflow. At Bernalillo, this occurred in July 1956 when the inflow was 53 acre-ft and the maximum storage was 47 acre-ft. At Tortugas, this occurred in August 1967 when inflow was 347 acre-ft and the maximum storage was 291 acre-ft. Different capacity-inflow ratios were calculated depending on how the capacity and inflow were defined; however, in each case, the result plotted very close to the Brune-Dendy relationship—assuming that the 96 percent trap efficiency was applicable for all the cases (Figure 15). The reservoir outlet configurations at Bernalillo and Tortugas, along with the relative coarseness of the

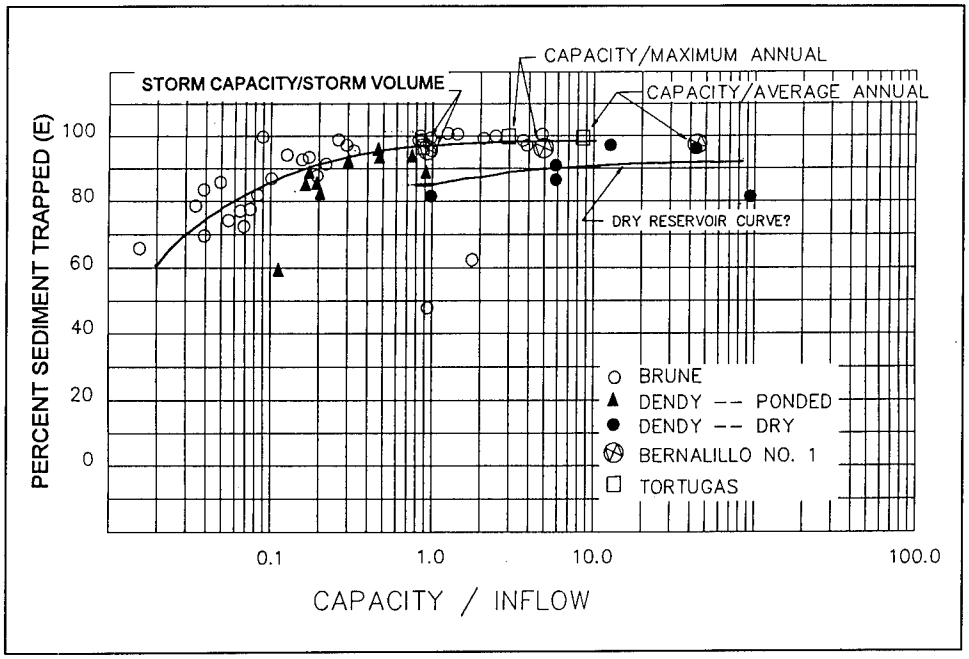

Figure 15. Trap efficiency for Tortugas and Bernalillo detention basins using Brune-Dendy's curve

sediment inflow, probably account for the relatively high trap efficiency of these dry reservoirs. Detention reservoirs and basins in Albuquerque have similar outlet configurations and sediment inflowing loads. Thus, this verification calculation establishes some confidence in using the Brune-Dendy method for the normally dry reservoirs in Albuquerque. Because using specific storm inflow and storage capacity to calculate the capacity-inflow ratio provides the best surrogate for detention time, these values were used to calculate trap efficiency with the Brune-Dendy method.

Application of the Churchill method to detention reservoirs in Albuquerque is questionable due to the dissimilarity between dry reservoirs and the major reservoirs of the Tennessee Valley Authority. Application of the method was modified herein to consider actual detention time of a storm event. The trap efficiency was calculated in a series of time steps where capacity was taken to be the average capacity of the detention reservoir during the time step, and average discharge through the detention reservoir was taken to be equal to the average outflow as suggested by Dendy (1974). Two storm events from the 1956 water year at Bernalillo reservoir were used to test the method. A July event had an average storage capacity of 53 acre-ft and an average outflow of 27 cfs. An August storm had an average storage capacity of 10.2 acre-ft and an average outflow of 15.5 cfs. Trap efficiencies of 83 and 70 percent were calculated for the July and August storms, respectively. These calculated trap efficiencies were considerably lower than the reported trap efficiency for the detention reservoir. Based on this result it was decided not to consider the Churchill method in estimating trap efficiencies for the Albuquerque Arroyos study.

The Hazen method will not provide a complete solution for trap efficiency unless the composition of the inflowing load is known. This method calculates trap efficiency by size class. There are insufficient data to establish sediment inflow concentrations by size class at either Bernalillo or Tortugas detention dams. However, measured concentrations at the outlet of Tortugas provide insight into the maximum size class that passes through the detention dam. Measurements at Bernalillo and Tortugas indicated that 99 percent of the sediment passing through the outlet was finer than 0.016 mm, which is the lower limit of medium silt.

It was determined that reasonable calculated trap efficiencies could be obtained with the Hazen method when the performance variable n was set equal to 0.5. Calculations indicated that 99.7 percent of the medium silt and 100 percent of the coarse silt would be trapped in the detention reservoir. Although these results are not directly comparable because the percentage of each size class in the inflow is unknown, it can be inferred that the Hazen method does an adequate job of predicting the maximum size class that can be passed through the detention dams.

Data were insufficient to completely verify any of the trap efficiency methods. However, it was demonstrated that predictions of trap efficiency could be obtained with a reasonable level of confidence, in Albuquerque detention dams, using the Brown (with K = 0.32), Brune-Dendy, or Hazen (with n = 0.5) method.

Calculated Trap Efficiencies

Trap efficiencies were calculated for each of the flood-control detention structures and sediment traps upstream from the North Diversion Channel. The sediment traps have insignificant storage capacity, so only the Hazen method is appropriate for application. Required data for the calculations are tabulated below.

The Brown method was used to calculate trap efficiencies for the detention structures. A K factor of 0.32 was used, based on the analysis of measured data at Bernalillo Reservoir. This method supplies a rough estimate of long-term trap efficiency.

The Brune-Dendy method was used to calculate trap efficiency for a storm event. The maximum storage during the 100-year-frequency flood was used as the capacity, and the 100-year-frequency inflow volume was used as the inflow. The 100-year-frequency flood used for this analysis was based on storm centering No. 1 (USAED Albuquerque 1992), which results in the highest peak discharge in the North Diversion Channel. At each of the detention dams, this flood is considerably less than the design flood, which would be based on storm centerings above each detention dam.

Location	Drainage Area square mile	Reservoir Capacity acre-ft	100-yr Reservoir Storage acre-ft	100-yr Inflow acre-ft	100-yr Peak Outflow cfs	100-yr Peak Surface Area square ft
Detention Structures						
Embudo	3.7	152	48	101	230	300,000
Piedra Lisa	0.6	29	13	21	50	174,000
John B. Robert	10.2	458	58	209	660	282,000
Arroyo Del Oso	13.7	323	54	364	820	623,000
Pino	6.2	517	107	136	70	574,000
South Domingo	4.4	345	43	97	140	285,000
North Domingo Baca	1.8	134	23	53	100	151,000
Glenwood	0.20	3.4	3.4	6	77	38,000
Hidden Valley	0.12	1.6	1.58	3	54	12,400
Sediment Traps						
Wyoming					1100	75,400
Bear					1800	167,200
South Pino					2300	142,700
North Pino					1800	176,400
Domingo Baca					2600	220,100

Calculated trap efficiencies for each of the detention structures are listed in the following tabulation. Arroyo Del Oso Detention Dam is downstream from John B. Robert Detention Dam on Bear Canyon Arroyo; therefore applicability of Brown's watershed-capacity method is questionable. However, the calculated trap efficiency of 88 percent was identical to that calculated using the Brune-Dendy method. For the rest of the detention dams, the Brune-Dendy method predicts an average trap efficiency of about 95 percent. Trap efficiencies calculated using the Brown method are similar for the detention reservoirs, but for the Glenwood and Hidden Valley detention basins, calculated trap efficiencies are about 13 percent lower. Both methods predict that a very high percentage of the inflowing sediment load will be trapped by the detention structures. This result effectively eliminates the steep mountain watersheds from consideration as significant sediment sources to the improved channels downstream from the detention structures.

The Hazen method was used to assess the trap efficiency of individual size classes through the detention structures and sediment traps. This information is important in the analysis of deposition in the North Diversion Channel,

Location	Calculated Trap Efficiency, percent	
	Brown Method	Brune-Dendy Method
Embudo	93	95
Piedra Lisa	94	96
Glenwood	84	96
Hidden Valley	81	95
John B. Robert	93	93
Arroyo Del Oso	88	88
Pino	96	96
South Domingo Baca	96	95
North Domingo Baca	96	95

where only the sand sizes are expected to deposit. Calculated results are tabulated on the following page.

These results indicate that most of the inflowing clay, varying percentages of silt, and almost none of the sand will pass through the detention structures. This result further supports the conclusions based on results from the Brown and Brune-Dendy methods which indicated that the steep mountain watersheds would not be significant sediment sources.

The calculations indicated that the sediment traps were effective in reducing sand delivery to the North Diversion Channel. During the 100-year-frequency flood, on the average, about 70 percent of the very fine sand size class, 90 percent of the fine size class, and almost all of the medium sand and larger size classes were trapped by the sediment traps. Trap efficiency would be less at lower discharges when the ponding feature in the sediment traps and detention time are reduced. The calculated trap efficiencies for the sediment traps were used to reduce sediment inflow by size class to the numerical model of the North Diversion Channel.

Sediment traps designed using the Hazen method should have applied shear stresses that are less than the critical shear stresses. In the sediment traps upstream from the North Diversion Channel, this was not the case. This means that some of the sediment that deposits in the traps will be re-entrained, adding uncertainty to the calculations. The effect of re-entrainment is somewhat accounted for by the choice of the performance variable n; in this case performance was assumed to be "poor."

A check of the Hazen method was conducted at Domingo Baca sediment trap. Sediment-transport rating curves were developed by RCE that represented sediment-transport capacity in the Domingo Baca Arroyo upstream

Location	Trap Efficiency by Size Class Using Hazen Method, percent									
	Clay	Very Fine Silt	Fine Silt	Medium Silt	Coarse Silt	Very Fine Sand	Fine Sand	Medium Sand	Coarse Sand	Very Coarse Sand
Detention Structures										
Embudo	4	15	40	77	96	99.6	100			
Piedra Lisa	10	29	67	93	99.3	99.9	100			
Glenwood	1	4	16	45	82	97	99.6	99.9	100	
Hidden Valley	1	2	8	26	62	91	98	99.6	99.9	100
John B. Robert	2	6	23	50	85	98	99.7	100		
Arroyo Del Oso	3	10	31	67	93	99.2	99.9	100		
Pino	25	60	90	98.7	99.9	100				
South Domingo Baca	5	17	48	83	98	99.8	100			
North Domingo Baca	4	14	39	77	97	99.6	100			
Sediment Traps										
Wyoming	0.2	0.4	1.5	7.5	29	64	90	97	99.2	99.7
Bear	0.2	0.5	2.6	13	36	73	93	98	99.6	99.8
South Pino	0.2	0.4	1.5	7	28	62	88	96	99	99.6
North Pino	0.2	0.5	2.6	13	37	74	94	98	99.6	99.8
Domingo Baca	0.2	0.5	2.5	9	34	71	92	98	99.4	99.8

from the trap and through the trap. Integrating the rating curve over the 100-year-frequency flood, RCE calculated a trap efficiency of 96 percent. This result adds circumstantial support to the applicability of the Hazen method for analyzing the sediment traps.

5 The Numerical Model

Description

The TABS-1 one-dimensional sedimentation program was used to develop the numerical model for this study. Development of this computer program was initiated by Mr. William A. Thomas at the U.S. Army Engineer District, Little Rock, in 1967. Further development at the U.S. Army Engineer Hydrologic Engineering Center (USAEHEC) and at the U.S. Army Engineer Waterways Experiment Station (WES) by Mr. Thomas has produced the widely used HEC-6 generalized computer program for calculating scour and deposition in rivers and reservoirs (USAEHEC 1993). Additional modifications and enhancements to the program by Mr. Thomas at WES led to the TABS-1 program currently in use. This study was conducted using version 2.06, dated August 1992. This version of TABS-1 is fully compatible with HEC-6 version 4.1, dated October 1993, for the Albuquerque Arroyos numerical model. The program produces a one-dimensional model that simulates the response of the riverbed profile to sediment inflow, bed-material gradation, and hydraulic parameters. The model simulates a series of steady-state discharge events and their effects on the sediment transport capacity at cross sections and the resulting degradation or aggradation. The program calculates hydraulic parameters using a standard-step backwater method assuming subcritical flow. The program assigns critical depth for water-surface elevation if the backwater calculations indicate transitions to supercritical flow. However, for supercritical flow, hydraulic parameters for sediment transport are calculated assuming normal depth in the channel. A more detailed description of the program capabilities is found in Appendix B.

For numerical sedimentation models to completely simulate the behavior of a stream channel, computations would have to account for all of the basic processes of sedimentation: erosion, entrainment, transportation, deposition, and compaction of both bed and the streambanks for the complete range of particle sizes found in nature. The state of the art has not advanced to such a complete simulation. The computer program used in this study, TABS-1, is a state-of-the-art program for use in mobile-bed channels. It incorporates procedures for describing the complex sedimentation processes when these procedures have been established by research and published. Where knowledge gaps exist, the TABS-1 program contains logic that bridges those gaps. When

applied by experts using good engineering judgment, the TABS-1 program will provide good insight into the behavior of mobile-bed channels. Because the program has given reliable results at similar projects, it is expected to give reliable answers to the questions being addressed here. In the Albuquerque Arroyos application, the channels are concrete-lined, so that degradation is limited to removal of sediment deposited in the channel.

Numerical Model Geometry

The North Diversion Channel was modeled from its outlet at sta 18+90 to sta 476+25. Embudo Channel was modeled from its confluence with the North Diversion Channel at sta 412+50 to sta 471+00, a distance of about one mile. In the numerical model, the Embudo Channel was treated as an extension of the North Diversion Channel; and the North Diversion Channel, upstream from its confluence with Embudo Channel, was modeled as a tributary. This was done because flow in the Embudo Channel is normally much greater than in the North Diversion Channel upstream from the confluence. Cross-section geometry was developed from data provided in Design Memorandums No. 4 and 5 (USAED Albuquerque 1964, 1965) and from as-built plans of the Embudo Channel provided by the Albuquerque Metropolitan Arroyo Flood Control Authority (AMAFCA). A channel profile of the modeled reaches of the concrete-lined channels is shown in Figure 16. Each asterisk in Figure 16 represents a cross-section location in the numerical model.

Bear and Domingo Baca Arroyos were modeled for about one mile upstream from their confluences with the North Diversion Channel. These were modeled primarily to obtain calculated sediment inflow from these unlined channels. Cross sections for the improved portion of the Bear Arroyo were based on plans provided by AMAFCA. Cross sections in the unimproved sections of Bear Arroyo were developed from 1973 topographic maps, with 2-ft-contour intervals, which were provided by AMAFCA. Cross sections for the Domingo Baca Arroyo were developed from the same topographic maps.

The designated movable beds for the trapezoidal cross sections in the numerical model were adjusted to account for deposition. This was accomplished by adding extra points on each side slope to define the movable-bed width. The purpose of these adjustments was to obtain, as much as possible, a horizontal bed across the bottom of the channel without significant deposition on the side slopes (Figure 17). Initially, the movable-bed width was set to allow for a deposition depth of 1 ft for all cross sections. Final movable-bed width designations were determined iteratively; adjustments were based on calculated deposition from the previous iteration.

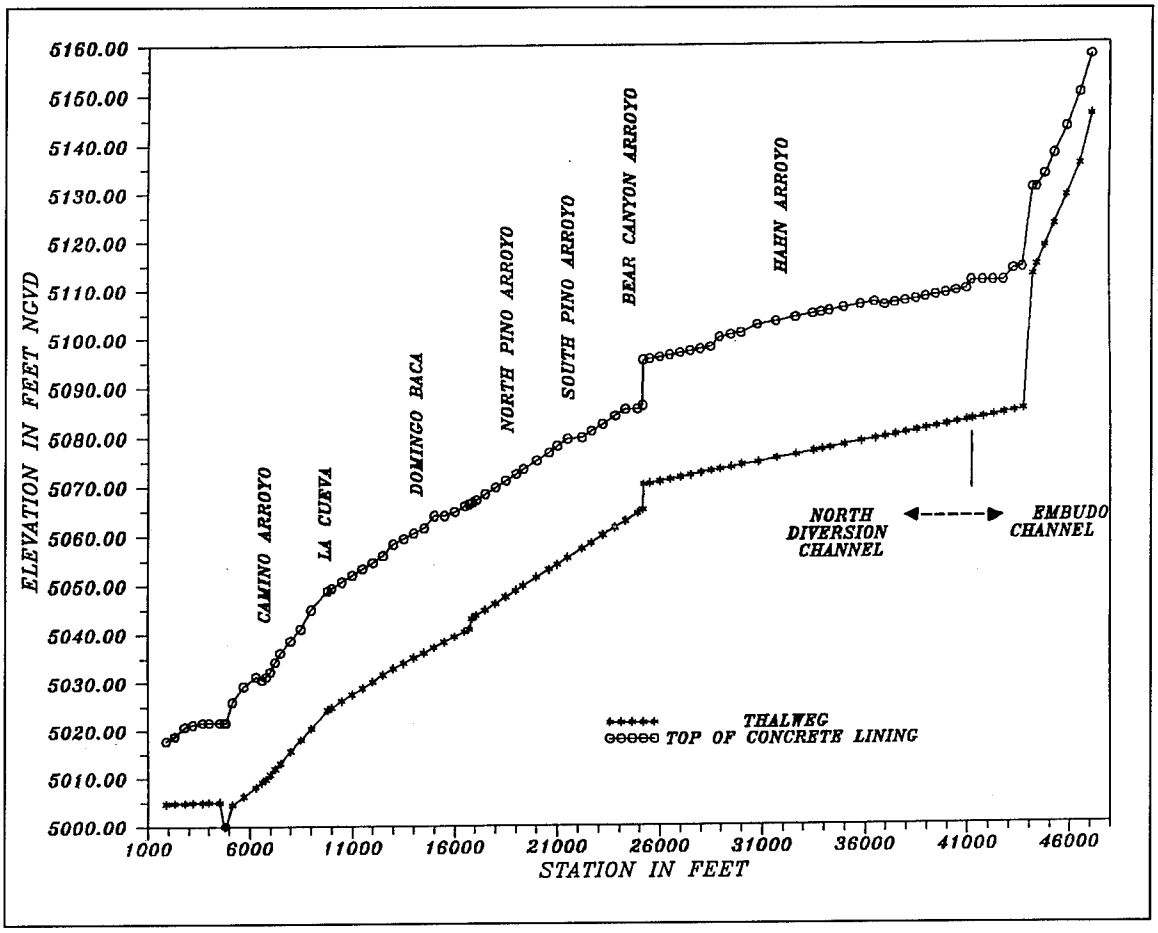

Figure 16. Channel profile for North Diversion and Embudo Channels

Hydrology

Discharge hydrographs are simulated in the numerical model by a series of steady-state events. The duration of each event is chosen such that changes in bed elevation due to deposition or scour do not significantly change the hydraulic parameters during that event. Simulating the rapidly rising 100-year-frequency flood in the North Diversion Channel required relatively short computational time-steps. Computational time-steps as short as 1 minute were used.

The 100-year-frequency flood hydrograph, used in the TABS-1 sedimentation model, was developed by the Albuquerque District (USAED Albuquerque 1992) using the HEC-1 hydrologic model. The hydrograph calculated using storm centering No. 1 (Plate 1), which produced the largest discharges in the North Diversion Channel, was used in the TABS-1 numerical model. Peak discharges used in the numerical model are listed in Table 1. Storm centering No. 4 (Plate 2), which produced the largest discharges on the Embudo watershed, was used to determine the peak discharges and runoff from the Embudo

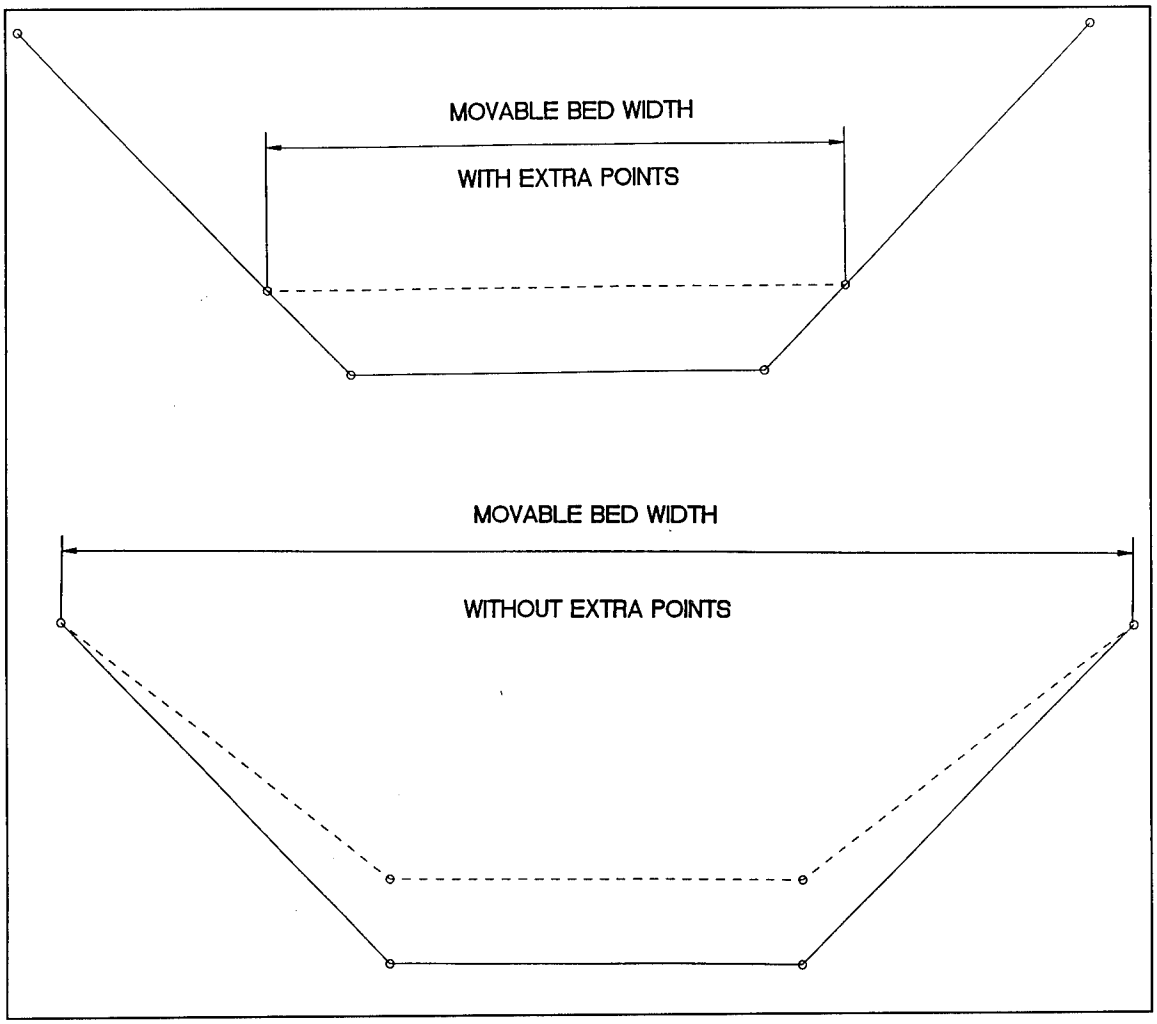

Figure 17. Movable bed widths in numerical model

tributaries. The HEC-1 model was also used by the Albuquerque District to develop a flood hydrograph for the July 1988 historical flood runoff. Peak discharges determined using the HEC-1 model with reported rainfall data produced a peak runoff in the North Diversion Channel downstream from Embudo Arroyo considerably higher than the peak discharge of 7,250 cfs reported by the USGS. After a systematic study (USAED Albuquerque 1992), it was concluded that the difference in 1988 flood peak results was most likely due to errors in the stream gage data. The HEC-1 hydrograph was used in the TABS-1 sedimentation model to calculate sediment deposition for the July 1988 storm, which was in turn compared with reported sediment removal records for the Embudo Channel. The 100-year-frequency hydrographs for storm centering No. 1 and for the July 1988 storm are shown in Plates 3 and 4, respectively.

Storm centerings No. 2 and No. 3 (Plates 5 and 6) were used to obtain maximum runoff for some tributaries to the North Diversion Channel.

Table 1
Peak Discharges, 100-Year-Frequency Flood

Location	Station	Discharge cfs
North Diversion Channel	18+90	20,700
	68+00	19,900
	97+95	19,300
	150+00	18,500
	193+50	17,800
	215+00	16,700
	249+00	15,700
	343+00	13,800
	412+50	2,400
Camino Arroyo		800
La Cueva Arroyo		1,300
Domingo Baca Arroyo		1,400
North Pino Arroyo		1,100
South Pino Arroyo		1,400
Bear Arroyo		1,200
Hahn Arroyo (includes Grantline and Vineyard Arroyos)		5,700
Embudo Arroyo		12,100

Maximum volume hydrographs were used to calculate sediment yield with the MUSLE as reported in Chapter 3 of this report and in Tables A5-A14.

The downstream water-surface elevation for the numerical model was calculated at sta 18+90 assuming normal depth. Cross-section geometry, slope, and the roughness coefficient of 0.030 for the normal depth calculation were taken from Design Memorandum No. 4 (USAED Albuquerque 1964).

Bed Material Gradations

The arroyos that feed into the North Diversion Channel are coarse-sand-and-gravel-bed streams. Twenty-seven bed samples were collected from various locations in the watershed by removing the top 1/2 in. of surface material and then collecting about a 6-in.-deep sample with a shovel. Nineteen samples were collected by engineers from the Albuquerque District

and WES in 1990 and 1992. Eight additional samples were collected by RCE as part of the geomorphic study. Bed-material gradation data are listed in Table 2; sampling locations are shown in Plate 7.

Analysis of the gradation data showed no obvious longitudinal variation in bed-material size. Any downstream tendency for streambed fining was obscured in the normal scatter of gradation data attributed to sampling technique. The arroyo beds upstream of Tramway Boulevard were just about as coarse as the arroyo beds at the confluence with the North Diversion Channel. Samples collected from reservoir fan deposits also showed no significant variation. All of the bed-material samples were used to develop an average bed-material gradation, which is shown along with an envelope of all the samples taken in Figure 18. The average bed-material gradation was used to calculate sediment-transport capacity in the unlined channels.

Sediment Inflow

The geomorphic and sediment yield studies determined that the primary sources of sediment to the Embudo and North Diversion Channels are bed and bank erosion in the unlined arroyos. Localized sources are created when developments significantly alter the natural sediment regime and induce the creation or expansion of gully erosion. The primary sediment sources are:

a. Embudo Arroyo upstream from Monte Largo.

b. North Glenwood Hills Arroyo.

c. South Glenwood Hills Arroyo Tributary.

d. Embudito Arroyo.

e. Piedra Lisa Outlet Channel.

f. Bear Canyon Arroyo at the North Diversion Channel.

g. Domingo Baca Arroyo at the North Diversion Channel.

Measured Sediment Concentrations

Regression equations were developed from the measured data for sand and fines at the USGS gage on the North Diversion Channel near Alameda. Separate regression equations were developed from the data with discharges greater than 600 cfs and combined with the regression curves for the total data set. This action is necessary to provide reasonable values when sediment concentrations are determined from extrapolation of the regression equations.

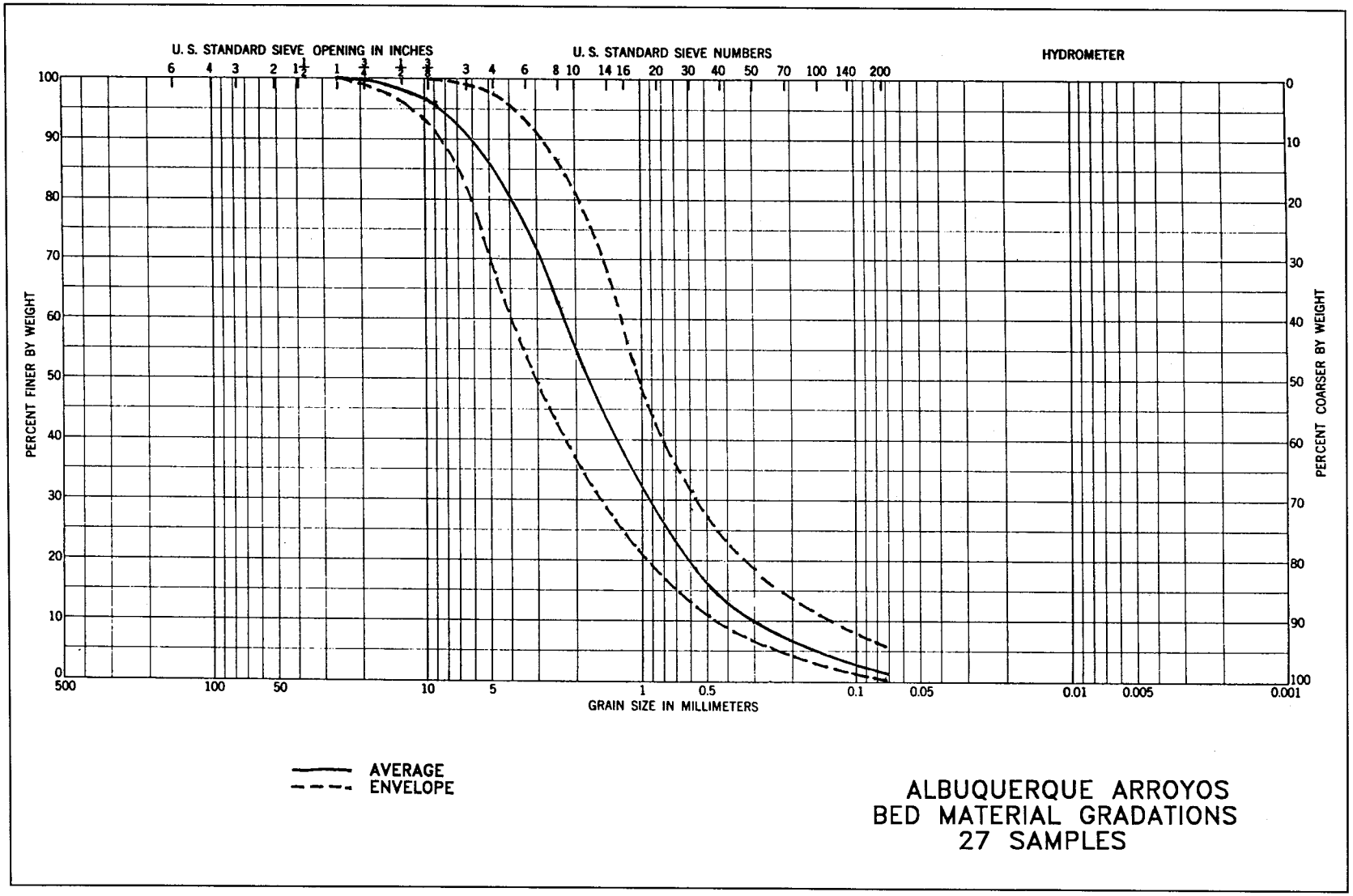

Figure 18. Average bed material gradations

Table 2
Bed Material Gradation Data from Three Sources

Sample No.	Location	Grain Size, mm		
		d_{85}	d_{50}	d_{15}
1990 WES Sediment Impact Assessment				
E1	Embudo Arroyo d/s Embudo Dam	5.0	2.0	0.37
E2	Embudo Channel at NDC	2.0	0.7	0.46
Albuquerque District and WES (1992)				
1	Embudo Arroyo d/s Embudo Dam	7.2	3.2	0.35
2	Pino Arroyo at NDC	5.3	2.3	0.50
3	Pino Arroyo u/s Tramway Blvd.(south trib.)	2.3	1.0	0.35
4	Pino Arroyo at Albuquerque Academy	4.2	1.9	0.41
5	Domingo Baco at NDC	5.3	1.5	0.27
6	Bear Arroyo d/s San Mateo Blvd.	6.0	2.0	0.47
7	NDC at Edith Blvd.	6.6	2.1	0.51
8	Pino Arroyo at Eubank Basin	4.0	1.5	0.50
9	Bear Arroyo u/s Wyoming Blvd.	4.1	1.6	0.54
10	La Cueva Arroyo u/s San Pedro Rd.	3.6	1.2	0.23
11	Pino Arroyo at Wyoming Blvd. Basin	7.3	2.1	0.40
12	Pino Arroyo u/s Tramway Blvd.(north trib)	6.2	2.2	0.61
13	Bear Arroyo at John B. Robert Reservoir	3.8	1.4	0.30
14	Bear Arroyo at NDC	4.2	1.5	0.17
17	La Cueva Arroyo d/s Eagle Rock Ave.	3.0	1.3	0.23
18	South Domingo Baca u/s Bobcat Rd.	3.8	1.8	0.58
19	Lomas Channel u/s concrete lining	2.7	1.3	0.41
Resource Consultants and Engineers (1993)				
CA1	Camino Arroyo at NDC	6.0	1.3	0.40
NLC1	La Cueva Arroyo u/s of Airport	3.7	1.2	0.21
DB1	Domingo Baca u/s of NDC	5.0	1.7	0.30
SDB1	South Domingo Baca at Holbrook St.	3.7	1.3	0.30
NGH1	N. Glenwood Hills d/s Montgomery Blvd.	5.5	2.0	0.25
HV1	u/s Hidden Valley Detention Basin	4.3	2.3	0.40

NOTE: NDC = North Diversion Channel.
u/s = upstream
d/s = downstream

(Continued)

Table 2 (Concluded)

		Grain Size, mm		
Sample No.	Location	d_{85}	d_{50}	d_{15}
PL1	Piedra Lisa Outlet Channel	4.7	2.1	0.40
EA1	Embudo Arroyo u/s Monte Largo Dr.	7.0	2.7	0.50

The adopted sediment concentration rating curve for wash-load is shown in Figure 19. This curve was used to determine the wash-load sediment inflow to the numerical model. Wash load is defined in this study to be material less than 0.25 mm in diameter, and it was assumed to be supplied from all the tributaries regardless of their stage of improvement. For tributaries with no calculated bed-material (material greater than 0.25 mm in diameter) inflow, the medium sand fraction from the measured load was included as sediment inflow.

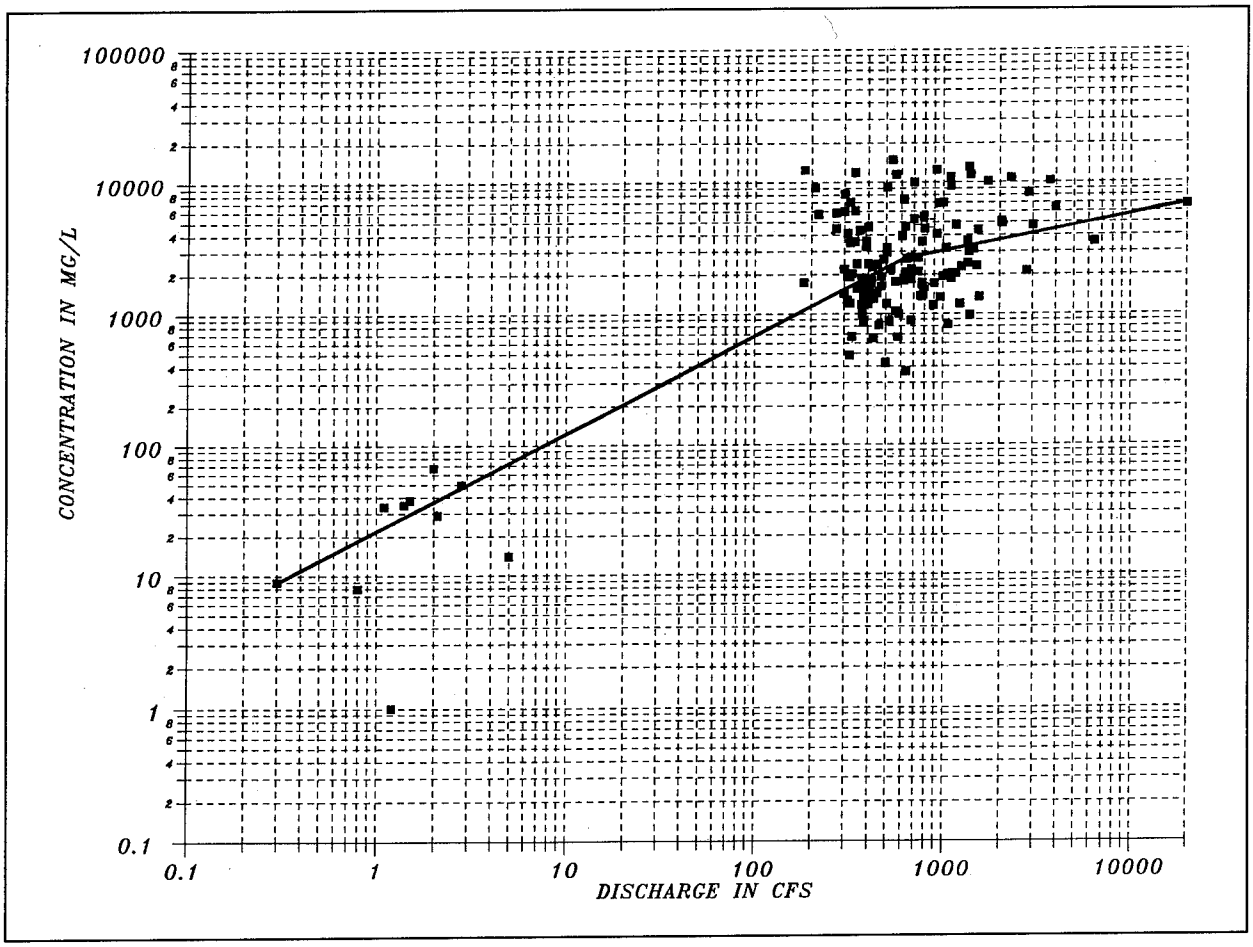

Figure 19. Measured suspended sediment rating curve in North Diversion Channel

Size class distributions for the wash load were determined from the particle size analyses of the measured suspended sediment data. A sand-silt break was established for all the samples, but a complete particle size analysis was conducted for only four samples. The average size class fractions for the four data sets are tabulated below.

Size Class	Range, mm	Fraction
Clay	< 0.004	0.22
Very-fine and fine silt	0.004 - 0.016	0.11
Medium and coarse silt	0.016 - 0.062	0.36
Very-fine sand	0.062 - 0.125	0.24
Fine sand	0.125 - 0.25	0.06
Medium sand	0.25 - 0.50	0.01

These fractions were used to determine the size class breakdown of the wash load in the numerical model.

Sediment-Transport Functions

Several sediment-transport equations are available in the TABS-1 numerical model in which transport is calculated by size class for all the sediment-transport functions. If the original equation was developed as a representative-grain-size equation, TABS-1 treats each size class separately, ignoring the hiding effect. This may lead to excessively high transport rates initially. However, the hydraulic sorting and armoring algorithm in the numerical model partially accounts for the hiding effect. The sediment-transport equations tested for the Albuquerque Arroyos sediment study were the Yang (1973,1984), Ackers-White (1973), a combination of Toffaleti (1968) and Schoklitsch (Shulits 1935), a combination of Toffaleti and Meyer-Peter and Muller (1948), Madden's 1985 modification of the Laursen equation (Madden 1993), and Copeland's modification of the Laursen equation (Copeland and Thomas 1989). The equations based on the Toffaleti and Laursen methods were specifically developed for size-class analysis.

RCE developed a new sediment-transport function to calculate sediment yield. The new equation, called the Mussetter equation herein, calculates bed load by size class using the Meyer-Peter Muller equation as modified by the U.S. Bureau of Reclamation (1960). Suspended load is calculated for the median size of the bed material only; the gradation of the suspended load is assumed to be the same as the gradation of the bed. The effect of high sediment concentration is considered by using the modifications to the Rouse (1937) equation proposed by Woo, Julien, and Richardson (1988). The thickness of the bed layer for the reference concentration is computed based on the ratio of the shear velocity to the critical shear velocity for the median particle

size as proposed by Karim and Kennedy (1983). The Mussetter equation is not available in the HEC-6 program, but calculated sediment transport using the equation was compared with that calculated using other sediment transport equations.

Available data were insufficient to establish an appropriate sediment-transport function for the Albuquerque Arroyos. Several different transport functions were tested to determine the variation in calculated transport rates that could be expected under a range of hydrologic conditions. Two were eventually chosen for use in the TABS-1 numerical model; the Laursen-Copeland function was used to represent a high sediment-loading condition, and the Yang function was used to represent a low sediment-loading condition. Rationale for choosing these equations is given in Chapter 6 of this report.

6 Numerical Model Circumstantiation

July 1988 Flood

Deposition in the Embudo Channel was calculated with TABS-1, using several sediment-transport functions and a synthetic flood hydrograph for the July 1988 flood. The hydrograph was developed using the HEC-1 hydrologic model. Observations during the July 1988 flood indicated that almost all of the sediment supplied to the Embudo Channel, at its confluence with the North Diversion Channel, came from the unlined Embudo Arroyo channel downstream from Monte Largo Drive. (Since the 1988 flood, this section of Embudo Arroyo has been concrete-lined.) In the TABS-1 simulation of the July 1988 flood, sediment inflow of bed-material sizes was assumed to come only from the unlined portion of the Embudo Arroyo downstream from Monte Largo Drive. Sediment-transport capacity was calculated for an average cross section just upstream from the 1988 concrete-lined channel. Geometry for this cross section was developed from 1:6,000-scale topographic mapping with 2-ft-contour intervals, dated 1980. The base width of the trapezoidal channel was 20 ft; the channel side slope was assumed to be 1V:2H; and the channel slope was 0.053. The Manning's roughness coefficient was assigned a value of 0.05. The average bed-material gradation shown in Figure 18 was used in the calculations. The finer sediment sizes that do not appear in significant quantities in the bed should be considered as wash load and should be excluded from sediment-transport calculations. Einstein (1950) recommended that the lowest 10 percent of the bed-material gradation be excluded when calculating bed-material load. In the Albuquerque Arroyos study only sediment sizes greater than 0.25 mm were considered as bed-material load. Further, only 50 percent of the calculated medium sand fraction was included when the Laursen-Copeland function was employed to determine sediment inflow. Sediment inflow rating curves developed for several sediment-transport functions are shown in Figure 20. The TABS-2 model did not extend to Monte Largo Drive; therefore, the calculated sediment inflow associated with the hydrograph at Monte Largo was shifted to account for the routing time to the upstream boundary of the numerical model. Sediment sizes less than 0.25 mm were assumed to be supplied according to the measured concentration data from the USGS gage near Alameda.

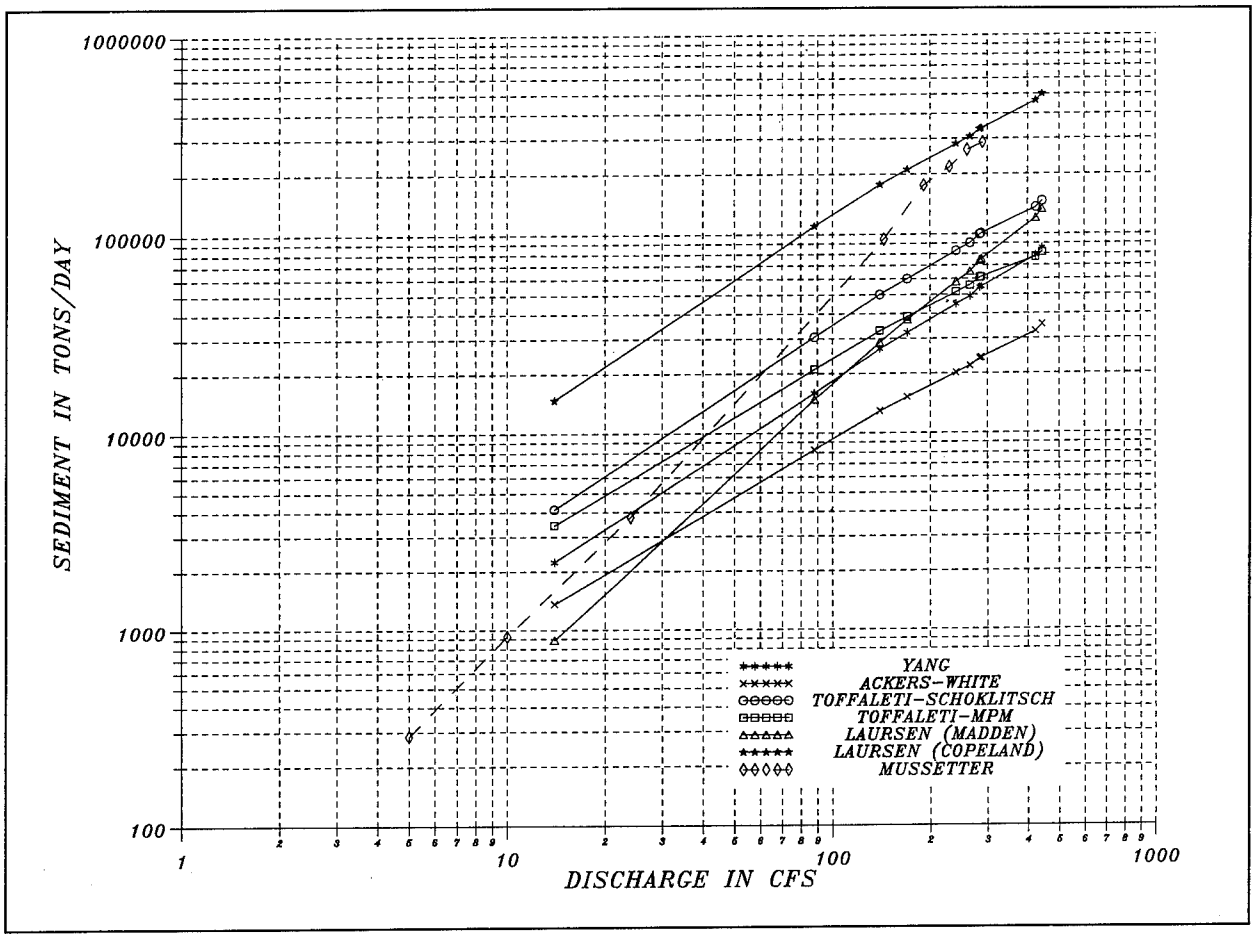

Figure 20. Sediment inflow rating curves—Embudo Arroyo

The exact quantity of deposition in the Embudo Channel between sta 412+50 and sta 437+40 during the July 1988 flood is uncertain. Channel sediment removal in the Embudo Channel had last been recorded on 2 January 1985. The next reported sediment removal, after the July 1988 flood, occurred on 31 March 1989, when 8,300 cu yd of sediment was removed. According to local sources, most of this material was deposited as a result of the July 1988 storm. However, it is uncertain if significant quantities of sediment were eroded by or deposited by subsequent flows.

Comparing reported sediment deposition with calculated deposition using six equations from TABS-1, the Laursen-Copeland, Laursen-Madden, Toffaleti-Schoklitsch, and Yang equations produced results within 50 percent of the reported quantity of 8,300 cu yd. The Laursen-Copeland equation overestimated deposition while the other equations underestimated deposition. Calculated sediment depositions in Embudo Channel between sta 412+50 and 437+40 for the July 1988 flood using these six transport equations are tabulated below.

Sediment-Transport Function	Sediment Deposition cu yd
Ackers - White	700
Laursen - Copeland	11,300
Laursen - Madden	6,600
Toffaleti - Meyer-Peter and Muller	3,800
Toffaleti - Schoklitsch	6,300
Yang	4,500

Wyoming Boulevard Basin

Calculated sediment yields into the Wyoming Boulevard Basin were compared with measured deposition. Without any measured runoff data, the measured and calculated depositions cannot be compared directly; only qualitative comparisons of results are possible. Sediment yield was calculated by integrating the 100-year-frequency hydrograph and sediment-transport rating curves using the SAM (Thomas, Copeland, Raphelt, and McComas, in preparation) computer program. In this test both storm centerings Nos. 1 and 2 were used. Storm centering No. 1 produces the largest discharges in the North Diversion Channel. Storm centering No. 2 produces the largest discharges on South Pino Arroyo at the Wyoming Basin. The hydrographs were taken from the HEC-1 hydrologic model. The sediment-transport rating curve for the Mussetter equation was taken from the RCE report. Sediment-transport rating curves for the other sediment-transport functions were based on geometry developed by RCE from 1988 topographic mapping (1 in. = 300 ft scale). Hydraulic variables were calculated using the SAM computer program with the Brownlie equations to determine bed roughness, with an assigned bank roughness coefficient of 0.08. The average bed-material gradation shown in Figure 18 was employed in the calculations; only sediment sizes greater than 0.25 mm were considered as bed-material load. Only 50 percent of the medium sand fraction was used with the Laursen-Copeland function. The sediment-transport rating curves are shown in Figure 21.

The Wyoming Boulevard Basin was completed in July 1991. Since that time two sediment surveys have been taken by Bohannan-Huston, Inc. of Albuquerque. From these surveys RCE computed approximately 3,360 tons of sediment accumulation in the basin between July 1991 and March 1992, and an additional 2,140 tons between March 1992 and March 1993. According to AMAFCA personnel[1] the watershed above Wyoming Boulevard Basins experienced unusually large storms during both periods.

[1] Cliff Anderson, personal communication with RCE, 1993.

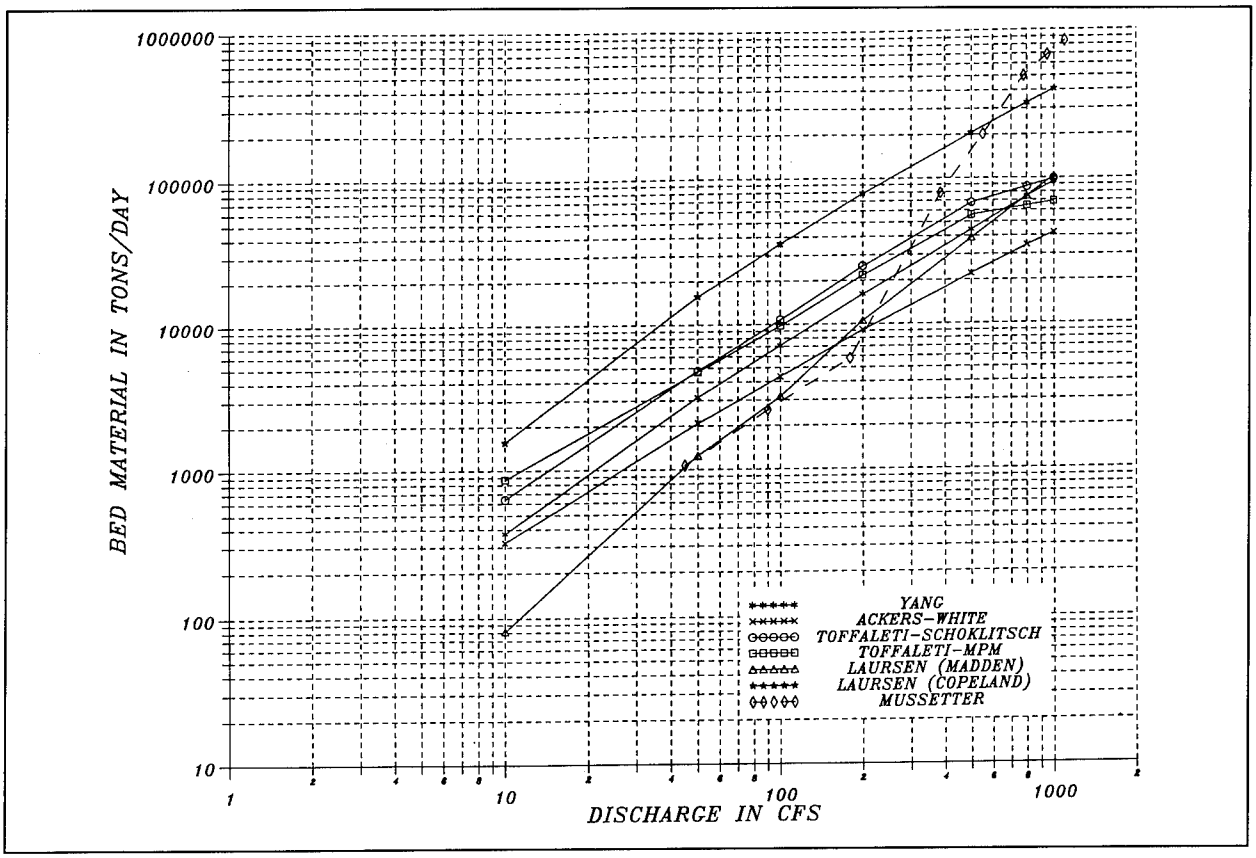

Figure 21. Sediment inflow rating curves—Pino Arroyo

The trap efficiency of the Wyoming Boulevard Basin was calculated using the Hazen method. The basin was assumed to have no sediment deposits for the calculations. Removal percentages calculated for each size class for the 100-year-flood peak discharge (storm centering No. 1) are tabulated below.

Size Class	Range, mm	Percent Removal
Clay	0.002-0.004	0
Very-fine silt	0.004-0.008	1
Fine silt	0.008-0.016	3
Medium silt	0.016-0.032	17
Coarse silt	0.032-0.062	45
Very-fine sand	0.062-0.125	82
Fine sand	0.125-0.250	96
Medium sand	0.250-0.500	99
Coarse sand	0.5-1.0	100
Very-coarse sand	1.0-2.0	100

The trap efficiency will be greater at lower discharges, but it will decrease as the basin fills. Almost all of the bed-material load that enters the basin is trapped. Bed-material load is material greater than 0.25 mm.

When one considers that nearly all of the inflowing bed-material load will be trapped in the Wyoming Boulevard Basins, the calculated yields from the 100-year-frequency flood should be considerably higher than the yields measured between July 1991 and March 1993. Results from the Laursen-Copeland equation showed the calculated sediment yield for the 100-year-frequency flood to be more than seven times greater than the average of the annual deposits when storm centering No. 1 is used and more than 13 times greater than the average of the annual deposits when storm centering No. 2 is used. Sediment yields calculated using the Toffaleti combinations were more than two or three times the average of the annual deposits with storm centerings No. 1 and 2, respectively. For storm centering No. 1, flood yields calculated using the Mussetter and Yang equations were less than two times the average of the annual deposits. For storm centering No. 2, sediment yields calculated using the Yang equation were greater than two times the average of the annual deposits, and about six times the average when the Mussetter equation was used. The 100-year-frequency-flood sediment yields calculated using the Laursen-Madden and Ackers-White equations for both storm centerings were about the same as those reported between July 1991 and March 1992. These two equations can be eliminated from consideration for this application. The Toffaleti-Meyer-Peter and Muller equation was eliminated from consideration because it underestimated deposition in Embudo Channel during the July 1988 flood simulation. Results are tabulated below.

Sediment-Transport Function	Calculated Sediment Yield at Wyoming Boulevard Basin, 100-year-Frequency Hydrograph, tons	
	Storm Centering No. 2	Storm Centering No. 1
Ackers - White	4,340	3,210
Laursen - Copeland	36,710	19,550
Laursen - Madden	4,680	2,080
Mussetter	16,370	4,570
Toffaleti - Meyer-Peter and Muller	9,500	6,300
Toffaleti - Schoklitsch	10,780	6,090
Yang	7.580	4,014

Sediment-Transport Function Evaluation

Data are insufficient to adjust the numerical model or to determine the appropriate sediment inflow. Different sediment transport equations predict different sediment loads and different deposition quantities. Circumstantiation

tests conducted using data from the July 1988 flood in Embudo Channel and in the Wyoming Boulevard Basin indicate that reasonable results can be obtained from the Laursen-Copeland, Toffaleti-Schoklitsch, and Yang equations. The Mussetter equation is not available in the TABS-1 program and therefore was eliminated from consideration in this study. The Laursen-Copeland function gave higher results in both tests and the Yang equation gave lower results. These two equations were used to evaluate the 100-year-frequency flood.

Sediment inflow rating curves used for the numerical model are shown in Plates 8 through 18. Separate rating curves were developed for the rising and falling limbs on Embudo Arroyo. This was necessary because the numerical model boundary did not extend to the end of the lined channels in the Embudo system and sediment routing had to be accomplished external to the model. This was done using output from the HEC-1 hydrology model by routing sediment transport quantities with the flow from sediment-contributing tributaries to the upstream boundary of the numerical model.

7 Numerical Model Results

The TABS-1 numerical model was used to evaluate deposition and its effect on channel roughness in the North Diversion and Embudo Channels. Sediment inflow was composed of wash load and bed-material load. Wash load was based on measured sediment concentrations at the USGS gage in the North Diversion Channel at Alameda. Sediment inflow of bed-material load was calculated assuming equilibrium conditions at the upstream boundaries. Bed-material inflow was calculated for Embudo, Bear Canyon, and Domingo Baca Arroyos.

Due to the lack of calibration data, sediment inflow and deposition quantities cannot be predicted with certainty. Sensitivity studies were conducted using a reasonable range of sediment loadings. Sediment loadings were determined by calculating sediment-transport capacity in the unlined channels just upstream from the end of concrete-lined sections. These calculations were made assuming normal depth and equilibrium sediment-transport potential in a representative cross section. High sediment loading was calculated using the Laursen-Copeland sediment-transport function, and low sediment loading was calculated using the Yang sediment transport function. In most cases, sediment yields calculated using the Laursen-Copeland function were similar to sediment yields calculated in the geomorphic study using the Mussetter equation.

Sediment Deposition

Sediment deposition rates in the North Diversion and Embudo Channels are significantly greater during the recession of the flood hydrograph. The HEC-1 model indicated that the flood flows, which preceded the peak discharge, occur primarily from local urban runoff. High sediment loads from the upstream unlined arroyos begin to reach the confluence of the Embudo and North Diversion Channels coincidental with the peak flow. High sediment loads continue through the recession of the flood hydrograph.

Results were similar for both loading conditions in the North Diversion Channel downstream from its confluence with Embudo Channel. At the peak flow, with both a high and low sediment loading, less than 0.5 ft of sediment

had deposited in the North Diversion Channel between the Embudo confluence and sta 252+00. About 1 ft of sediment had deposited in a short reach just downstream from the Domingo Baca confluence at sta 150+00. Sediment deposition should be considered when calculating a roughness coefficient for these reaches of the channel, but it is not necessary to modify channel geometry for the hydraulic capacity calculations.

Sediment deposition depths in the Embudo Channel were greater than in the North Diversion Channel, and the quantity of sediment deposition depended on the prescribed sediment loading. The results from the high sediment loading are recommended for design calculations. Most of the deposition occurred during the recession of the flood hydrograph, but enough deposition had taken place by the time the peak flow occurred to require modification of cross-section shape for the hydraulic capacity calculations. Deposition depths calculated using the TABS-1 numerical model, with the maximum loading condition, at the peak of the 100-year-frequency flood, are shown in Table 3. It is recommended that these data be used to develop a smooth deposition profile line to modify cross-section shape for the hydraulic capacity calculations.

Sediment deposition increased during the recession of the flood hydrograph. Calculated deposition depths at the end of the flood are shown in Table 4 for both the high and low sediment loadings. Calculated deposition quantities in the North Diversion and Embudo Channels for the 100-year-frequency flood were 49,000 cu yd for the high loading condition and 23,000 cu yd for the low loading condition. Calculated deposition quantities in the North Diversion Channel Outlet were 67,000 cu yd and 34,000 cu yd for the high and low loading conditions, respectively. These deposits reduce channel capacity in two ways: by reducing the cross-sectional flow area, and by increasing the boundary roughness. The variation of stage and bed elevation during the 100-year-frequency flood at sta 437+40 in the Embudo Channel is shown in Figure 22. These variations at other stations in the Embudo and North Diversion Channels are shown in Plates 19-23.

Design Roughness Coefficients

Manning's roughness coefficients in the numerical model were determined in a progressive fashion, by considering the increasing effect of boundary roughness with increasing deposition in the concrete-lined channel during the course of the 100-year-frequency flood. The model was run several times, increasing roughness coefficients as sediment deposition increased. This makes the roughness coefficients in the model unique to the particular hydrograph and sediment loading used in the study. The effect of deposition on channel roughness was most significant in the Embudo Channel due to the greater quantity of deposition and because the deposited material was coarser than the material deposited in the North Diversion Channel. Calculated bed-material gradation at the upstream end of the deposition zone in the Embudo

Table 3
Deposition in Embudo and North Diversion Channels At Peak of 100-Year-Frequency Flood, High Sediment Loading

Station	Discharge cfs	Deposition ft
Embudo Channel		
437+40	12,100	3.7
432+95		2.5
428+00		2.0
423+00		1.5
418+00		1.0
North Diversion Channel Downstream from Embudo		
412+50	13,800	0.8
410+00		0.5
405+00		0.4
400+00		0.3
395+00		0.2
390+00		0.2
385+29		0.2
380+00		0.2
375+00		0.2
370+00		0.2
365+00		0.1
358+13		0.1
350+00		0.1
343+00		0.0
North Diversion Channel Downstream from Domingo Baca		
155+00	19,300	0.0
150+00		0.1
145+00		0.1
140+00		1.0
135+00		0.1
130+00		0.0

Table 4
Deposition in Embudo and North Diversion Channels At End of 100-Year-Frequency Flood

Station	Deposition, ft, Above Invert	
	High Loading	Low Loading
Embudo Channel		
437+40	20.2	6.3
432+95	14.1	4.3
428+00	11.4	3.6
423+00	10.0	2.8
418+00	7.4	2.0
North Diversion Channel		
412+50	6.8	1.8
410+00	6.0	1.4
405+00	4.8	1.0
400+00	3.9	0.6
395+00	3.2	0.3
390+00	2.6	0.2
385+29	2.4	0.1
380+00	1.8	0.1
375+00	1.5	0.1
370+00	1.2	0.1
365+00	1.0	0.1
358+13	0.7	0.0
350+00	0.6	0.1
343+00	0.5	0.2
339+00	0.0	0.0

Channel, for the 100-year-frequency peak, is compared with the calculated bed-material gradation at sta 412+50 in the North Diversion Channel in Figure 23. The coarseness of the calculated bed-material gradation decreased longitudinally down the channel, and the calculated gradations at a given point became coarser with the progression of the hydrograph. A bed-material sample obtained from the Embudo Channel after the July 1988 flood is shown in Figure 23.

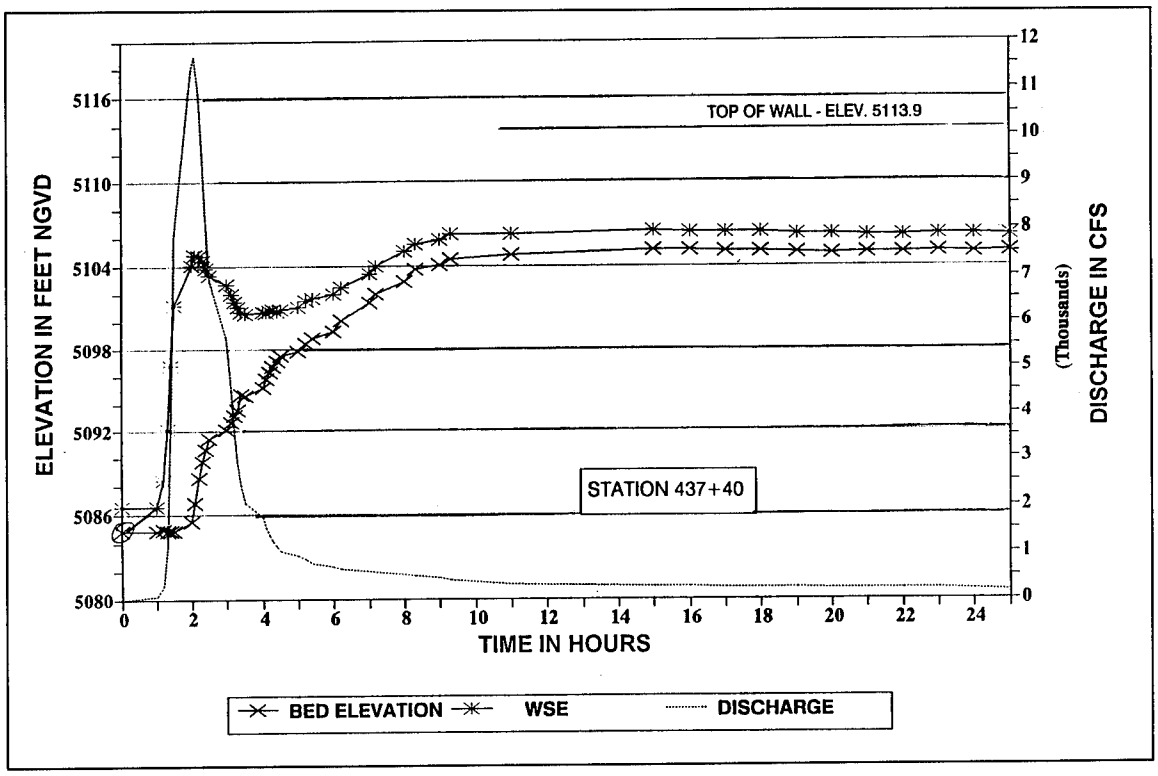

Figure 22. Variation of stage and bed elevation during 100-year-frequency flood at sta 437+40

The Manning's roughness coefficient was calculated external to the TABS-1 numerical model by compositing the roughness of the concrete side slopes with the bottom deposits of sand. The Einstein-Horton compositing equation was used:

$$\overline{n} = \frac{\left[\sum_{i=1}^{3} P_i\, n_i\right]^{\frac{2}{3}}}{\left[\sum_{i=1}^{3} P_i\right]^{\frac{2}{3}}} \qquad (14)$$

where

$\overline{n}$ = composite roughness coefficient for the cross section

P = wetted perimeter

Subscripts 1 and 3 = associate variables with the side slopes

Subscript 2 = channel bottom

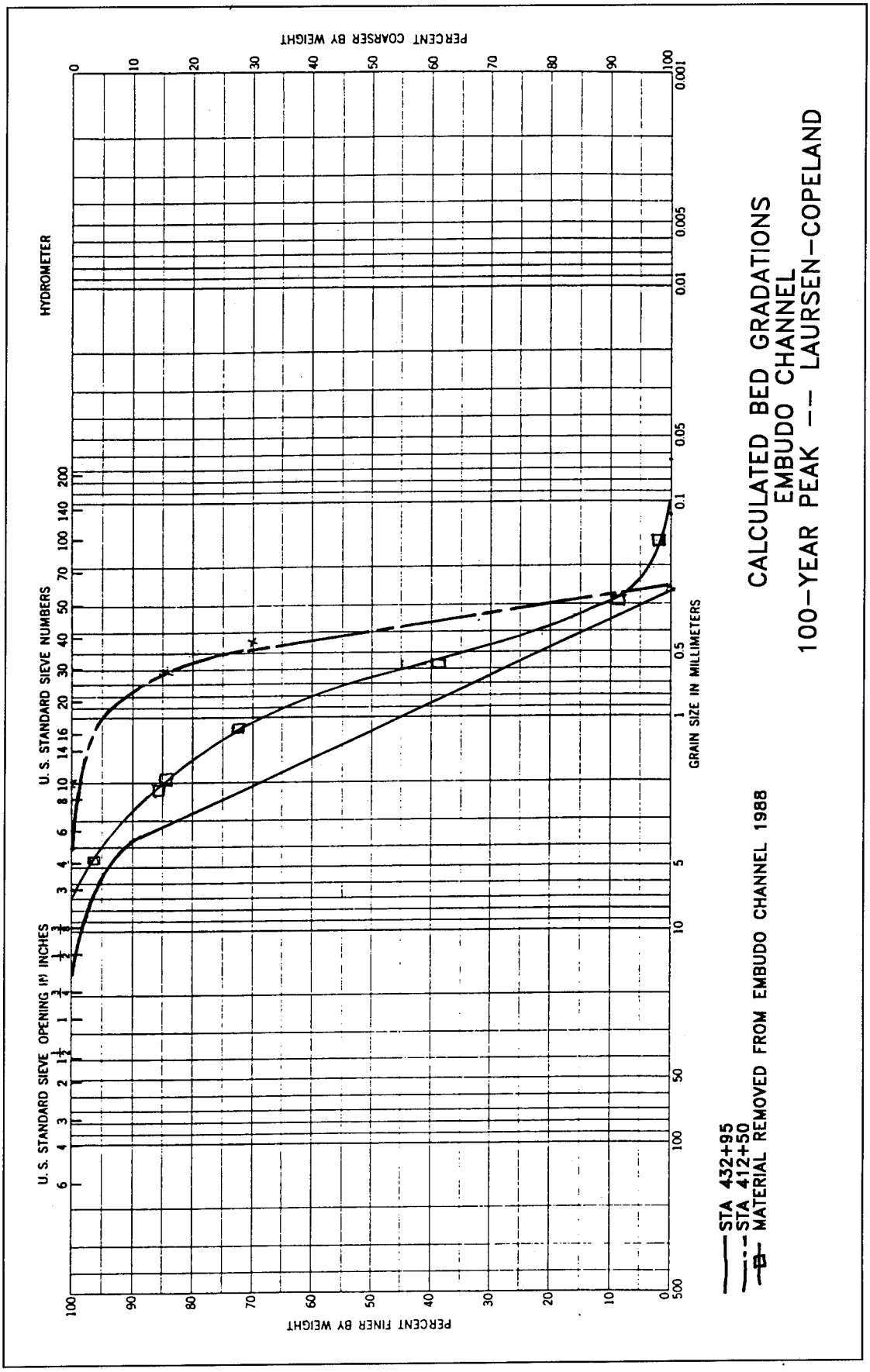

Figure 23. Calculated bed material gradations

Roughness for concrete was calculated using resistance equations based on the Keulegan and Colebrook-White equations as recommended in EM 1110-2-1601 (USAEHQ 1991). The equations have been modified here to calculate Manning's roughness coefficient directly:

$$n = \frac{-1.486\ R^{\frac{1}{6}}}{32.6\ \log_{10}(A+B)}$$

$$A = \frac{1.048\ R^{\frac{1}{6}}}{n\ \mathbb{R}\ 10^{0.1739 A_r}} \qquad (15)$$

$$B = \frac{k_s}{R\ 10^{0.1739 A_r}}$$

$$\mathbb{R} = \frac{4RV}{\nu}$$

where

R = hydraulic radius, ft

V = average channel velocity, fps

ν = kinematic viscosity, fps

k_s = roughness height, ft

A_s = Iwagaki's coefficient for smooth flow

A_r = Iwagaki's coefficient for rough flow

Iwagaki's coefficients vary with Froude Number (Chow 1959). A roughness height of 0.007 ft was assigned for calculating maximum water-surface elevations, as recommended in EM 1110-2-1601.

When sediment deposits completely covered the concrete bottom, bed roughness was calculated using the Brownlie resistance equations.

For lower regime flow:

$$n = \left[1.6940 \left(\frac{R}{d_{50}} \right)^{0.1374} S^{0.1112} \sigma_g^{0.1605} \right] 0.034 d_{50}^{0.167} \quad (16)$$

For upper regime flow:

$$n = \left[1.0213 \left(\frac{R}{d_{50}} \right)^{0.0662} S^{0.0395} \sigma_g^{0.1282} \right] 0.034 d_{50}^{0.167} \quad (17)$$

where

R = hydraulic radius, ft

d_{50} = median grain size, ft

S = energy slope

σ_g = geometric standard deviation of the bed sediment

These equations, which account for both grain and form roughnesses, were developed for alluvial channels.

The sediment bed gradation used in the Brownlie equation was calculated with the TABS-1 model. The calculated bed gradation varied longitudinally in the channel, with the coarser gradations at the upstream end of the Embudo Channel. Bed gradations were finer in the North Diversion Channel, resulting in lower calculated roughness coefficients. The bottom width of the channel increases with deposition in the Embudo Channel. This results in an additional increase in roughness due to the increased fraction of the wetted perimeter composed of sediment. The calculated variations of Manning's roughness coefficient with discharge for the maximum sediment loading condition for three reaches of the North Diversion Channel and the Embudo Channel are shown in Figures 24-27. Roughness may decrease with discharge, in channel sections with sediment deposition, because as depth increases with discharge, a lessor percentage of the channel wetted perimeter is covered by sediment in the trapezoidal channel. In order to demonstrate the influence of

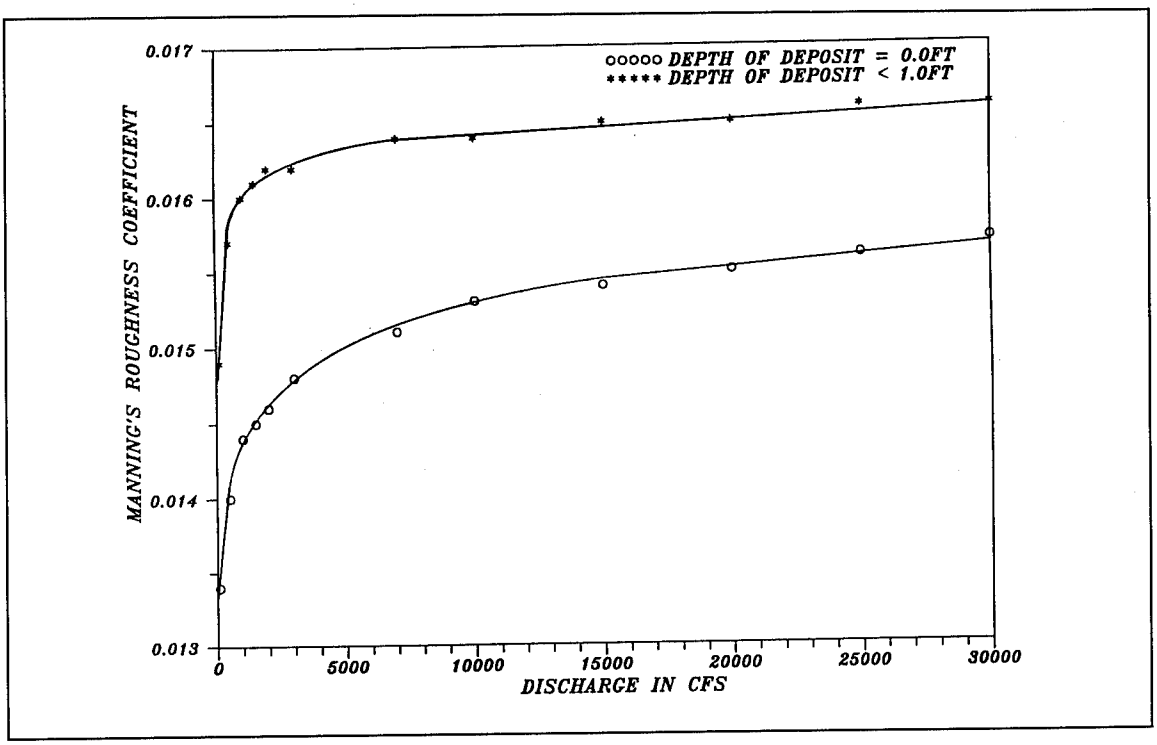

Figure 24. Variation of Manning's n with depth of sediment deposit, North Diversion Channel, sta 73+00—97+94

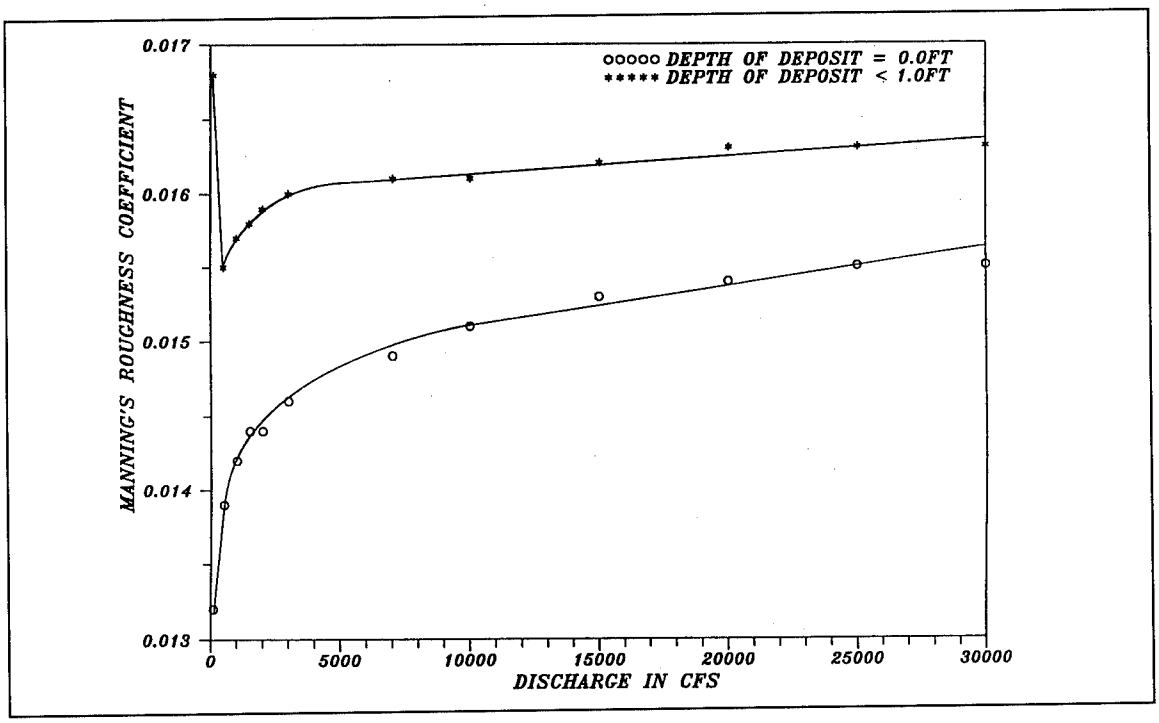

Figure 25. Variation of Manning's n with depth of sediment deposit, North Diversion Channel, sta 97+94—252+00

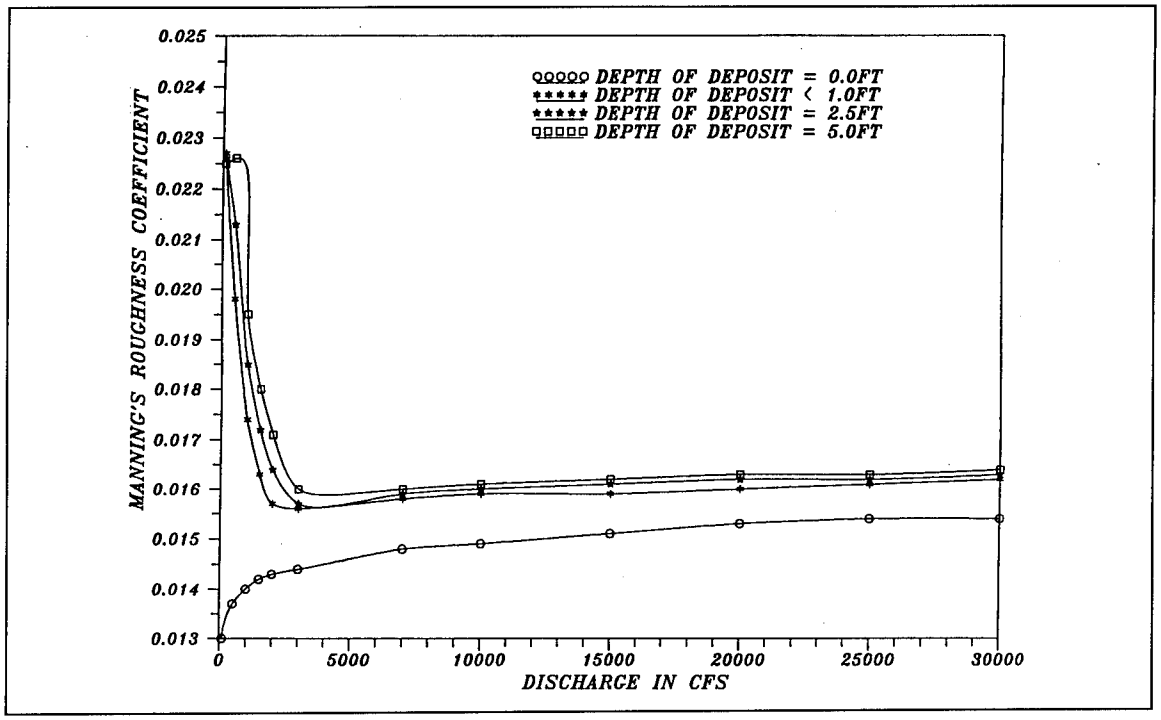

Figure 26. Variation of Manning's n with depth of sediment deposit, North Diversion Channel, sta 252+00—412+50

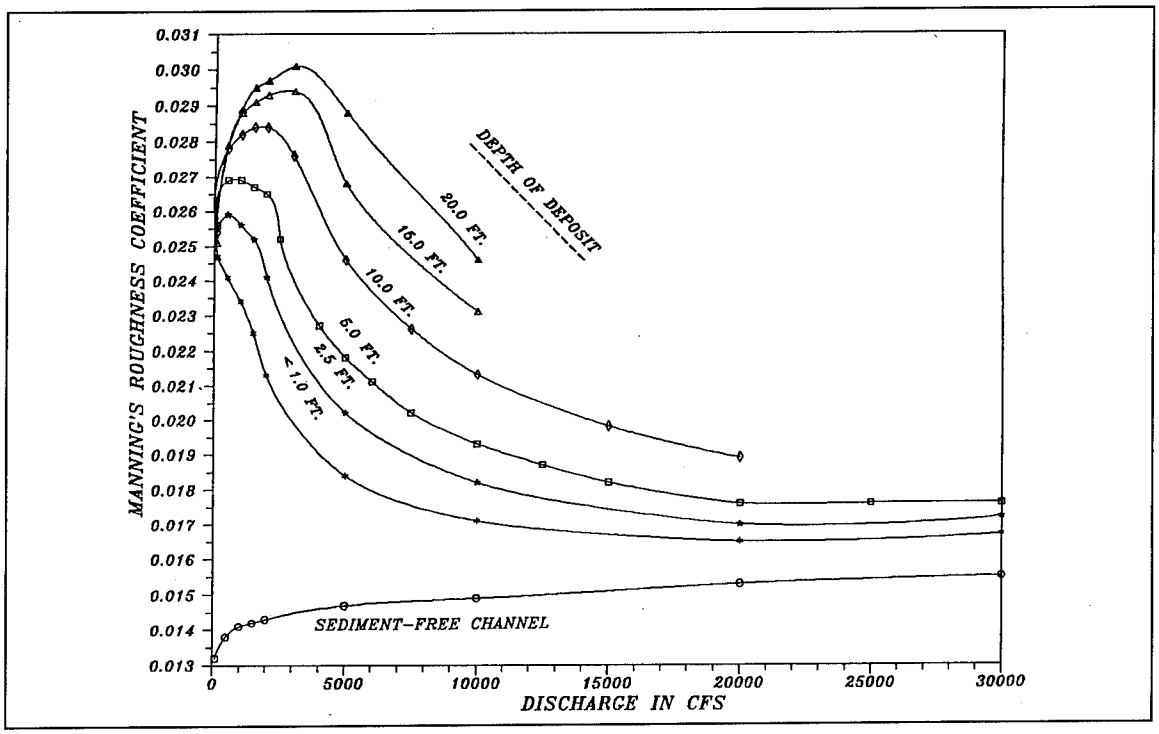

Figure 27. Variation of Manning's n with depth of sediment deposit, Embudo Channel, sta 412+50—437+40

Table 5
Recommended Design Roughness Coefficients, Maximum Water-Surface Elevations

Station ft	Discharge cfs	Manning Roughness Coefficient
North Diversion Channel		
51+50-97+94	19,300-20,700	0.017
97+94-252+00	15,900 - 19,300	0.017
252+00-412+50	13,800-15,900	0.017
Embudo Channel		
412+50-437+40	12,100	0.019

deposited sediment on the roughness coefficient, a roughness coefficient for a sediment-free channel is also shown in the figures.

Recommended design roughness coefficients for calculating maximum water-surface elevations for the 100-year peak discharge, listed in Table 5, vary between 0.017 for the North Diversion Channel and 0.019 for Embudo Channel. Recommended design values were rounded up from the calculated values shown in the figures. Increased roughness due to curvature of the channel was not considered in the above calculations. The roughness coefficient in Embudo Channel would increase with increased deposition and with falling discharge.

A lower design roughness coefficient was calculated to determine maximum velocities. The channel was considered to be sediment free for maximum velocity conditions, and a k_s of 0.0002 ft was selected for the roughness height. This k_s value is considerably lower than recommended in EM 1110-2-1601 for maximum velocity calculations. However, recent prototype data collected by the Los Angeles District (Stonestreet, Mulvihill, and Copeland 1993) suggest that this lower value is possible in concrete-lined channels, such as the North Diversion Channel. Data from the North Diversion Channel at Alameda USGS gage also support this lower k_s value. The recommended design roughness coefficient for maximum velocity is 0.011.

Effect of Additional Sediment Inflow at Camino Arroyo

Currently (1993), gravel mining operations have left a very large depression upstream from the Camino Arroyo Inlet. The depression will effectively trap any sand or larger sediment before it reaches the North Diversion Channel. Therefore, the numerical model did not include any medium sand or greater inflow at Camino Arroyo Inlet.

It is possible that future development could result in concrete channels through the existing depression that are capable of delivering sediment to the North Diversion Channel. This scenario was tested with the numerical model. Camino Arroyo has two branches upstream from Interstate Highway 25. Channel geometry was estimated from ortho-topo maps for both of these channels, and sediment transport capacity was calculated using both the Yang and Laursen-Copeland sediment-transport functions. The calculated transport rates were combined to establish a rating curve for the Camino inlet. The numerical model was then run to assess the effect of the increased sediment loading during the 100-year-frequency flood.

Calculated results indicated an insignificant change in water-surface elevation at the peak, but there was increased deposition in the North Diversion Channel at the end of the flood. Differences in calculated water-surface elevations were less that 0.1 ft for simulations using both transport functions. There was no sediment deposition in the vicinity of the Camino Inlet during the peak. Most of the sand load that entered the channel from Camino Arroyo deposited downstream in the North Diversion Channel or in the outlet. However, at the end of the 100-year-frequency flood, there was an increase in deposition for about 1,000 ft upstream from the Camino Inlet. The total increase in deposition at the end of the flood was about 10,600 cu yd using the Laursen-Copeland function and about 5,000 cu yd using the Yang function. The maximum increase in bed elevation occurred using the Laursen-Copeland function; 600 ft upstream from the inlet, an increase in deposition of 1.2 ft was calculated. Construction of a sediment trap or debris basin at the inlet to the concrete channel would reduce or eliminate the increased deposition in the North Diversion Channel. An economic study comparing maintenance costs related to increased deposition in the North Diversion Channel and in a sediment trap would determine which is more practical.

8 Conclusions and Recommendations

Conclusions

A geomorphic analysis was conducted to assess the stability of the arroyos that drain into the North Diversion Channel and to determine the primary sources of sediment. The arroyos located on the alluvial mesa are naturally unstable in that they fluctuate between episodes of aggradation and incision. Sediment transport through the system depends to a great extent on antecedent local topography and the duration and magnitude of flood events. Urbanization of the watershed has resulted in greater runoff and greater concentration of flows, and these factors tend to increase erosion potential. However, flood-control measures that include detention dams, concrete-lined channels, channel stabilization, and sediment traps have compensated for the hydrologic effects and the overall trend is reduced erosion from the urbanized area. As, a result, the primary sources of sediment to the North Diversion Channel are bed and bank erosion in the unlined arroyos.

Sediment yield was calculated for each watershed that drained into the North Diversion Channel. Estimates of both wash load and bed-material load were calculated. Yields were compared with detention reservoir capacity. There is no generally accepted method for calculating sediment yield, so several methods were used to calculate yield and compared with limited measured data.

Limited measured data from natural arroyos in the Albuquerque Arroyo drainage area, and in similar areas, indicated suspended sediment concentrations as high as 300,000 mg/l, with average concentrations on the order of 47,000 mg/l. Limited data indicated that between 12 and 21 percent of this suspended load was sand or larger sized sediment. Due to the effects of urbanization, measured suspended sediment concentrations in the North Diversion Channel itself were considerably lower, ranging between 300 and 15,000 mg/l; about 30 percent of the measured suspended load was sand or larger sized sediment. The measured data must be considered approximate due to sampling difficulties in flashy arroyos, the uncertainty associated with the

equipment used, the lack of bed-load measurements, and the lack of an adequate range of sampled discharges.

Reservoir surveys and deposition in the North Diversion Channel were used to determine an estimate of average-annual sediment yield. Two detention reservoirs in the vicinity of Albuquerque had measured sediment yields of 0.16 and 0.28 acre-ft/square mile/year over 30- and 12-year monitoring periods, respectively. Based on haul records, sediment is deposited in the North Diversion Channel at the rate of 0.20 acre-ft/square mile/year. These rates compare with a calculated sediment yield of 0.58 acre-ft/square mile/year using measured suspended sediment records on the natural arroyos.

The haul record data indicate a general decline in annual sediment deposition in the North Diversion Channel. This is attributed to the construction of detention dams and lined channels in the Albuquerque Arroyos study area.

Calculated sediment yields using methods in which surface erosion is the primary source produced generally low sediment yields. Using the SCS soil erosion rates, an average-annual sediment yield of 0.23 acre-ft/square mile/year was calculated. Sediment yields calculated using MUSLE averaged about 0.11 acre-ft/square mile/year. Rainfall simulator experiments on the natural watershed produced runoff with concentrations less than 1,000 mg/l.

Sediment yield calculated assuming equilibrium sediment-transport capacity in the arroyos produced results more in line with measured data. Bed-material load was calculated using a sediment-transport equation and combined with wash-load concentrations determined using MUSLE. Average annual yields at the canyon mouths were high, ranging between 1.02 and 0.88 acre-ft/square mile/year. Downstream near the confluence with the North Diversion Channel, sediment yields ranged between 0.53 and 0.03 acre-ft/square mile/year; the drainage areas with the fewest flood control improvements had the greatest yields.

Sediment yields from mountainous drainage areas for the 100-year-frequency storm were calculated using the Tatum and Los Angeles District methods. Concentrations were high using these methods, but existing detention structures had sufficient capacity to contain the sediment loads.

Trap efficiencies for the detention structures and sediment traps were estimated. These results were used to determine inflow into the North Diversion Channel. The detention structures had calculated trap efficiencies between 88 and 96 percent. In the larger reservoirs, almost all of the sediment larger than 0.0625 mm is trapped. The sediment traps effectively remove between 62 and 74 percent of the sediment larger than 0.0625 and almost all of the sediment larger than 0.50 mm.

Deposition and scour in the North Diversion and Embudo Channels were modeled with a numerical sedimentation model. The effect of deposited sediment on conveyance and roughness was determined. The model was

circumstantiated using data from the July 1988 storm where 8,300 cu yd of sediment deposition was reported in the Embudo Channel. Sediment inflow into the model was calculated by means of two sediment-transport equations, one of which produced calculated sediment deposition about 45 percent lower than the reported, and another which produced calculated sediment deposition about 35 percent higher than the reported deposition. These amounts were employed in the numerical model to provide high and low estimates of 100-year-frequency flood deposition. This type of sensitivity analysis is necessary due to the high degree of uncertainty associated with the sediment data.

Sediment deposition can be expected in the North Diversion and Embudo Channels during the 100-year-frequency storm. The high sediment load assumption is recommended for design purposes. At the flood peak, less than a foot of deposition would occur in the North Diversion Channel for a distance of about 7,000 feet downstream from the Embudo confluence. Deposition in the Embudo Channel at the peak would range from 1.0 ft at the North Diversion Channel confluence to 3.7 ft at the supercritical chute, located 1,900 ft upstream. Less than a foot of deposition in the North Diversion Channel downstream from Domingo Baca was calculated at the peak of the 100-year-frequency flood. At the end of the 100-year-frequency flood, deposition in Embudo Channel ranged between 7.4 and 20.2 ft. In the North Diversion Channel, deposition ranged between 6.8 ft at the Embudo Confluence and 0.5 ft, 7,000 ft downstream.

Because of the limited deposition in the North Diversion Channel at the flood peak no adjustment to the conveyance is required to compute 100-year-frequency water-surface profiles. However, in the Embudo Channel, cross-section geometry should be adjusted for water-surface calculations.

Roughness coefficients at the peak of the flood were calculated analytically external to the numerical model using compositing techniques. At the peak of the flood, recommended Manning's roughness coefficients ranged between 0.017 and 0.019 when the depth of deposition in the channel was less than 1 ft. Roughness coefficients increase with deposition, up to 0.030. These high roughness values are attributed to bed forms. There is a decline in these high roughness coefficients with increasing discharge because the percentage of channel wetted perimeter covered by sediment decreases with water depth in the trapezoidal channel.

Recommendations

The following recommendations are made for a data collection program that would be useful for future sedimentation studies.

a. Install a continuous recorder stream gage upstream from the Wyoming Street Basin on South Pino Arroyo. Monitor deposition in the basin following major runoff events. This survey should include sediment density and size class determinations. Data from such a data collection

effort would be especially useful in determining an appropriate sediment-transport equation for arroyos in Albuquerque.

b. Conduct periodic reservoir surveys in order to monitor storage capacity and to determine sediment yield. The survey data should include sediment density determinations.

c. Survey and monitor the sediment traps after storm events to assess the need for removal and to aid in assessing their trap efficiencies. Bed-material gradations should be determined.

d. A cooperative program with the USGS to collect suspended sediment data at the North Diversion Channel gaging station would be useful. Correlations with the pumping sampler samples and samples collected using a standard US P-61 sampler would prove useful.

e. Hydrologic studies should be conducted to determine the effect of reduced storage due to sediments for design or analysis of the arroyos downstream from detention dams.

References

Ackers, P., and White, R. W. (1973). "Sediment transport: new approach and analysis," *Journal, Hydraulics Division,* American Society of Civil Engineers, 99 (HY11), 2041-60.

Andrews, E. D. (1980). "Effective and bankfull discharges of streams in the Yampa River Basin, Colorado and Wyoming," *Journal of Hydrology* 46, 311-30.

Benson, M. A., and Thomas, D. M. (1966). "A definition of dominant discharge," *Bulletin, International Association of Science and Hydrology*, XI, 76-80.

Brown, C. B. (1950). "Sedimentation." *Engineering Hydraulics*. Hunter Rouse, ed., Proceedings, Fourth Hydraulics Conference, Iowa Institute of Hydraulic Research, Iowa City, IA.

Brownlie, William R. (1983). "Flow depth in sand-bed channels," *Journal of Hydraulic Engineering,* American Society of Civil Engineers, 109(7), 959-90.

Brune, Gunnar M. (1953). "Trap efficiency of reservoirs." *Transactions,* American Geophysical Union. 34(3).

Chow, Ven T. (1959). *Open channel hydraulics*. McGraw Hill, New York.

Churchill, M. A. (1948). Discussion of "Analysis and use of reservoir sedimentation data," by L.C. Gottschalk, pp 139-40, *Proceedings, Federal Inter-Agency Sedimentation Conference,* Denver, CO, 139-40.

Copeland, R. R., and Thomas, W. A. (1989). "Corte Madera Creek sedimentation study; Numerical model investigation," Technical Report HL-89-6, U.S. Army Engineer Waterways Experiment Station, Vicksburg, MS.

Dendy, F. E. (1974). "Sediment trap efficiency of small reservoirs." *Transactions*, American Society of Agricultural Engineers, 17(5), 898-901.

Einstein, Hans A. (1950). "The bed-load function for sediment transportation in open channel flows," Technical Bulletin No. 1026, U.S. Department of Agriculture, Soil Conservation Service, Washington D.C.

Fair, Gordon M., Geyer, John C., and Okum, Daniel A. (1968). "Water and wastewater engineering." *Volume 2, Water purification and wastewater treatment and disposal.* John Wiley and Sons, New York, 25-1 through 25-16.

Funderburg, D. E. (1977). "Trap-efficiency investigation Bernalillo floodwater retarding reservoir No. 1 (Piedra Lisa Arroyo) near Bernalillo, New Mexico, water years 1956-1974," Open-File Report 77-261, U.S. Geological Survey, Albuquerque, NM.

Funderburg, D. E., and Roybal, F. E. (1977). "Sediment-trap efficiency of Tortugas Arroyo near Las Cruces, New Mexico, water years 1963-1974," Open-File Report 77-586, U.S. Geological Survey, Albuquerque, NM.

Hazen, Allen. (1904). "On sedimentation." *Transactions*, American Society of Civil Engineers, 53(63).

Karim, F., and Kennedy, J. F. (1983). "Missouri River computer-based predictors for sediment discharges and friction factors of alluvial streams," Iowa Institute of Hydraulic Research Report No. 242, University of Iowa, Iowa City, IA.

Laursen, Emmett M. (1958). "Total sediment load of streams," *Journal, Hydraulics Division,* American Society of Civil Engineers, 84(HY1), 1530-1 to 1530-36.

Madden, Edward B. (1993). "Modified Laursen method for estimating bed-material sediment load," Contract Report HL-93-3, prepared for U.S. Army Engineer Waterways Experiment Station, Hydraulics Laboratory, Vicksburg, MS.

Meyer-Peter, E., and Müller, R. (1948). "Formulas for bed-load transport." *Second Meeting of the International Association for Hydraulics Research,* Stockholm, Sweden, Appendix 2, 39-64.

Pickup, G., and Warner, R. F. (1975). "Bed-material characteristics and transmission losses in an ephemeral stream," *Hydrology and Water Resources in Arizona and the Southwest,* 2, 455-72.

Resource Consultants and Engineers Inc. (RCE) (1993). "Geomorphic and sediment yield analyses for Albuquerque Arroyos," prepared for U.S. Army Engineer Waterways Experiment Station, Vicksburg, MS, RCE Ref No. 92-916, Fort Collins, CO.

Rouse, H. (1937). "Modern conceptions of the mechanics of fluid turbulence," *Transactions*, American Society of Civil Engineers, 102, 463-543.

Shulits, S. (1935). "The Schoklitsch bed-load formula," *Engineering*, London, England, June 21, 644-46, and June 28, 687.

Stonestreet, Scott E., Mulvihill, Michael E., and Copeland, Ronald R. (1993). "Determination of hydraulic roughness for concrete-lined, super-critical channels," *American Society of Civil Engineers National Hydraulics Conference*, San Francisco, July 1993.

Tatum, Fred E. (1963). "A new method of estimating debris-storage requirements for debris basins," *Second Federal Interagency Sedimentation Conference,"* Jackson, MS, USDA-ARS Miscellaneous Publication No. 970.

Thomas, William A., Copeland, Ronald R., Raphelt, Nolan K., and McComas, Dinah N. "User's Manual for the Hydraulic Design Package for Channels (SAM)" (in preparation), U.S. Army Engineer Waterways Experiment Station, Vicksburg, MS.

Toffaleti, F. B. (1968). "A procedure for computation of the total river sand discharge and detailed distribution, bed to surface," Technical Report No. 5, Committee on Channel Stabilization, U.S. Army Corps of Engineers, Vicksburg, MS.

U.S. Army Engineer District (USAED), Albuquerque. (1956). *Albuquerque Diversion Channels Project, Rio Grande and Tributaries, Albuquerque, New Mexico - Design Memorandum No. 1 : Hydrology*, Albuquerque, NM.

_____. (1964). *Albuquerque Diversion Channels Project, Rio Grande and Tributaries, Albuquerque, New Mexico,and Vicinity - Design Memorandum No. 4: Alameda Outlet Structure - Phase I*, Albuquerque, NM.

_____. (1965). *Albuquerque Diversion Channels Project, Rio Grande and Tributaries, Albuquerque, New Mexico,and Vicinity - Design Memorandum No. 5 : North Diversion Channel - Phases II and III, Alameda Outlet Structure to Campus Wash,* Albuquerque, NM.

_____. (1992). *Appendix A: Albuquerque Arroyos Feasibility Study, Hydrology and Hydrologic Model Calibration Analysis,* Albuquerque, NM, December.

U.S. Army Engineer District (USAED), Los Angeles. (1992). "Debris method - Los Angeles District method for prediction of debris yield," Los Angeles, CA.

U.S. Army Engineer Headquarters (USAEHQ). (1989). *Sedimentation investigations of rivers and reservoirs*. EM 1110-2-4000, Washington, DC.

_____. (1991). *Hydraulic design of flood control channels,* EM 1110-2-1601, Washington DC.

U.S. Army Engineer Hydrologic Engineering Center (USAEHEC). (1981). *Users manual HEC-1 flood hydrograph package*. Davis, CA.

_____. (1990). *Users manual HEC-2 generalized computer program, water surface profiles*. Davis, CA.

_____. (1993). *Users manual HEC-6 generalized computer program for scour and deposition in rivers and reservoirs*. Davis, CA.

U.S. Bureau of Reclamation (USBR). (1960). *Design of stable channels with tractive forces and competent bottom velocity*. Sedimentation Section, Hydrology Branch, Denver, CO.

_____. (1987). *Design of small dams*. U.S. Government Printing Office, Denver, CO.

USDA Soil Conservation Service (USDA SCS). (1977). *Soil survey of Bernalillo County and parts of Sandoval and Valencia Counties, New Mexico*. Albuquerque, NM.

_____. (1987). *Report on sediment survey of Sandia Mountain tributaries, Site No. 1, Piedra Lisa Arroyo*. Albuquerque, NM.

_____. (1992). *Physical and chemical properties of the soils, Bernalillo County and parts of Sandoval and Valencia Counties, New Mexico,* Albuquerque, NM.

U.S. Geological Survey (USGS). (1982). "Water resources data, New Mexico, water year 1982," U.S. Geological Survey Water-Data Report NM-82-1, 216-17.

_____. (1983). "Water resources data, New Mexico, water year 1983," U.S. Geological Survey Water-Data Report NM-83-1, 184-85.

Ward, Tim J. (1992). "Rainfall simulation to estimate potential sediment loadings to the Albuquerque North Diversion Channel," Technical Completion Report, Project No. 01-4-23969, New Mexico Water Resources Research Institute, New Mexico State University, Las Cruces, NM.

Watson, C. C., Harvey, M. D., Biedenharn, D. S., and Combs, P. (1988). "Geotechnical and hydraulic stability numbers for channel rehabilitation: Part 1, the approach," *Hydraulic Engineering, Proceedings, 1988 National Conference, Hydraulics Division,* American Society of Civil Engineers, S.R. Abt and J. Gessler, Eds, New York, 120-125.

Williams, J. R., and Berndt, H. B. (1977). "Sediment yield prediction based on watershed hydrology." *American Society of Civil Engineers Transactions*.

Wischmeier, W. H., and Smith, D. D. (1978). *Predicting rainfall erosion losses—A guide to conservation planning*, Agricultural Handbook 537, USDA, Washington DC.

Woo, H. S., Julien, P. Y., and Richardson, E. V. (1988). "Suspension of large concentrations of sands," *Journal of Hydraulic Engineering,* American Society of Civil Engineers, 114(8), 888-98.

Wright Water Engineers, Inc. (1989). *Assessment of the July 1988 storm and the City of Albuquerque Flood Control System,"* prepared for Risk Management and Public Works Departments, City of Albuquerque, NM.

Yang, C. T. (1973). "Incipient motion and sediment transport," *Journal, Hydraulics Division*, American Society of Civil Engineers, 99(HY10), 1679-1704.

_____. 1984. "Unit stream power equation for gravel," *Journal, Hydraulics Division*, American Society of Civil Engineers, 110(HY12), 1783-1797.

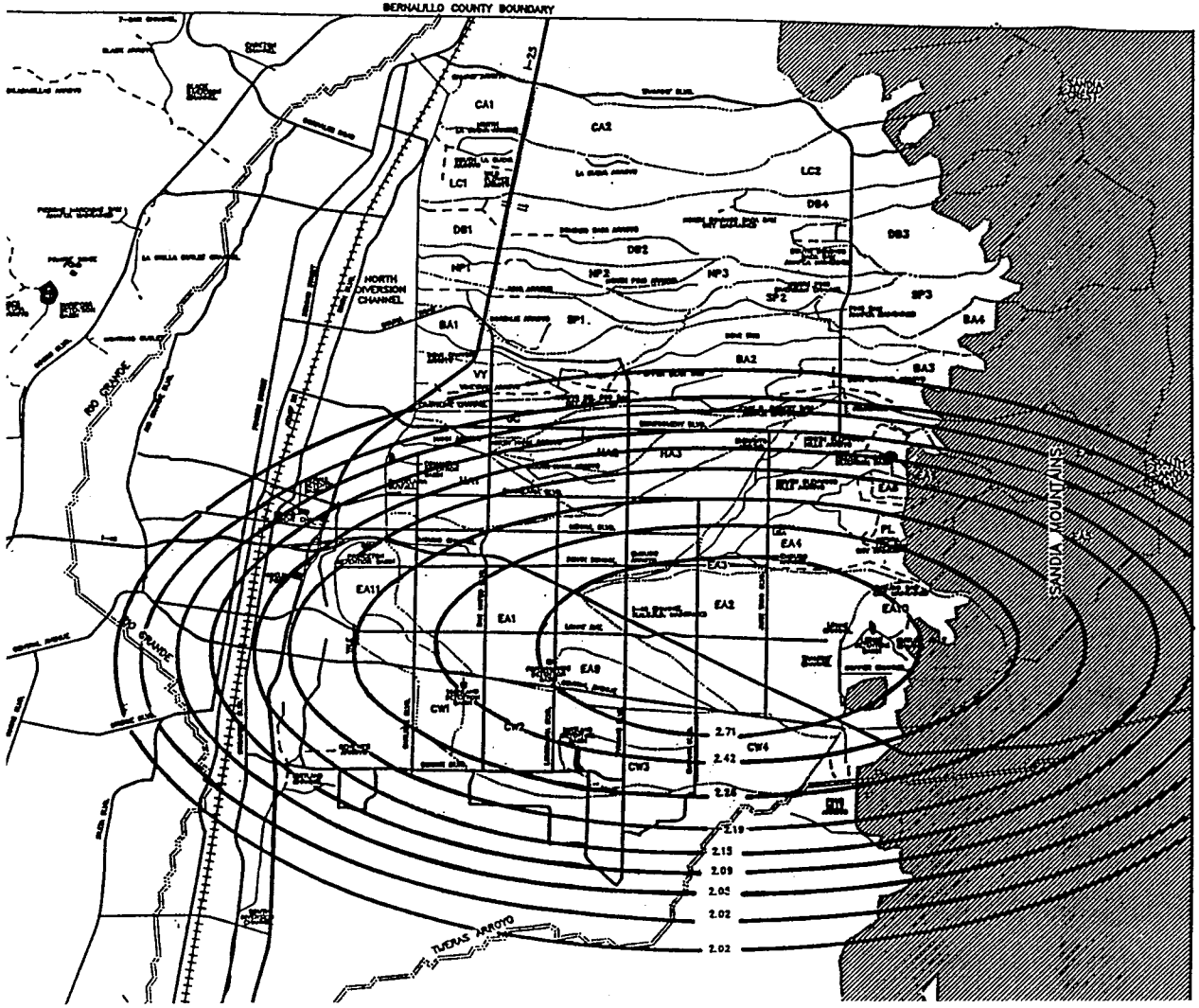

N

SCALE IN MILES

0 1 2

LEGEND

- DETENTION BASIN
- INTERSTATE HIGHWAY
- OTHER MAJOR ROAD
- LINED ARROYO OR CHANNEL
- UNLINED ARROYO OR CHANNEL
- EA1 SUBAREA DESIGNATION
- SUBAREA BOUNDARY

ISOHYET VALUES ARE FOR 24-HOUR 1.0% CHANCE FLOOD EVENT

100-YEAR-FREQUENCY STORM CENTERING NO. 1

Plate 1

Plate 2

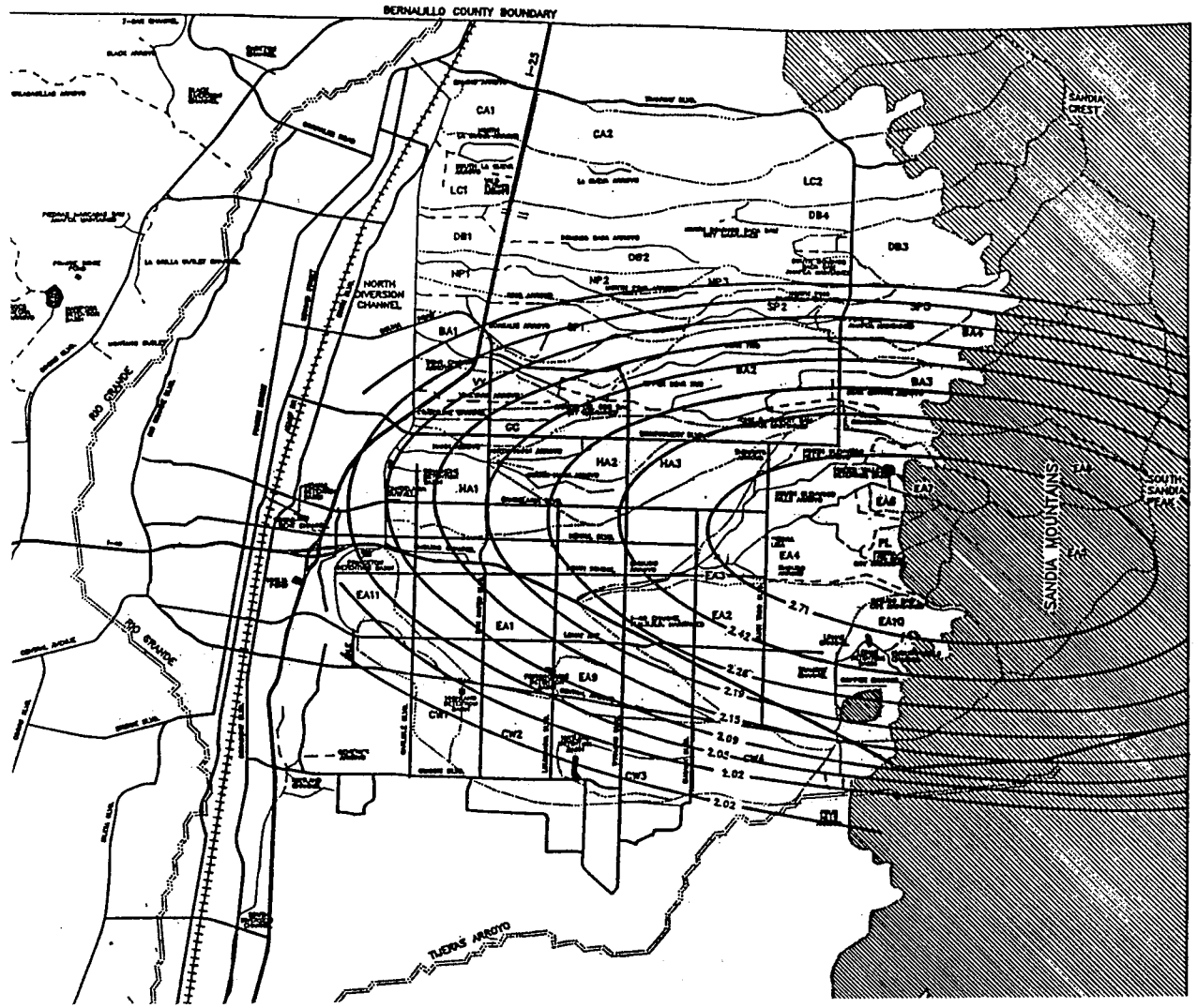

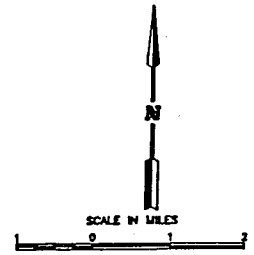

LEGEND

- DETENTION BASIN
- INTERSTATE HIGHWAY
- OTHER MAJOR ROAD
- LINED ARROYO OR CHANNEL
- UNLINED ARROYO OR CHANNE
- EA1 SUBAREA DESIGNATION
- SUBAREA BOUNDARY

ISOHYET VALUES ARE FOR 24-HOUR 1.0% CHANCE FLOOD EVENT

100-YEAR FREQUENCY STORM CENTERING NO. 4

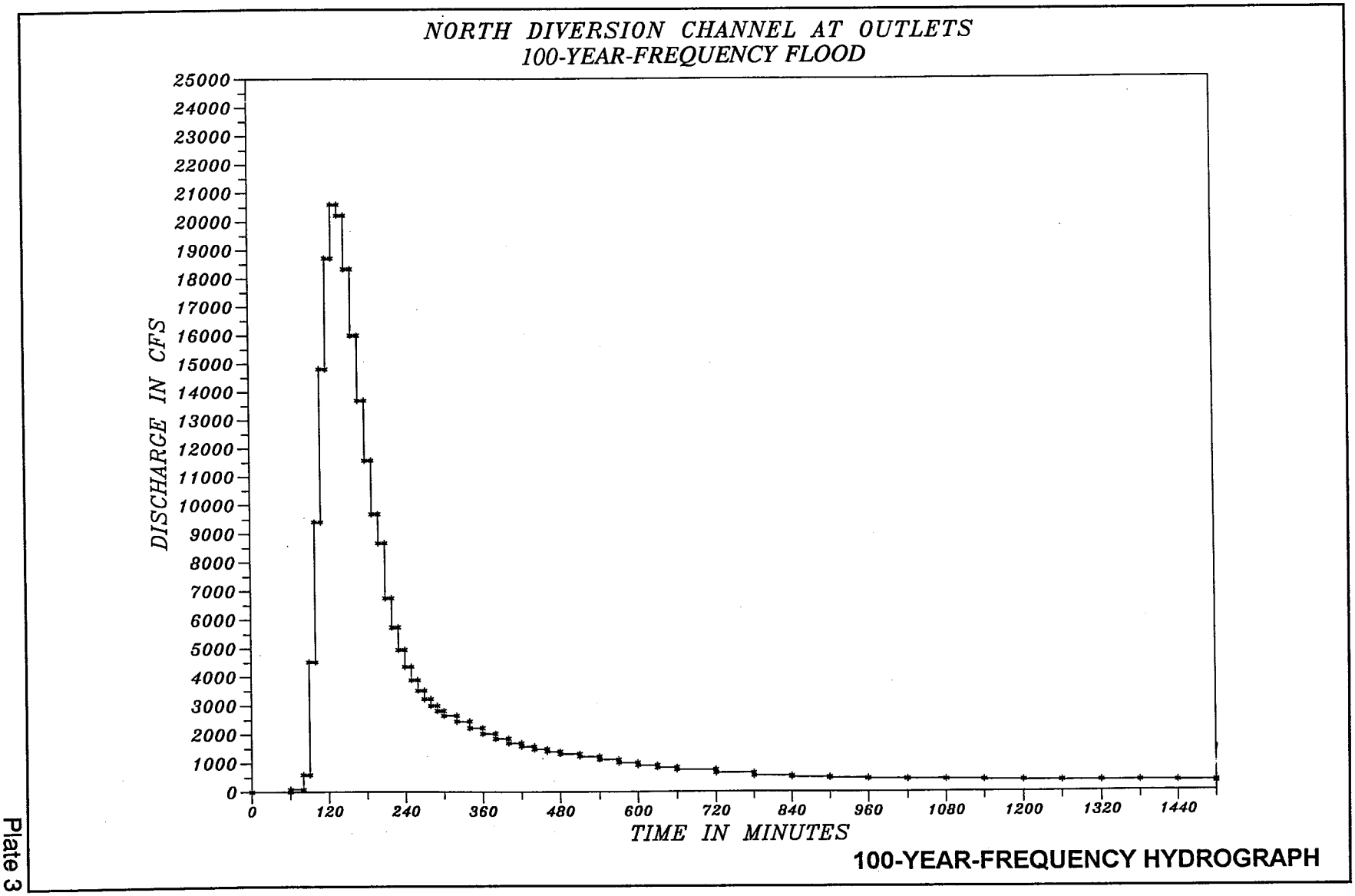

100-YEAR-FREQUENCY HYDROGRAPH

Plate 3

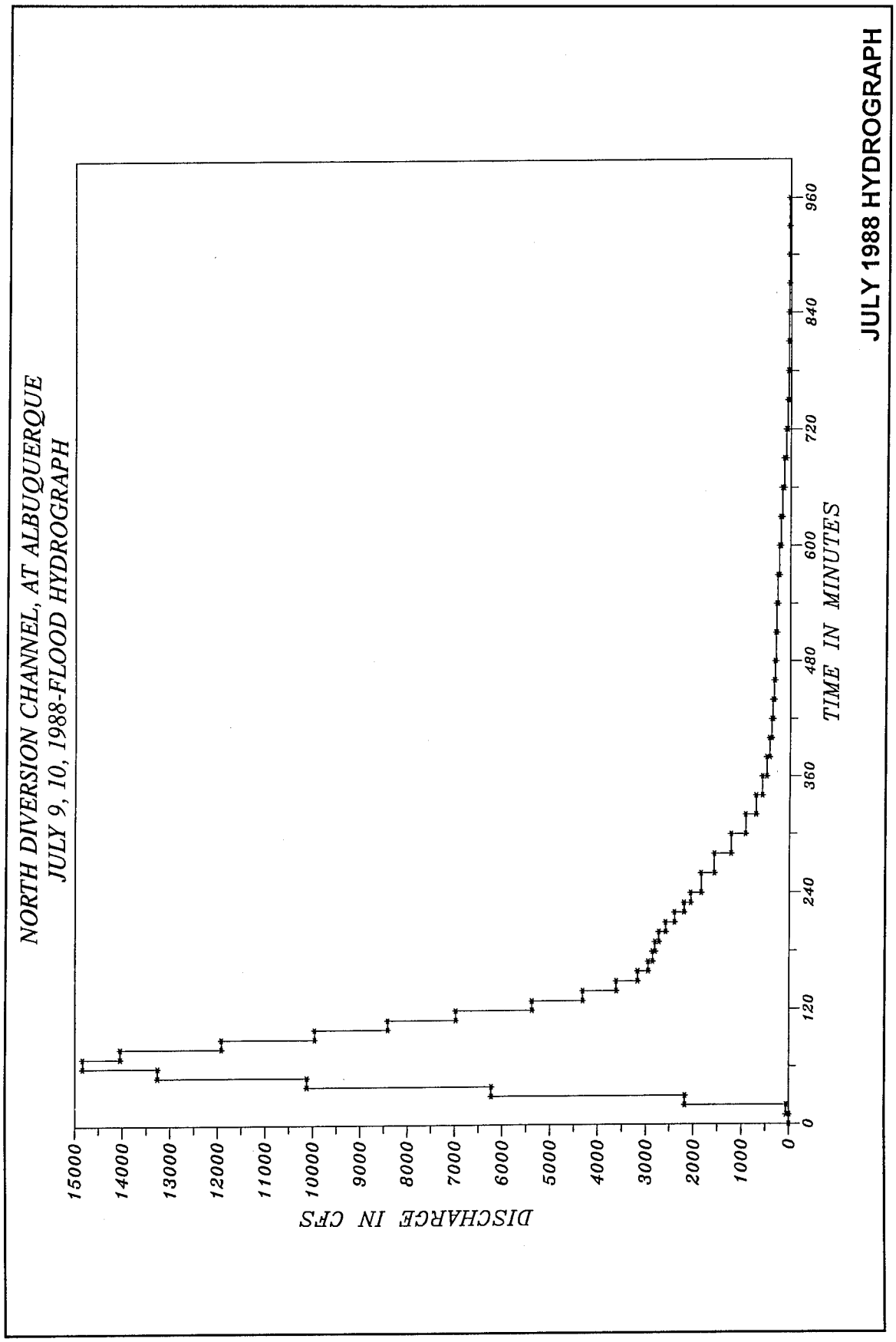
NORTH DIVERSION CHANNEL, AT ALBUQUERQUE
JULY 9, 10, 1988-FLOOD HYDROGRAPH
DISCHARGE IN CFS
15000
14000
13000
12000
11000
10000
9000
8000
7000
6000
5000
4000
3000
2000
1000
0
0
120
240
360
480
600
720
840
960
TIME IN MINUTES
JULY 1988 HYDROGRAPH

Plate 4

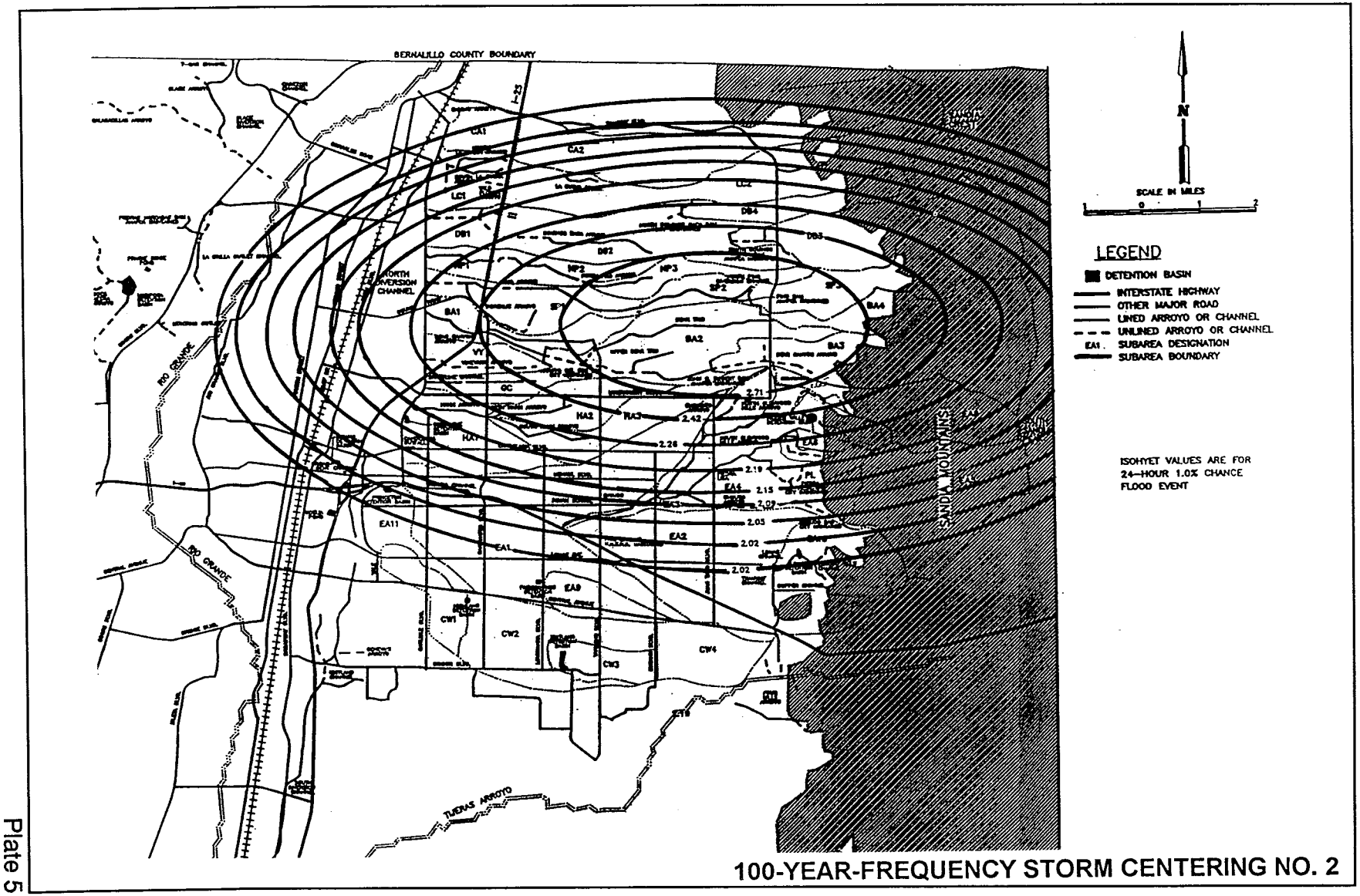

100-YEAR-FREQUENCY STORM CENTERING NO. 2

Plate 5

Plate 6

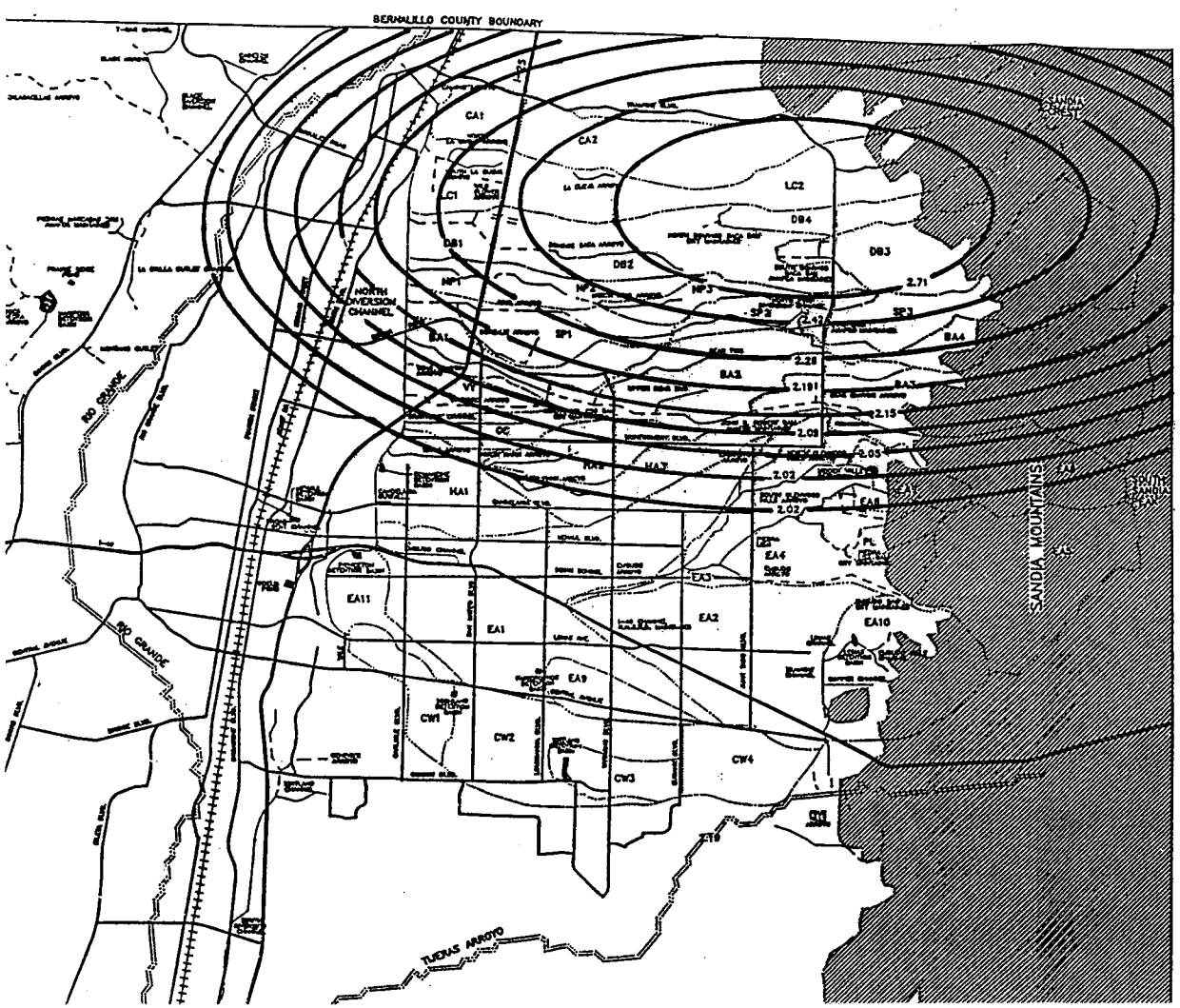

N

SCALE IN MILES

0 1 2

LEGEND

- DETENTION BASIN
- INTERSTATE HIGHWAY
- OTHER MAJOR ROAD
- LINED ARROYO OR CHANNEL
- UNLINED ARROYO OR CHANNEL
- EA1 SUBAREA DESIGNATION
- SUBAREA BOUNDARY

ISOHYET VALUES ARE FOR 24-HOUR 1.0% CHANCE FLOOD EVENT

100-YEAR-FREQUENCY STORM CENTERING NO. 3

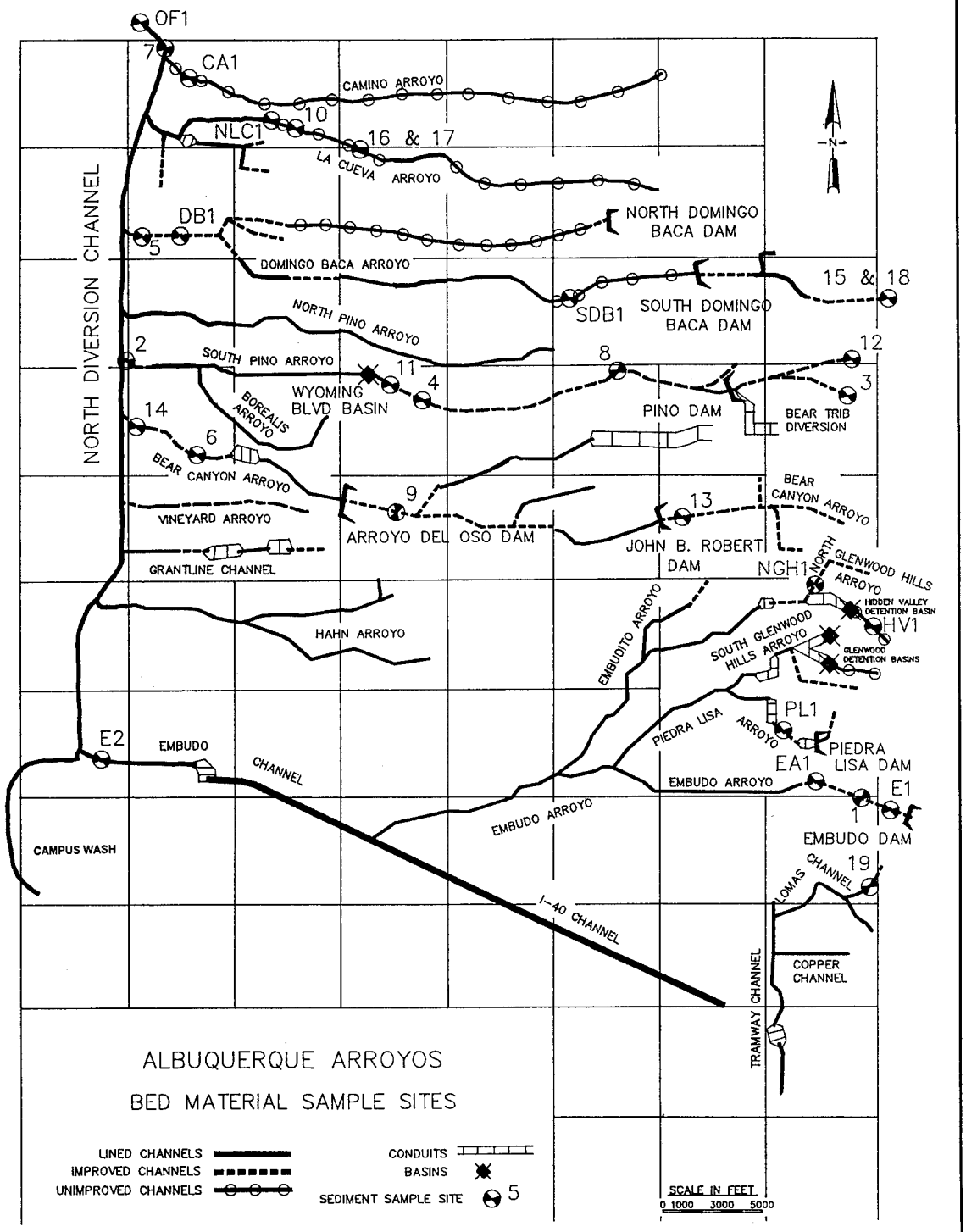

BED-MATERIAL SAMPLE SITES

Plate 7

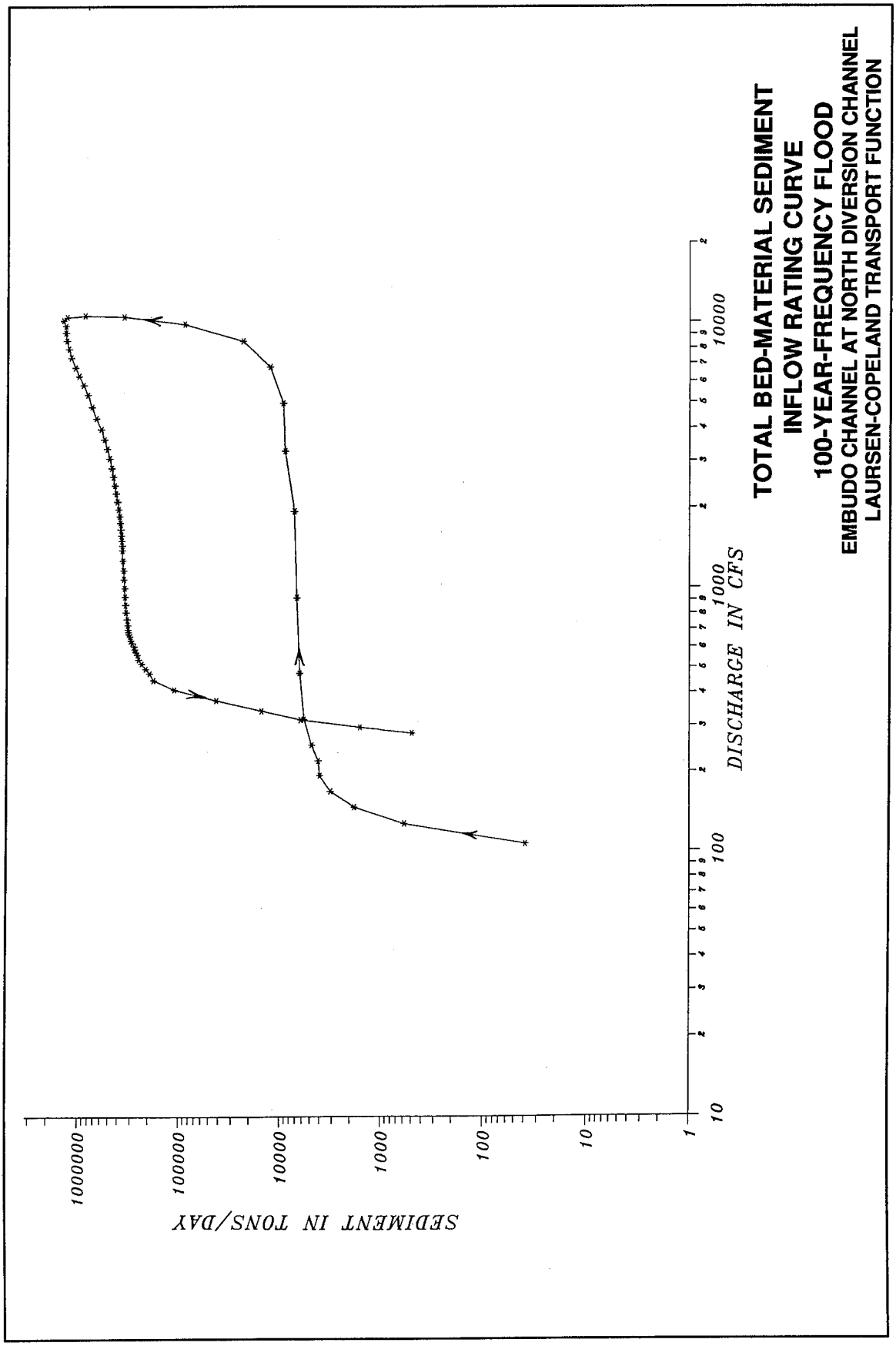
TOTAL BED-MATERIAL SEDIMENT
INFLOW RATING CURVE
100-YEAR-FREQUENCY FLOOD
EMBUDO CHANNEL AT NORTH DIVERSION CHANNEL
LAURSEN-COPELAND TRANSPORT FUNCTION
SEDIMENT IN TONS/DAY
1000000
100000
10000
1000
100
10
1
DISCHARGE IN CFS
10
100
1000
10000

Plate 8

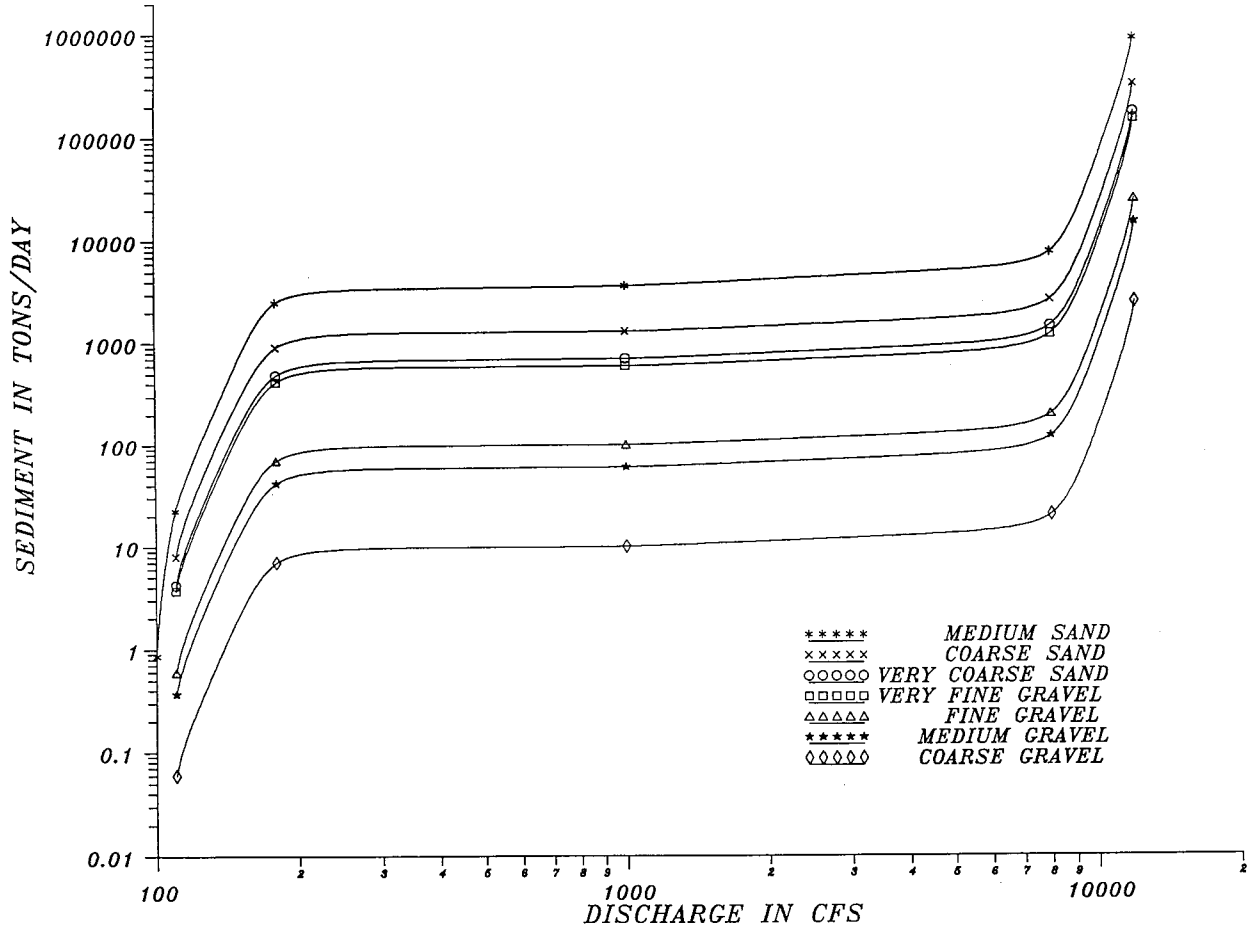

SIZE-CLASS SEDIMENT INFLOW RATING CURVES
100-YEAR-FREQUENCY FLOOD, RISING LIMB
EMBUDO CHANNEL AT NORTH DIVERSION CHANNEL
LAURSEN-COPELAND TRANSPORT FUNCTION

Plate 9

Plate 10

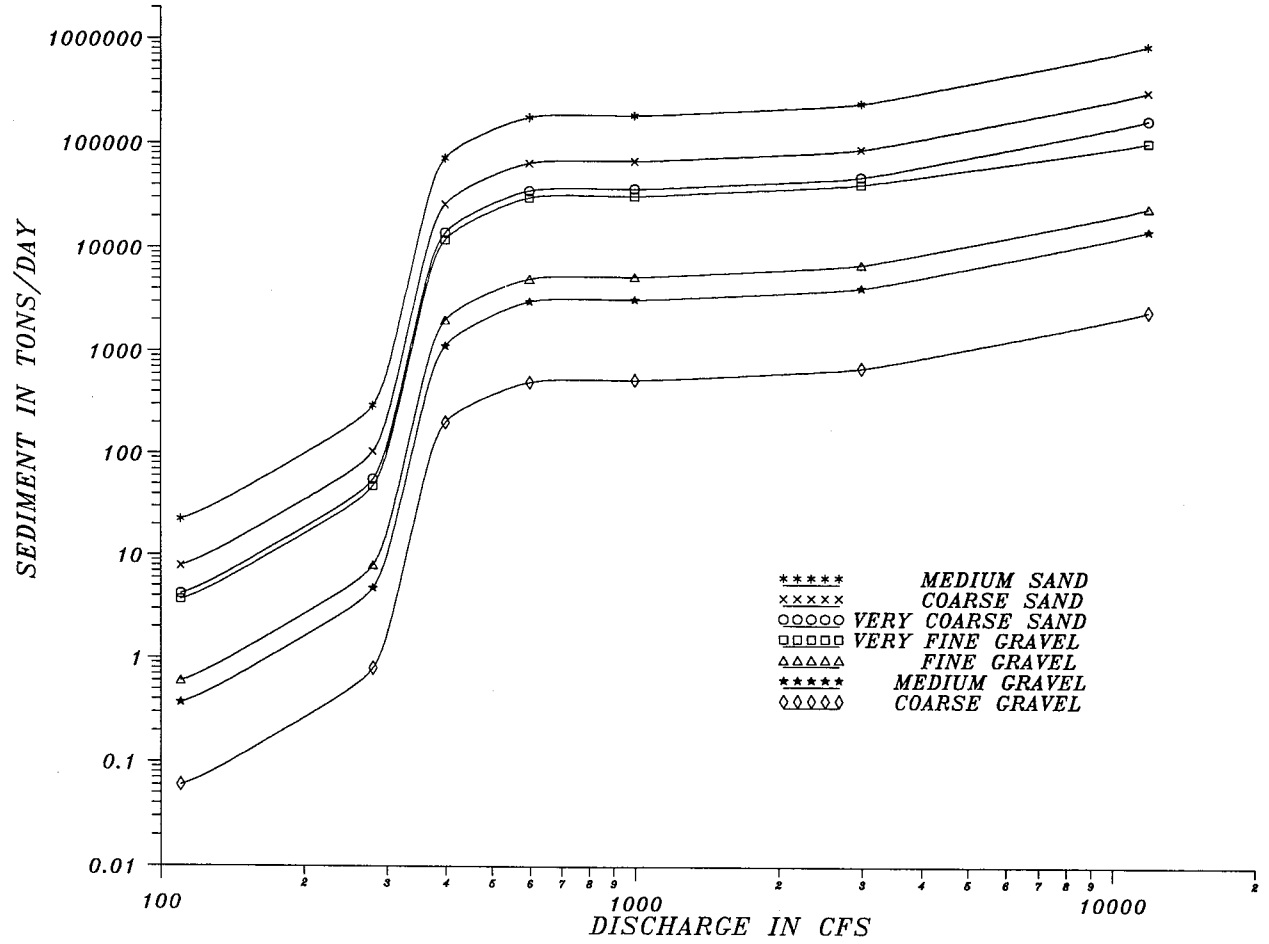

SIZE-CLASS SEDIMENT
INFLOW RATING CURVE
100-YEAR-FREQUENCY FLOOD, FALLING LIMB
EMBUDO CHANNEL AT NORTH DIVERSION CHANNEL
LAURSEN-COPELAND TRANSPORT FUNCTION

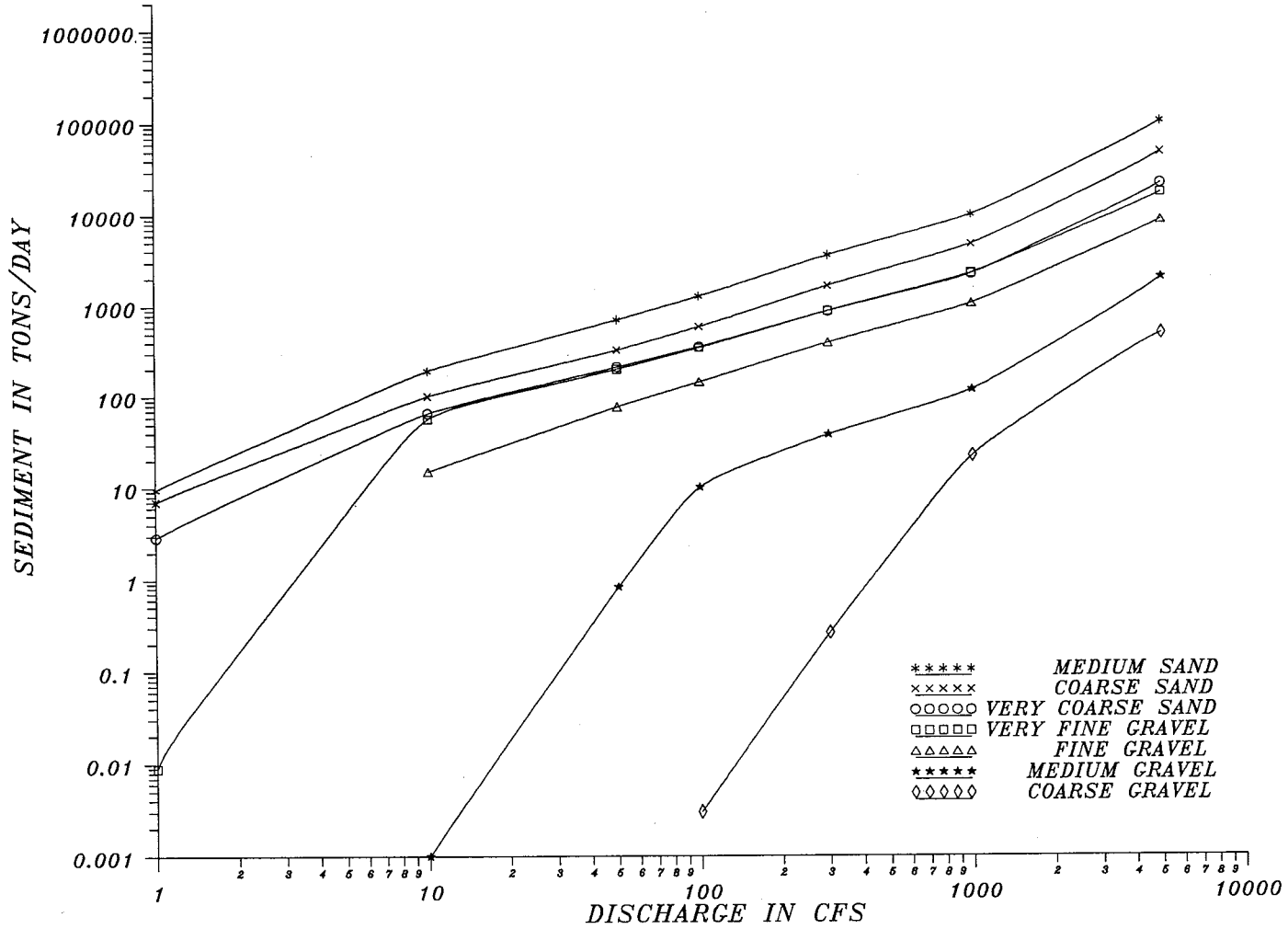

SIZE-CLASS SEDIMENT INFLOW RATING CURVES
BEAR CANYON ARROYO AT NORTH DIVERSION CHANNEL
LAURSEN-COPELAND TRANSPORT FUNCTION

Plate 11

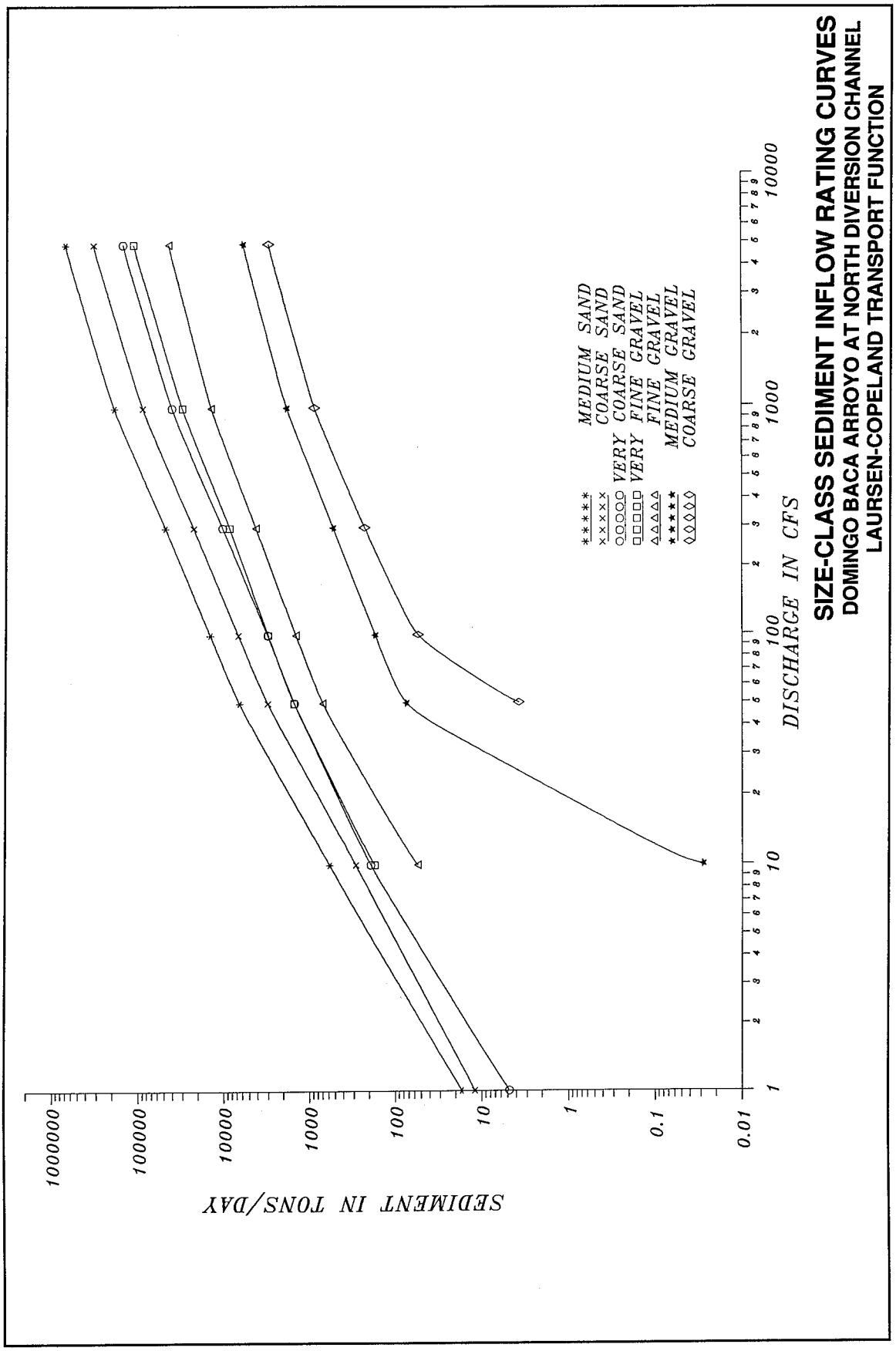
SIZE-CLASS SEDIMENT INFLOW RATING CURVES
DOMINGO BACA ARROYO AT NORTH DIVERSION CHANNEL
LAURSEN-COPELAND TRANSPORT FUNCTION
SEDIMENT IN TONS/DAY
DISCHARGE IN CFS
MEDIUM SAND
COARSE SAND
VERY COARSE SAND
VERY FINE GRAVEL
FINE GRAVEL
MEDIUM GRAVEL
COARSE GRAVEL

Plate 12

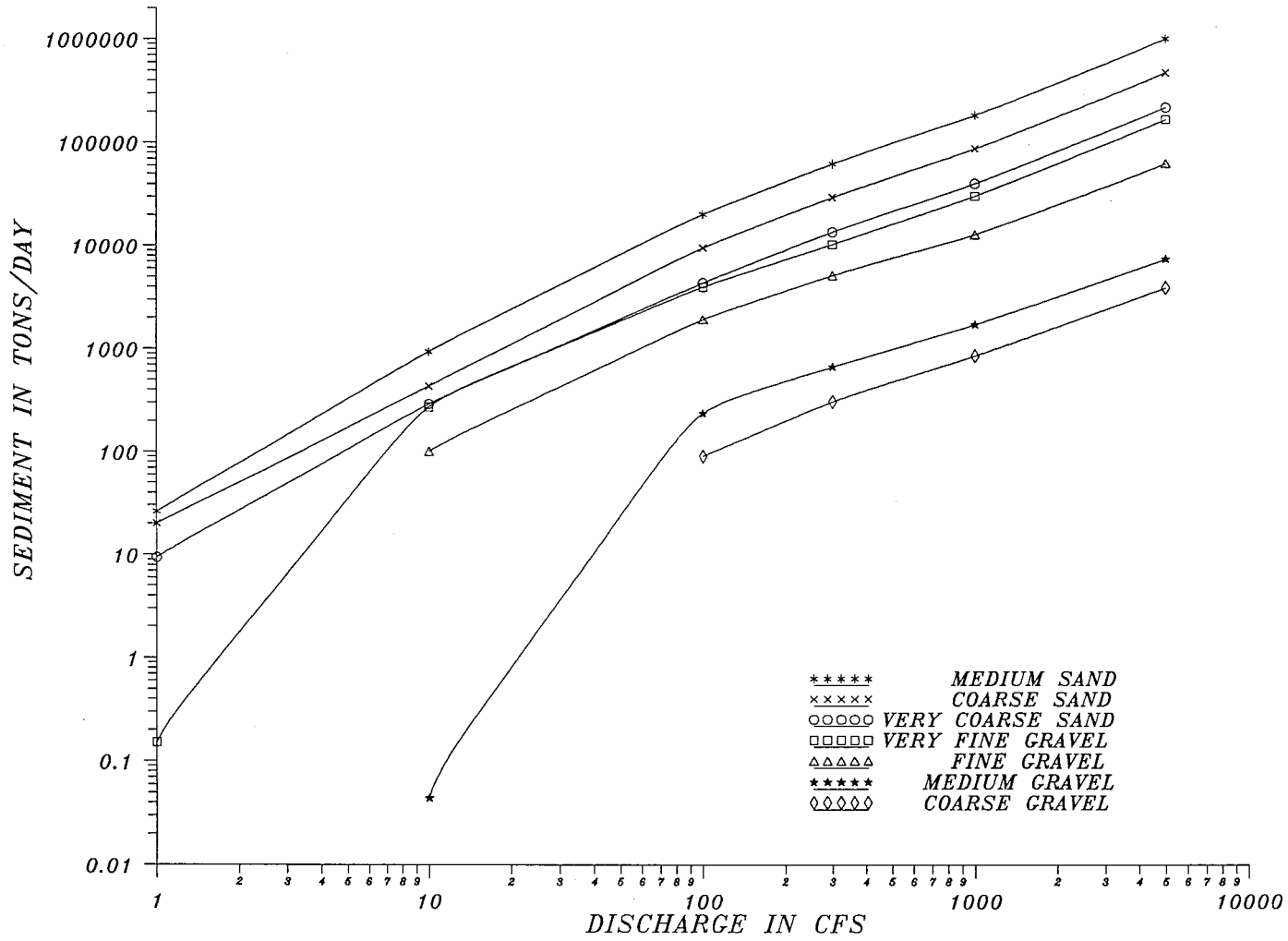

SIZE-CLASS SEDIMENT INFLOW RATING CURVES
LA CUEVA ARROYO AT NORTH DIVERSION CHANNEL
LAURSEN-COPELAND TRANSPORT FUNCTION

Plate 13

Plate 14

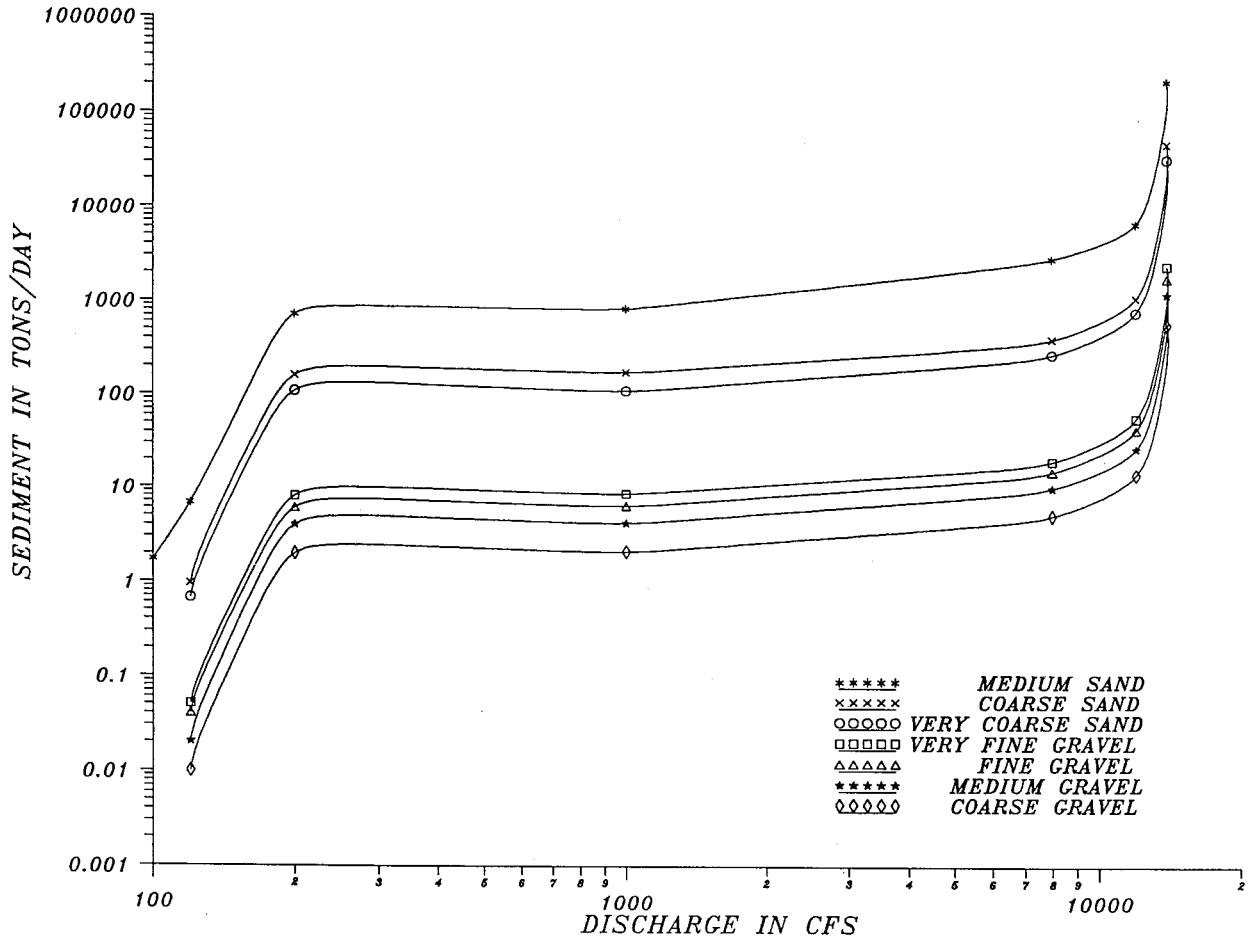

SIZE-CLASS SEDIMENT INFLOW RATING CURVES
100-YEAR-FREQUENCY FLOOD, RISING LIMB
EMBUDO CHANNEL AT NORTH DIVERSION CHANNEL
YANG TRANSPORT FUNCTION

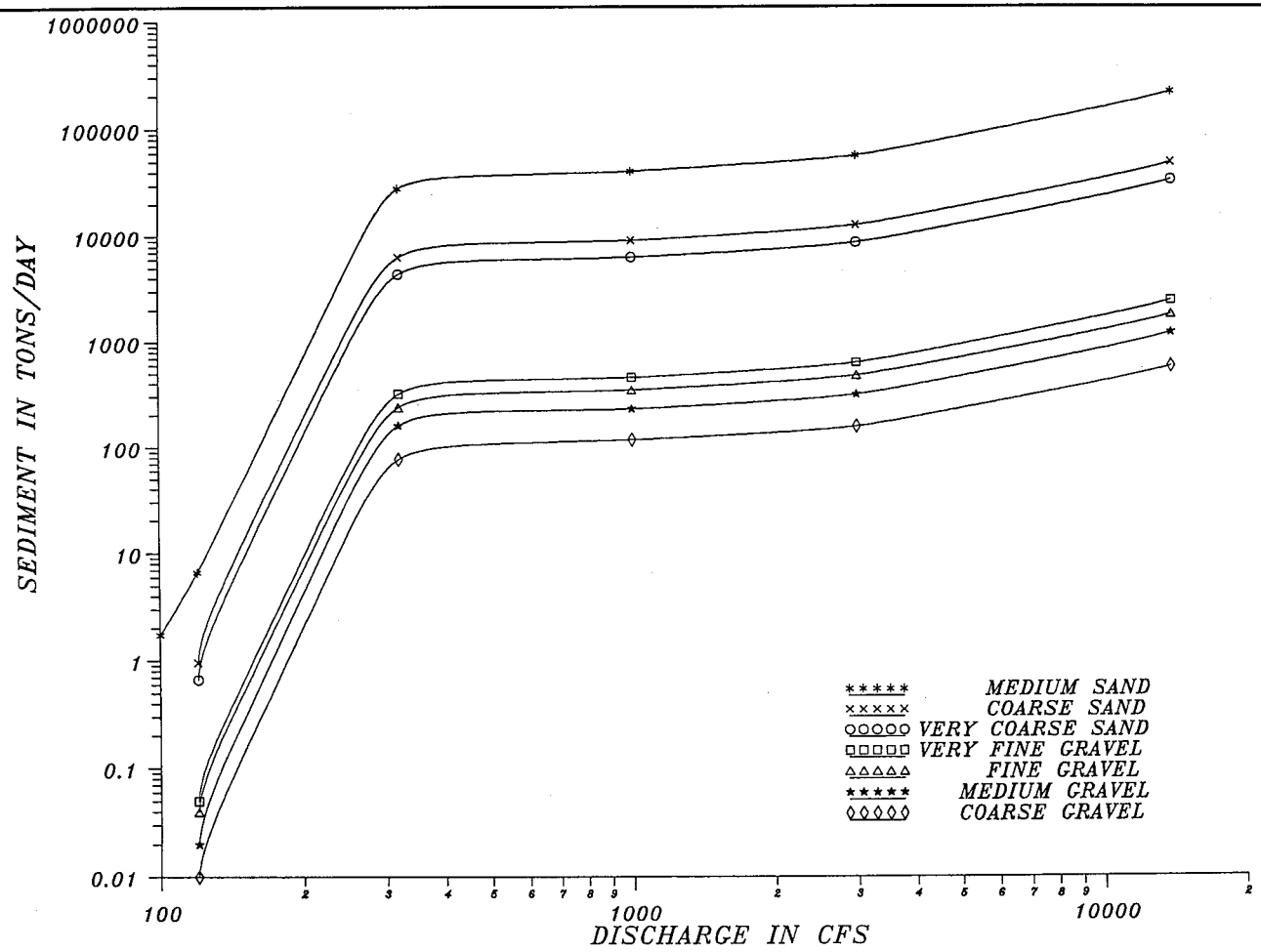

SIZE-CLASS SEDIMENT INFLOW RATING CURVE
100-YEAR-FREQUENCY FLOOD, FALLING LIMB
EMBUDO CHANNEL AT NORTH DIVERSION CHANNEL
YANG TRANSPORT FUNCTION

Plate 15

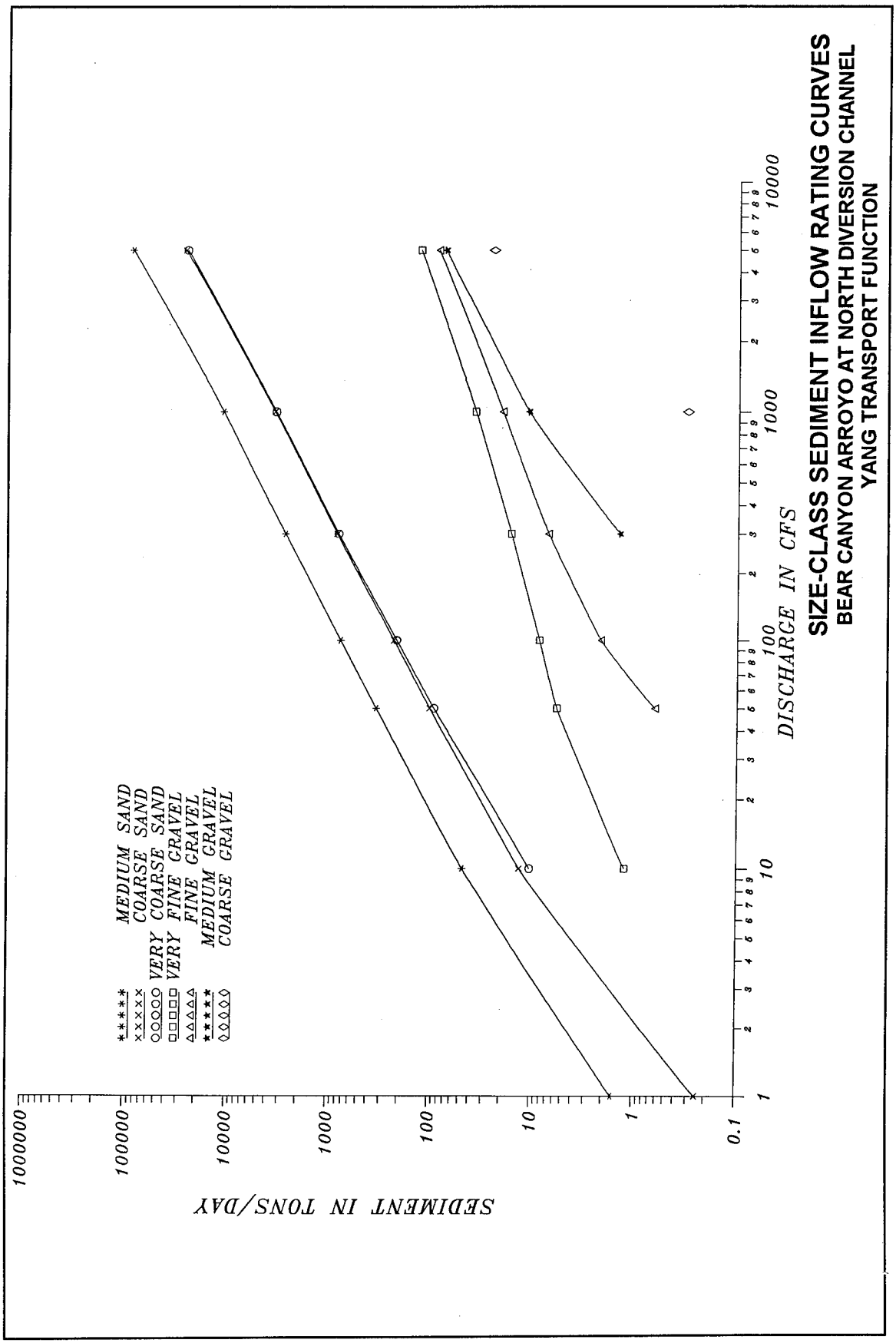
SIZE-CLASS SEDIMENT INFLOW RATING CURVES
BEAR CANYON ARROYO AT NORTH DIVERSION CHANNEL
YANG TRANSPORT FUNCTION
SEDIMENT IN TONS/DAY
DISCHARGE IN CFS
MEDIUM SAND
COARSE SAND
VERY COARSE SAND
VERY FINE GRAVEL
FINE GRAVEL
MEDIUM GRAVEL
COARSE GRAVEL
1000000
100000
10000
1000
100
10
1
0.1
1
10
100
1000
10000

Plate 16

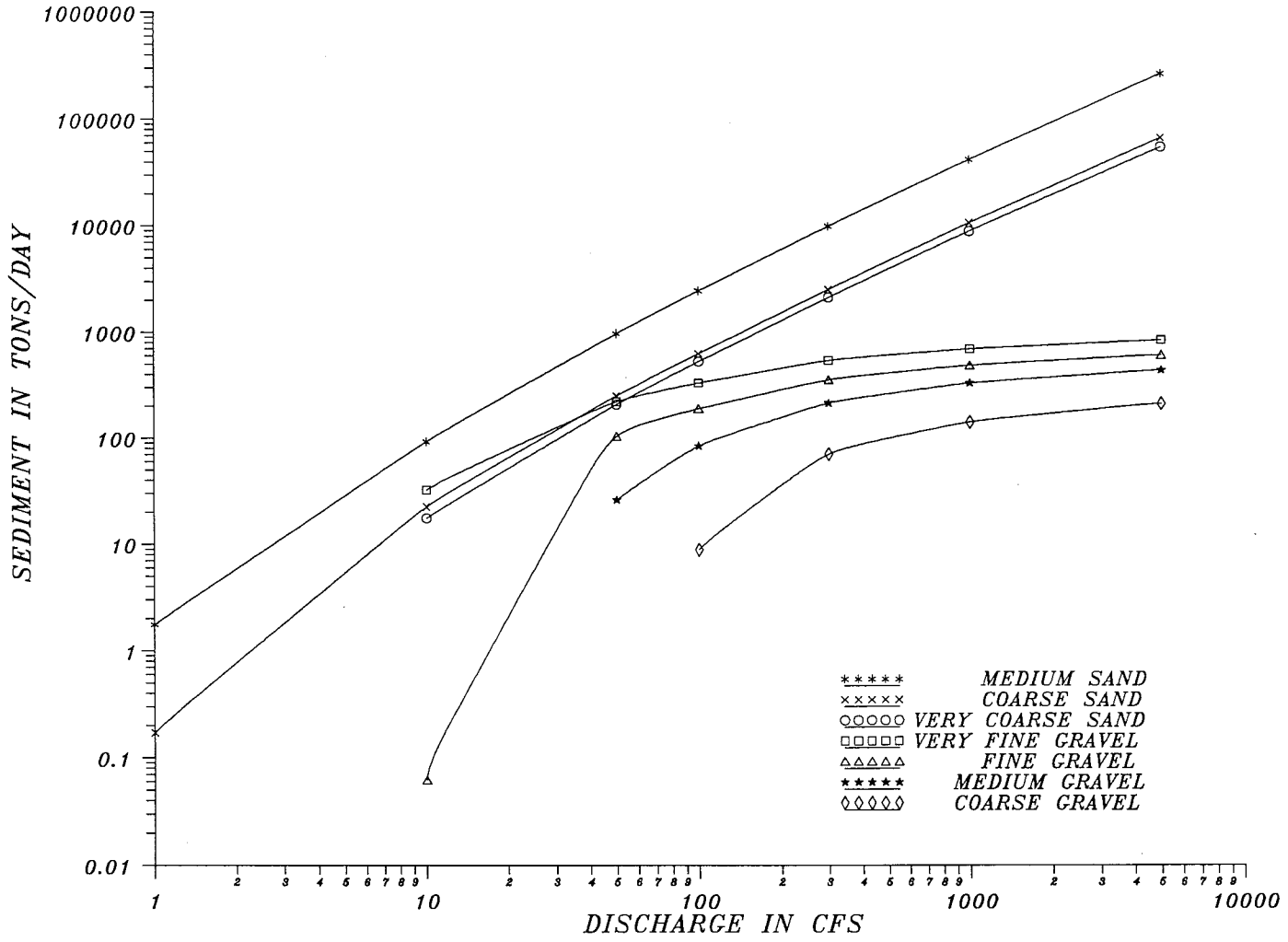

SIZE-CLASS SEDIMENT INFLOW RATING CURVES
DOMINGO BACA ARROYO AT NORTH DIVERSION CHANNEL
YANG TRANSPORT FUNCTION

Plate 17

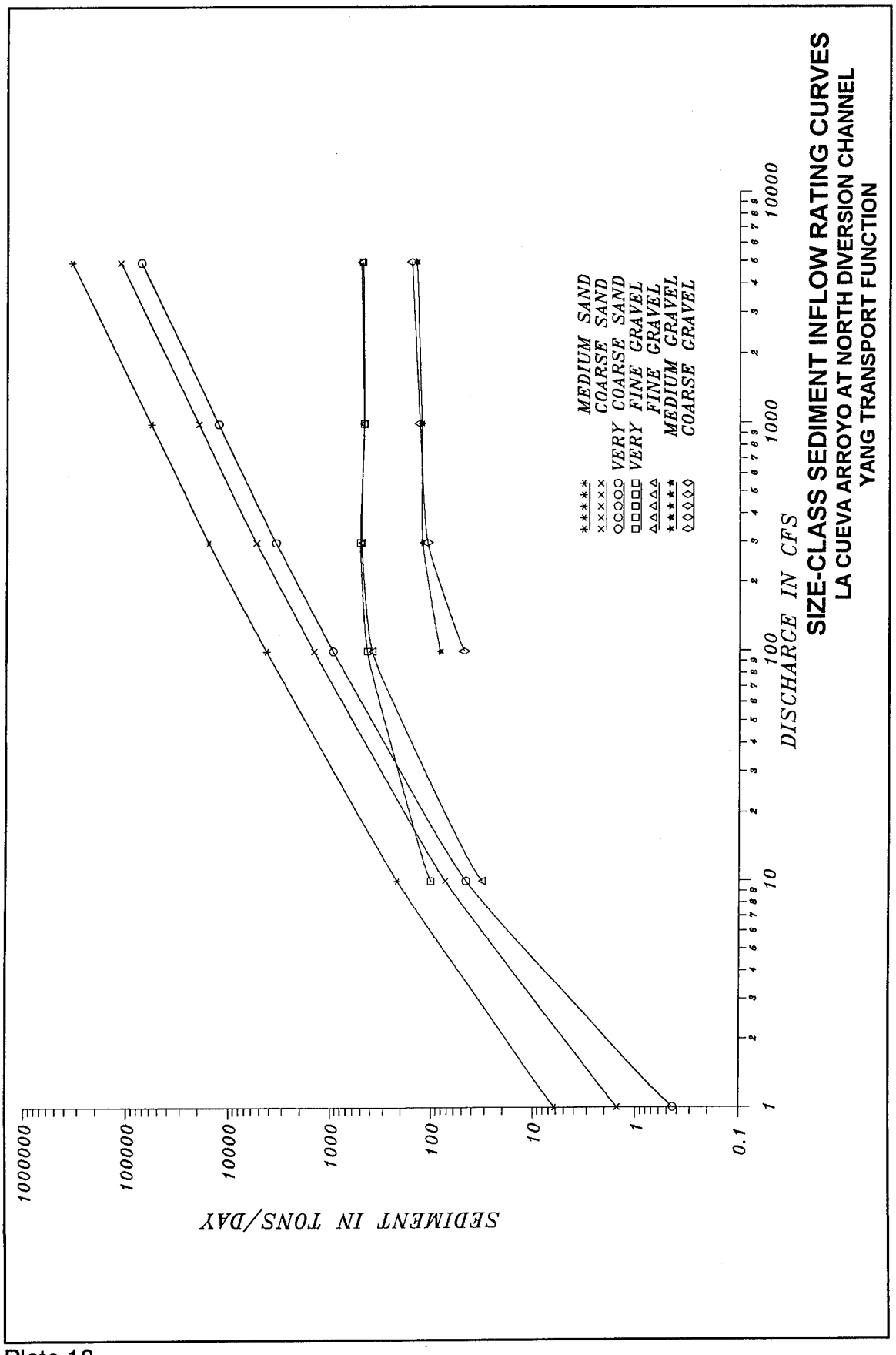
SIZE-CLASS SEDIMENT INFLOW RATING CURVES
LA CUEVA ARROYO AT NORTH DIVERSION CHANNEL
YANG TRANSPORT FUNCTION
SEDIMENT IN TONS/DAY
DISCHARGE IN CFS
MEDIUM SAND
COARSE SAND
VERY COARSE SAND
VERY FINE GRAVEL
FINE GRAVEL
MEDIUM GRAVEL
COARSE GRAVEL

Plate 18

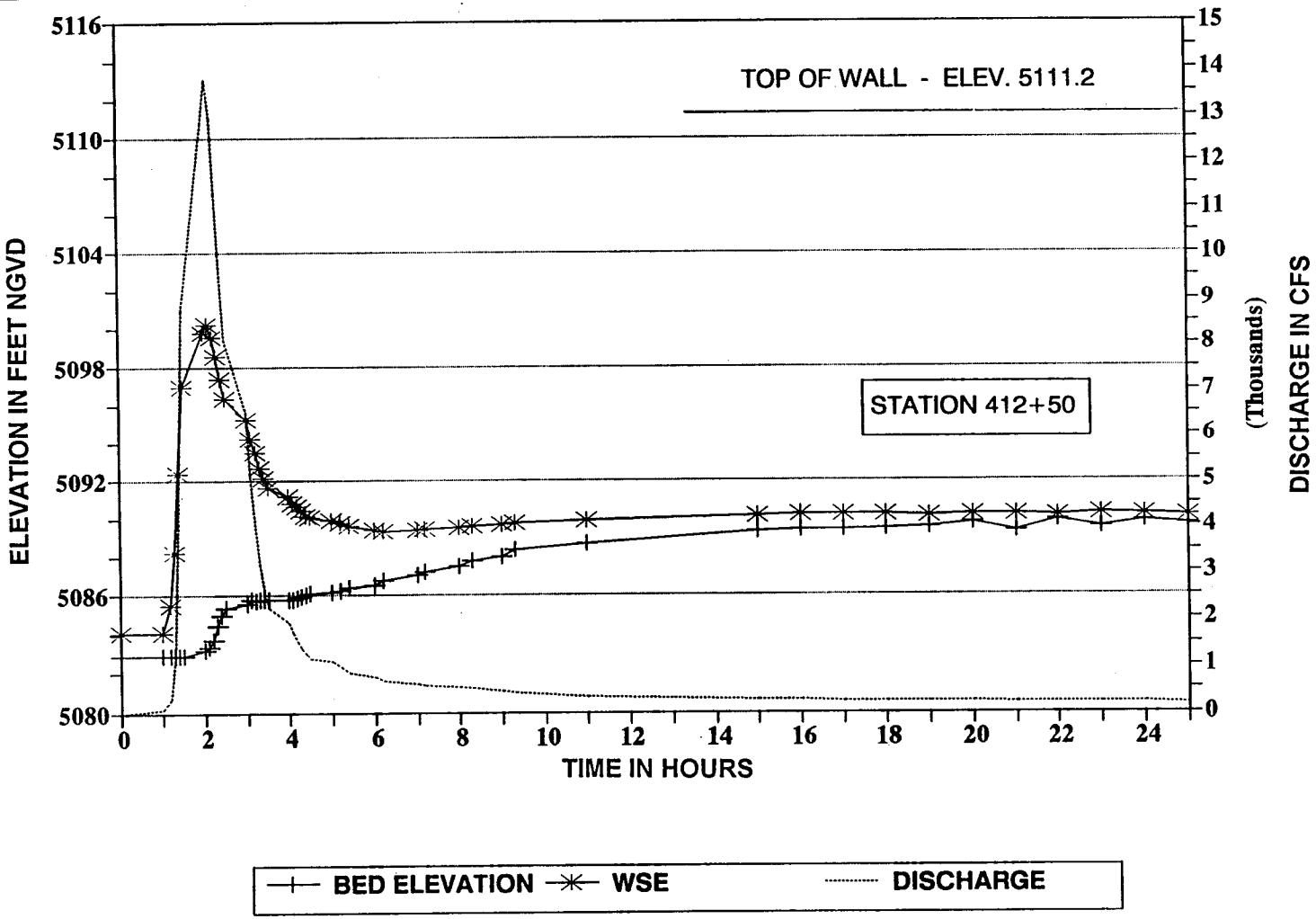

VARIATION OF STAGE AND BED ELEVATION
100-YEAR-FREQUENCY FLOOD
NORTH DIVERSION CHANNEL AT STATION 412+50

Plate 19

Plate 20

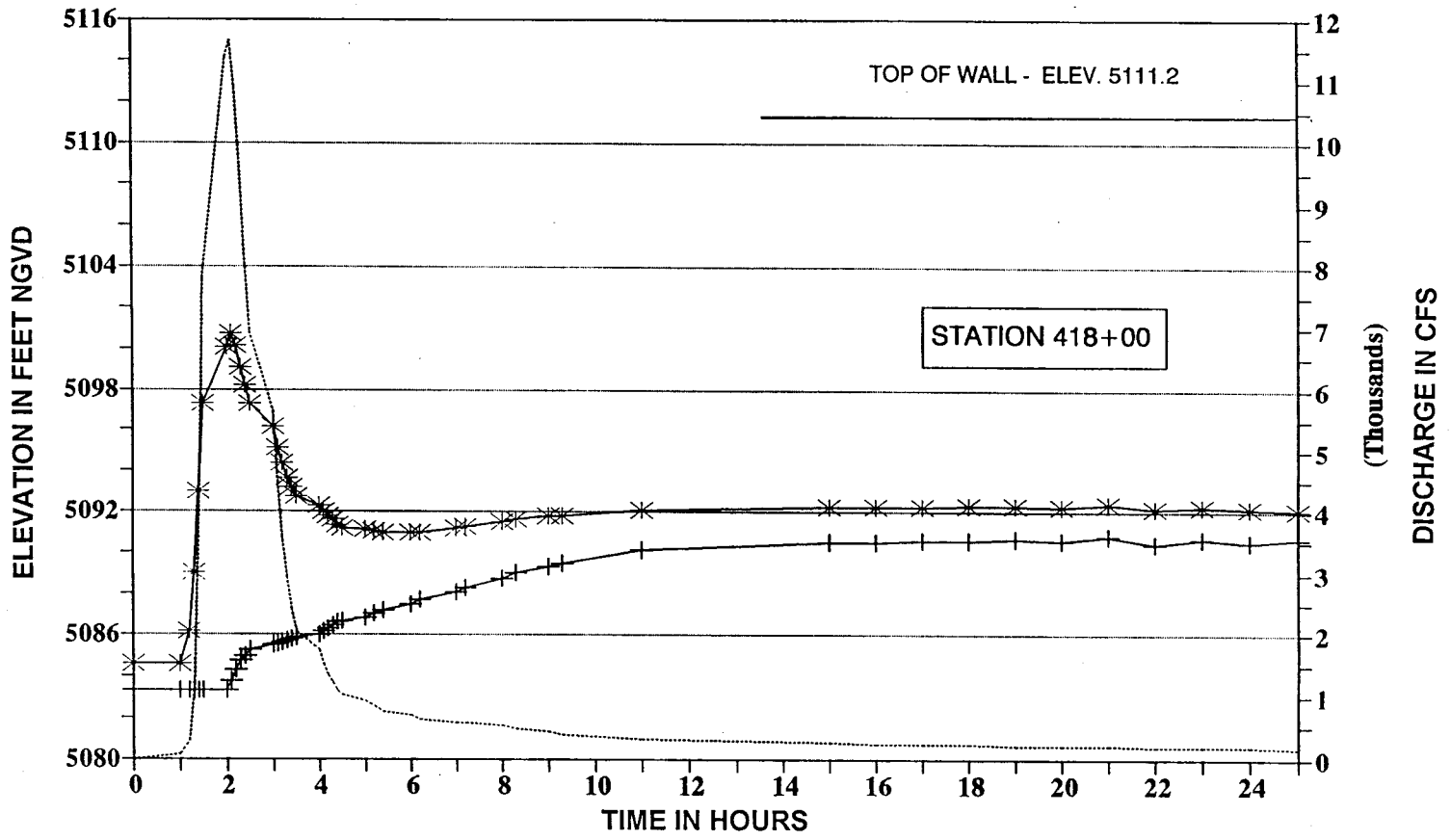

VARIATION OF STAGE AND BED ELEVATION
100-YEAR-FREQUENCY FLOOD
EMBUDO CHANNEL AT STATION 418+00

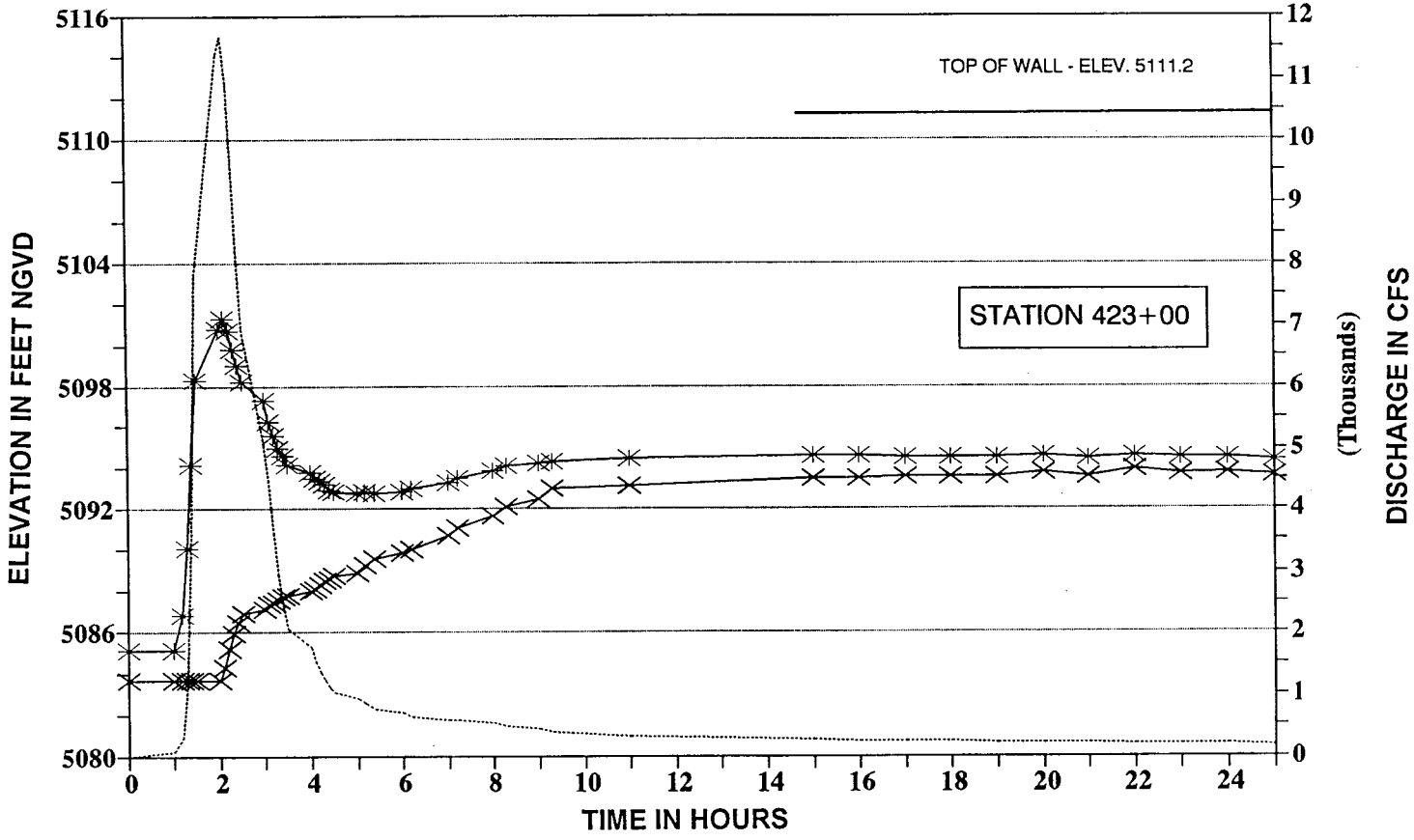

VARIATION OF STAGE AND BED ELEVATION
100-YEAR-FREQUENCY FLOOD
EMBUDO CHANNEL AT STATION 423+00

Plate 21

Plate 22

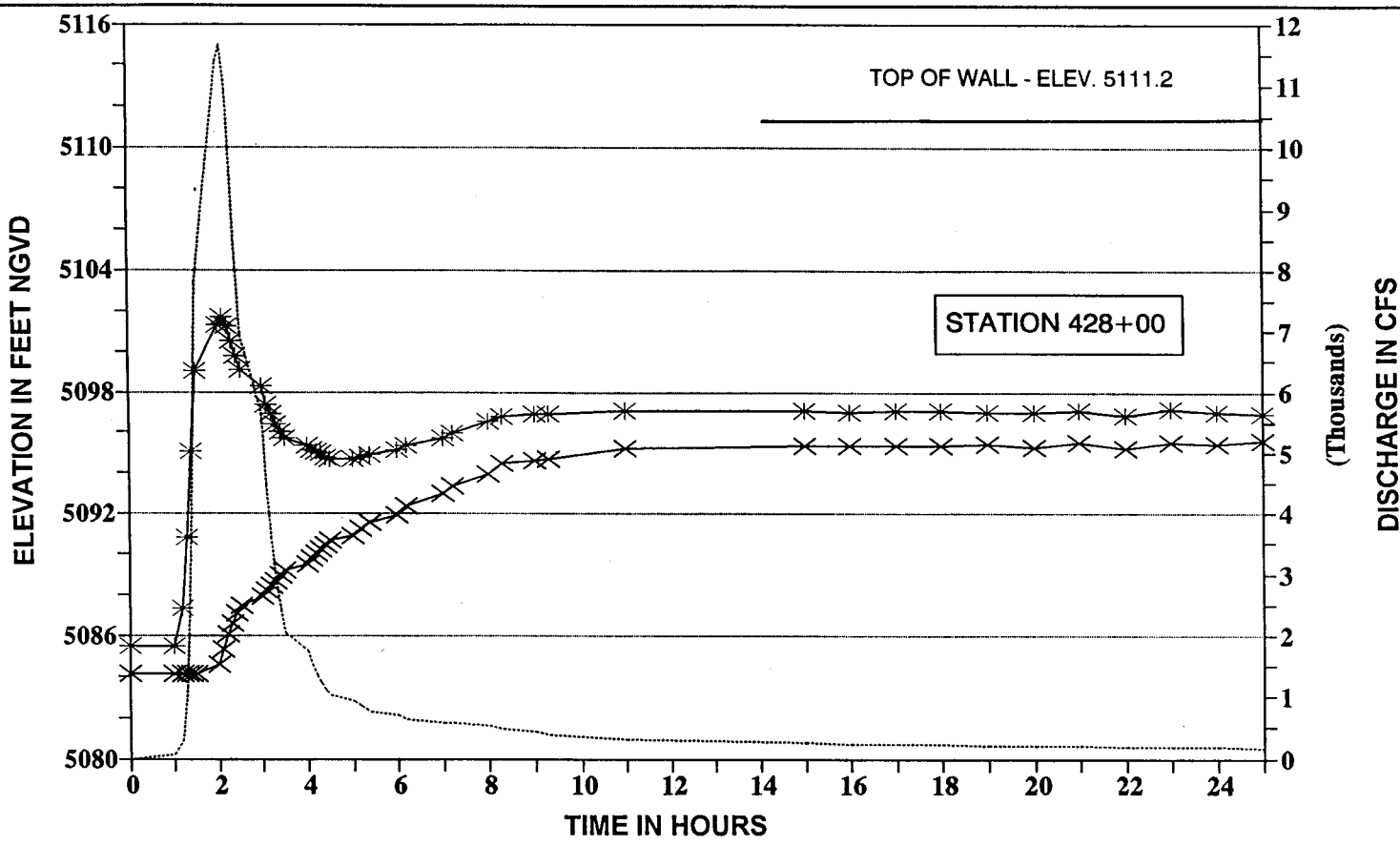

VARIATION OF STAGE AND BED ELEVATION
100-YEAR-FREQUENCY FLOOD
EMBUDO CHANNEL AT STATION 428+00

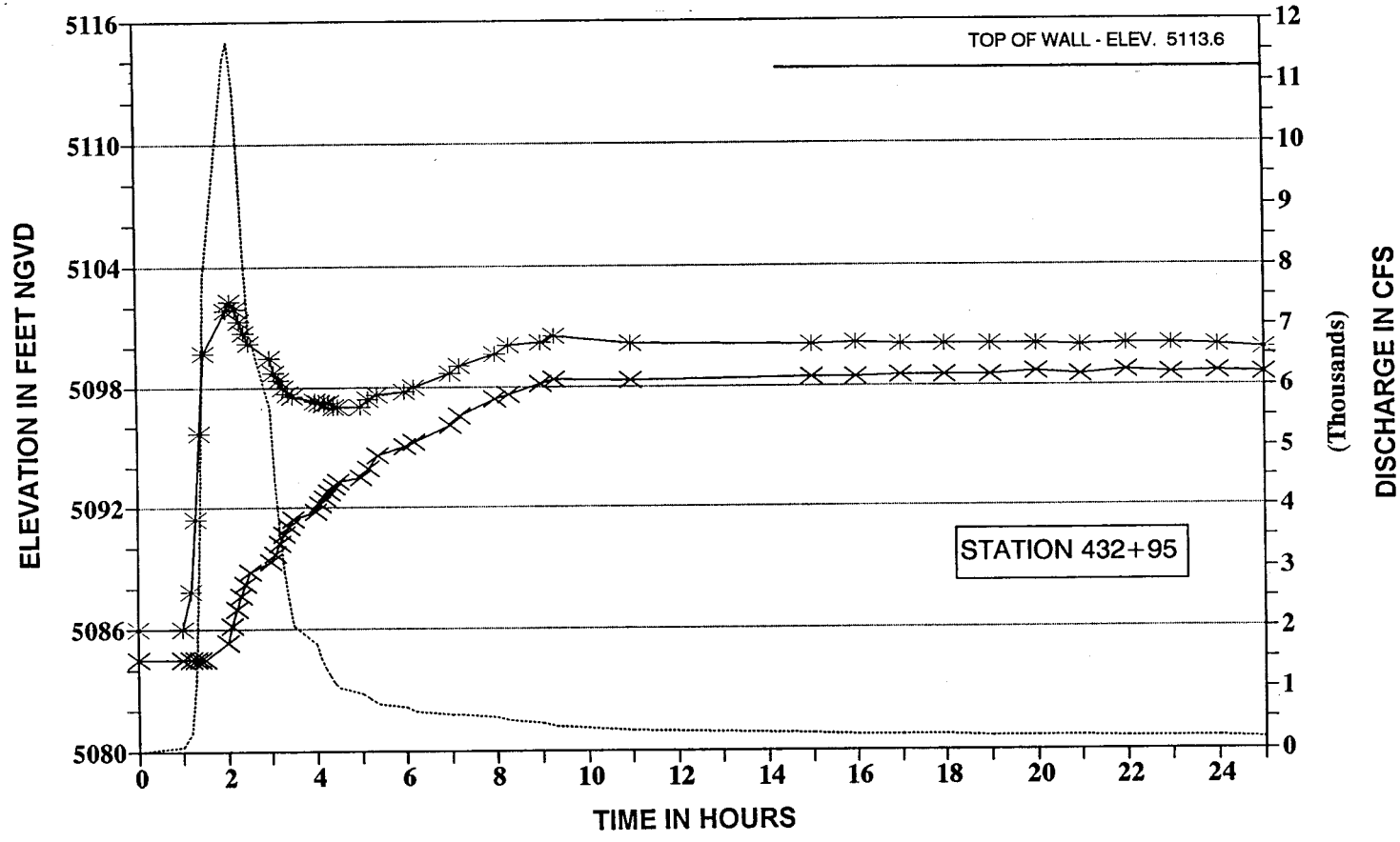

VARIATION OF STAGE AND BED ELEVATION
100-YEAR-FREQUENCY FLOOD
EMBUDO CHANNEL AT STATION 432+95

Plate 23

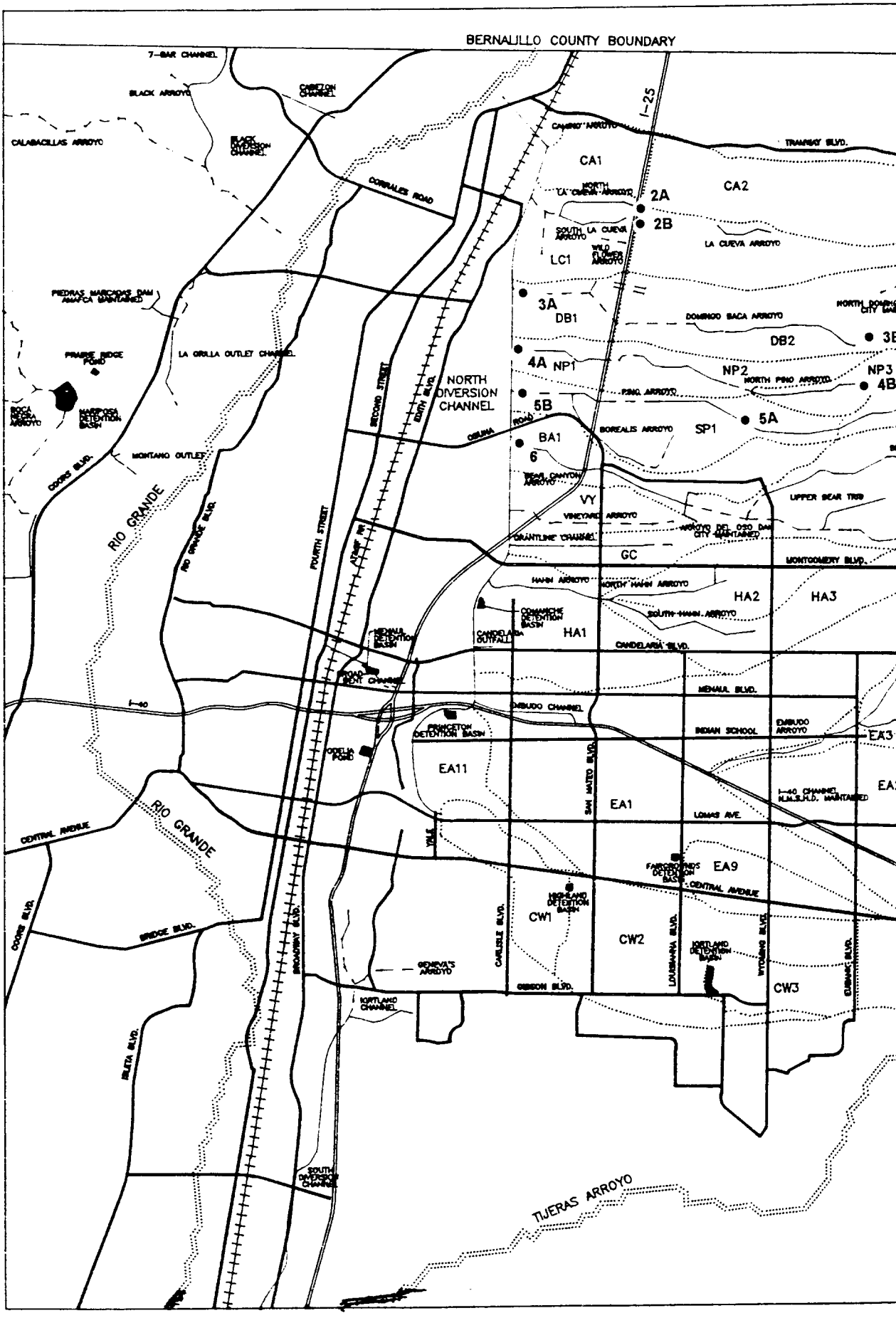
BERNALILLO COUNTY BOUNDARY
7-BAR CHANNEL
BLACK ARROYO
CARLTON CHANNEL
CALABACILLAS ARROYO
BLACK DIVERSION CHANNEL
CORRALES ROAD
I-25
CAMINO ARROYO
TRAMWAY BLVD.
CA1
CA2
NORTH LA CUEVA ARROYO
2A
2B
SOUTH LA CUEVA ARROYO
LA CUEVA ARROYO
WILD CHERRY ARROYO
LC1
PIEDRAS MARCADAS DAM AMAFCA MAINTAINED
3A
DB1
DOMINGO BACA ARROYO
DB2
3B
PRAIRIE BRIDGE POND
LA GRULLA OUTLET CHANNEL
4A
NP1
NP2
NP3
4B
NORTH PINO ARROYO
PINO ARROYO
NORTH DIVERSION CHANNEL
SECOND STREET
SOUTH 1ST ST.
5B
ROAD
OSUNA
BOREALIS ARROYO
SP1
5A
BA1
6
BOCA NEGRA ARROYO
MARIPOSA DETENTION BASIN
MONTANO OUTLET
COORS BLVD.
TIJERAS CANYON ARROYO
VY
VINEYARD ARROYO
UPPER BEAR TRIB
ARROYO DEL OSO DAM CITY MAINTAINED
RIO GRANDE
RIO GRANDE BLVD.
FOURTH STREET
ATRISCO DR.
GRANTLINE CHANNEL
GC
MONTGOMERY BLVD.
HAHN ARROYO
NORTH HAHN ARROYO
HA2
HA3
COMANCHE DETENTION BASIN
HA1
SOUTH HAHN ARROYO
CANDELARIA OUTFALL
CANDELARIA BLVD.
MENAUL BLVD.
I-40
EMBUDO CHANNEL
PRINCETON DETENTION BASIN
INDIAN SCHOOL
EMBUDO ARROYO
EA3
ODELIA ROAD
EA11
SAN MATEO BLVD.
EA1
I-40 CHANNEL N.M.S.H.D. MAINTAINED
LOMAS AVE.
YALE
CENTRAL AVENUE
RIO GRANDE
FAIRGROUNDS DETENTION BASIN
EA9
CENTRAL AVENUE
COORS BLVD.
BRIDGE BLVD.
BROADWAY BLVD.
HORNERS DETENTION BASIN
CW1
CARLISLE BLVD.
CW2
LOUISIANA BLVD.
HORTLAND DETENTION BASIN
WYOMING BLVD.
CW3
EUBANK BLVD.
GIBSON BLVD.
HORNERS ARROYO
HORTLAND CHANNEL
ISLETA BLVD.
SOUTH DIVERSION CHANNEL
TIJERAS ARROYO

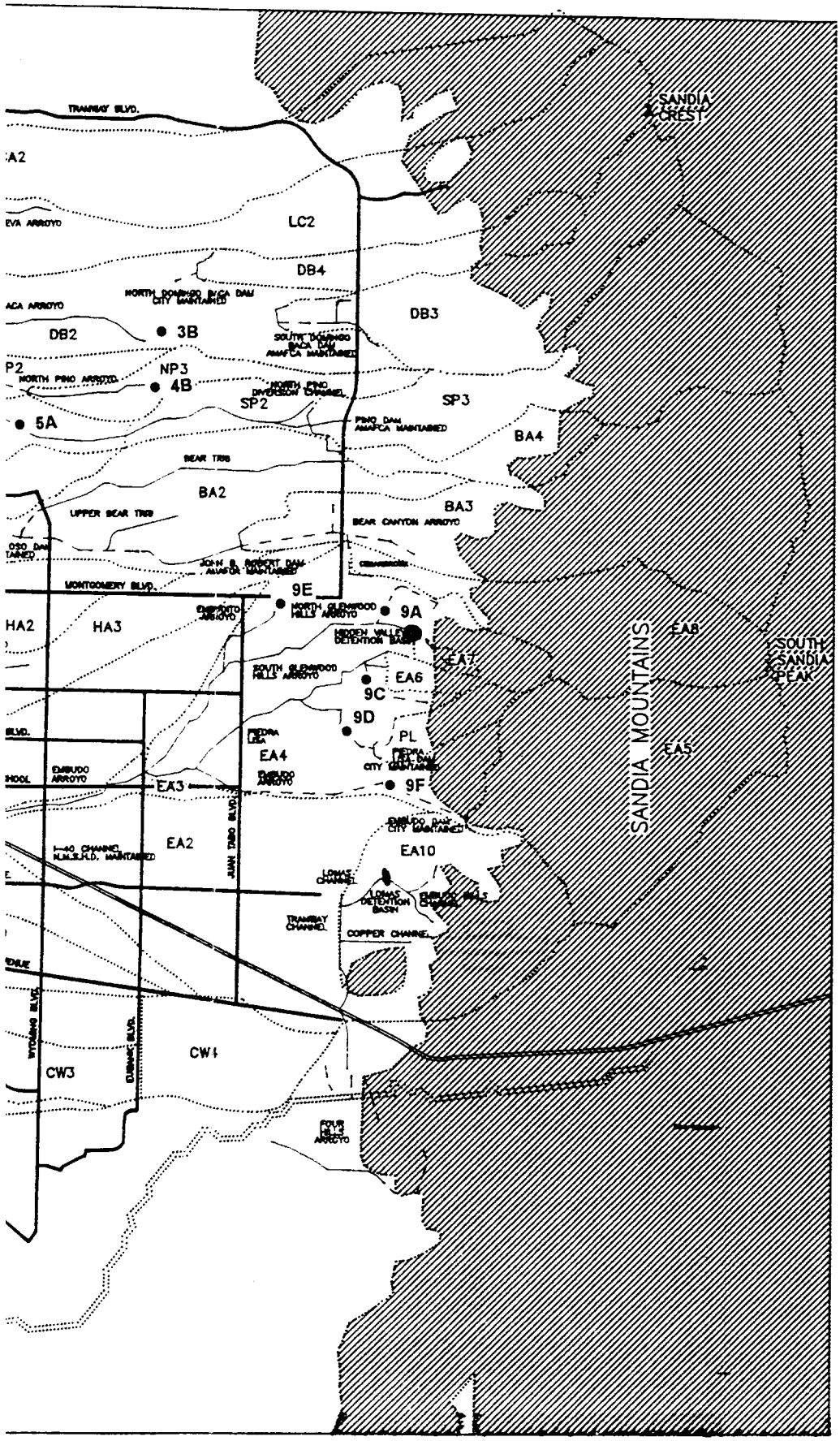

N

SCALE IN MILES

1 0 1 2

LEGEND

- DETENTION BASIN
- INTERSTATE HIGHWAY
- OTHER MAJOR ROAD
- LINED ARROYO OR CHANNEL
- UNLINED ARROYO OR CHANNEL
- EA1 SUBAREA DESIGNATION
- SUBAREA BOUNDARY
- 2A CONCENTRATION POINT

ALBUQUERQUE ARROYOS FEASIBILITY STUDY

WATERSHED MAP

ALBUQUERQUE DISTRICT, CORPS OF ENGINEERS

PLATE A-1

Appendix A
Geomorphic and Sediment Yield Computations

Table A1
Summary of Geomorphological Observation

Arroyo & Subreach	[1]Quadrant & Zone 1:2:3:4	Dams or Sediment Detention Structures	[2]Channel Type C:L:UL	Sediment Sources			Sediment Delivery to North Diversion Channel		
				Watershed Sources	Vertical Channel Stability Aggradation/ Degradation	Lateral Channel Stability	Stilling Basin Y:N	[3]Magnitude of Sediment Delivery H:M:L	Comments
Camino Downstream I-25	NE 3	Detention U/S I-25 - local scour D/S ~ 200'	UL	Small gullies, gullied headwall at gravel pit	Primarily aggradation	No evidence of lateral migration	Gravel Pit and detention basin	L	Local erosion over headwall of gravel pit
North LaCueva Upstream I-25	NE 3	Detention U/S of Runway culverts	UL	Gullying, local development runoff	Severe degradation (10') San Pedro to I-25 ~ 200' of erosion	Incised channel mass failure	N	M - derived from U/S I-25	Local channel incision U/S I-25
North La Cueva Downstream I-25	NE 3	None	L	Incision U/S of I-25	Lined	Lined	N	M - local source	Sediment Delivery = Sediment Yield to NDC
South LaCueva Upstream I-25	NE 3	U/S of cemetery culverts, U/S of I-25 culverts	C - U/S UL - local bank erosion	Mainly deposited U/S of cemetery	Aggradation U/S of I-25 culvert	Minor bank erosion U/S I-25	I-25 caused backwater	L	Some sediment derived from lot on E. side of I-25

[1]Quadrant and Zone

1 - Within the Sandias
2 - Upstream of Tramway Blvd.
3 - Downstream of Tramway Blvd.
4 - Rio Grande Floodplain

[2]Channel Type

C - Closed Conduit
L - Open Lined Conduit
UL- Unlined Channel

[3]Magnitude of Sediment Delivery

H - High
M - Medium
L - Low

Table A1 (Continued)

Arroyo & Subreach	Quadrant & Zone 1:2:3:4	Dams or Sediment Detention Structures	Channel Type C:L:UL	Sediment Sources			Sediment Delivery to North Diversion Channel		
				Watershed Sources	Vertical Channel Stability Aggradation/ Degradation	Lateral Channel Stability	Stilling Basin Y:N	Magnitude of Sediment Delivery H:M:L	Comments
Domingo Baca. Downstream I-25	NE 3	N. Domingo Baca. and S. Domingo Baca Dams	UL has been graded to ~1:3 side slopes	Bank erosion. Tributary gullying and widening due to base level lowering of Domingo Baca.	Aggradation U/S of Washington St. Local degradation on D/S side of Washington. Headcut and bank erosion (8-10'). Lateral on N. side (N. Domingo Baca.) degrading severely due to base level lowering	Meandering channel lateral erosion from Paseo del Norte culvert D/S eroding into 3:1 side slopes	Y	M - locally high D/S of Washington St. and at confluence with the north side lateral U/S of Jefferson St.	Washington St. and U/S too flat - sediment is depositing U/S. Local removal of sediment on road. Delivery to NDC depends on trap efficiency of stilling basin D/S of Washington St.
North Domingo Baca Downstream of dam	NE 2	North Domingo Baca Dam ~ 100% trap efficiency	UL 1st ~ 150' D/S of dam channel lined with gabion mattress	Clear water scour due to high trap efficiency of dam	Severe degradation D/S for ~ 900' D/S the channel is aggradational (local fans). Sediment supply ≈ transport capacity	Mass failure of banks due to incision. Retrogressive uphill failure on south bank.	N	L - depends on how much sediment makes it D/S of I-25	Good example of effects of very high trap efficiency dam - U/S watershed sediment supply is irrelevant to NDC

Table A1 (Continued)

Arroyo & Subreach	[1]Quadrant & Zone 1:2:3:4	Dams or Sediment Detention Structures	[2]Channel Type C:L:UL	Sediment Sources			Sediment Delivery to North Diversion Channel		
				Watershed Sources	Vertical Channel Stability Aggradation/ Degradation	Lateral Channel Stability	Stilling Basin Y:N	[3]Magnitude of Sediment Delivery H:M:L	Comments
South Domingo Baca Downstream of dam. (Garbage dump on valley floor U/S of Browning)	NE 2	South Domingo Baca Dam ~ 100% trap efficiency	UL, first ~ 200' is lined with rock and rubble D/S for ~ 1000' severe channel erosion, headcut is ~ 5-6' high	Clear water scour due to high trap efficiency of dam	~ 6-8' of degradation D/S of dam for about 1000' causing bank erosion. Very coarse bed material from old debris flow deposit	Mass failure of the banks in incised reach, lateral erosion by fluvial activity. $CaCo_3$ cementing older (Pliestocene) sediments	Y at Holbrook Street develop-ment. Start of lined channel.	M - sediment supply = transport capacity at Holbrook at start of lined section, but detention basin has high trap efficiency	Good example of channel compensation for clear water scour D/S of dam. Base level lowering at Holbrook St. increasing slope upstream
North Pino	NE 3	Grading on U/S side of Holbrook has blocked the channel and formed an informal basin	UL becomes L at Holbrook Street	Roads have concentrated and diverted flows, local small gullies relatively undeveloped	Aggradational	Stable - some minor lateral migration due to avulsive behavior on small in-channel fans	Y on D/S side of Holbrook head of lined section. Y at NDC	M (potential) transport will equal capacity if blockage is removed, but most sediment will be trapped in the basin	Large flood will probably cause removal of blockage and lead to severe erosion locally of the fill material
South Pino Upstream of Wyoming Blvd. (Albuquerque Academy) Downstream of Ventura	NE 3	Pino Dam and Tanoan golf course	UL in Academy reach but lined and grassed U/S	High trap efficiency of dam, golf course (Tanoan) and lined sections through developments	Aggradational. Local bank erosion in Academy grounds	Lateral migration in Academy grounds mass failure where h > hc, caliche reinforced on TLB	Y U/S of Wyoming at head of lined section, Y at NDC	L, paved and grassed watershed - local erosion sediment is trapped in stilling basin	Detention basin and USGS gage at concrete sill could be used to develop sediment yields if monitored

Table A1 (Continued)

Arroyo & Subreach	[1]Quadrant & Zone 1:2:3:4	Dams or Sediment Detention Structures	[2]Channel Type C:L:UL	Sediment Sources			Sediment Delivery to North Diversion Channel		
				Watershed Sources	Vertical Channel Stability Aggradation/ Degradation	Lateral Channel Stability	Stilling Basin Y:N	[3]Magnitude of Sediment Delivery H:M:L	Comments
Bear Downstream of Wyoming and Upstream of dam at Arroyo del Oso Park (start of lined section)	NE 3	Bear Canyon Dam (John B. B. Roberts). Dam at Arroyo del Oso Park	UL Lined on D/S side of ADO dam	Floodplain encroachment and filling, tributary degradation and widening	Some degradation D/S of Wyoming for ~ 2200' due to channel confinement. Aggradation D/S to dam, 2 concrete sills (5' drop) across channel	900' D/S of Wyoming channel has been narrowed by emplacement of gabions. Next 1200' some bank erosion but floodplain encroachment with concrete rubble etc. is limiting bank erosion	Y Arroyo del Oso Dam, very high trap efficiency	L, sediment trapped U/S of dam	Good example of the effects of constriction on channel incision, also increased runoff effects from urbanization
Bear North side tributary at Arroyo del Oso Park	NE 3	5 concrete sills - grade control structures between Wyoming Blvd. and Spain Rd.	UL, grade-control U/S of Spain Rd.	Local bank erosion	D/S of Spain Road about 10-15' of degradation due to channel shortening and base level lowering in Bear Arroyo	Mass failure of the banks due to incision	N	H, locally due to channel erosion, does not get beyond Arroyo del Oso Dam	Urbanization and channel relocation (> S) have caused severe channel erosion D/S of Spain Road

Table A1 (Continued)

Arroyo & Subreach	[1]Quadrant & Zone 1:2:3:4	Dams or Sediment Detention Structures	[2]Channel Type C:L:UL	Sediment Sources			Sediment Delivery to North Diversion Channel		
				Watershed Sources	Vertical Channel Stability Aggradation/ Degradation	Lateral Channel Stability	Stilling Basin Y:N	[3]Magnitude of Sediment Delivery H:M:L	Comments
Bear Downstream of San Mateo Blvd. to I-25	NE 3	Arroyo del Oso Dam and John B. Roberts Dam	UL, grade-control sill at San Mateo. 6-7' deep scour hole at D/S end of sill	Recent removal of vegetation has created potential for bank erosion	Controlled by grade-control U/S and box culverts under I-25, some degradation immediately D/S of San Mateo culvert outlet	First flows will cause some erosion of the disturbed banks	Y, flow expansion zone	L	Vegetation removal will locally increase sediment supply to NDC
Bear Downstream of I-25 to Kircher Blvd.	NE 3	Arroyo del Oso Dam and John B. Roberts Dam	UL 20' drop grade-control structure ~ 300' of toe rock on lower banks D/S of structure	No local sources	Controlled by grade-control structures. Aggradation extends ~ 500' U/S of next grade-control structure	Controlled by toe rock	Y, backwater from next D/S structure to give required tailwater for U/S grade-control structure	L	Wetland formed in D/S aggradation zone
Bear Kircher Blvd. NDC	NE 3	Arroyo del Oso Dam and John B. Roberts Dam	UL, 2 ~ 20' drop grade-control structures. Gabion contraction dikes at head of stilling basin	Minor local erosion from runoff from parking lots	Controlled by grade-control structures. Local aggradation U/S of both grade-control structures	Controlled by toe rock at U/S grade-control, but some lateral erosion D/S of lower grade-control - no toe rock	Y	L	Contraction dikes cause backwater U/S to provide suitable tailwater conditions for lower grade-control structure

Table A1 (Continued)

Arroyo & Subreach	[1]Quadrant & Zone 1:2:3:4	Dams or Sediment Detention Structures	[2]Channel Type C:L:UL	Sediment Sources			Sediment Delivery to North Diversion Channel		
				Watershed Sources	Vertical Channel Stability Aggradation/ Degradation	Lateral Channel Stability	Stilling Basin Y:N	[3]Magnitude of Sediment Delivery H:M:L	Comments
Embudito Downstream of Montgomery Blvd.	NE	—	UL, 18 concrete sills - grade-control vary from 2-3' drop. Grouted rock in bed for ~ 200' to start of D/S lined channel	Local bank erosion D/S of each grade-control structure, local gullying due to runoff from school grounds	Controlled by grade control structures, local scour on D/S side of each of the grade-control sills	Minor bank erosion between grade-control structures	N	L-M (high runoff potential due to urbanization). If sills do not fail, potential will decrease rapidly with each flow.	Highway runoff at U/S end has provided enough water to maintain a grass-lined channel ~ 400'
North Glenwood Hills Montgomery Blvd. N.E. to Tramway Blvd.	NE 2	Hidden Valley detention basin (A major storm could cause basin to fill completely-incised fan upstream)	UL, Glenwood Hills Dr. U/S grouted rock grade-control structures. D/S to Tramway gabion-type grade-control structures	Close to the Sandia's high potential, during large event, to supply a lot of sediment	U/S of Hidden Valley detention basin outlet. D/S of Glenwood Hills Dr. most of the grade-control is failing	Erosion between grade-control sills. The channel has been narrowed, could unravel very easily	N	H, (potential), if the channel erodes during an event, very steep channel	A large storm could cause this channel to unravel completely; lower reach in poor condition
South Glenwood Hills Camino de la Sierra to Embudito Dr.	NE 2	2 detention basins constructed at base of alluvial fans	C, closed conduits from detention basins	Hillslope erosion and alluvial fan incision	Local incision into fan	Local fan incision and channel widening	Y	L, detention basins on both branches	2 branches drain small valleys in Sandias; detention basins eliminate sediment delivery

Table A1 (Concluded)

Arroyo & Subreach	[1]Quadrant & Zone 1:2:3:4	Dams or Sediment Detention Structures	[2]Channel Type C:L:UL	Sediment Sources			Sediment Delivery to North Diversion Channel		
				Watershed Sources	Vertical Channel Stability Aggradation/ Degradation	Lateral Channel Stability	Stilling Basin Y:N	[3]Magnitude of Sediment Delivery H:M:L	Comments
Tributary South Glenwood Hills	NE 2	—	UL, D/S of Graham Dr. the channel is eroding - failed concrete grade-control structures	Incised fan U/S of Camino de la Sierra (probably dug out to concentrate flows)	Degrading D/S of Graham Dr. Concrete grade-control sills have been undermined and have failed	Bank erosion where there has been channel incision in the lower reach	N	H, potential channel erosion	Bonita Dr. is the channel for flows from U/S of Camino de la Sierra
Piedra Lisa Punta da Vista to Tramway Blvd.	NE 2	Piedra Lisa Dam	UL, 23 concrete grade-control sills in a channel distance of ~ 1500'	Dam has very high trap efficiency, local erosion of slopes D/S of dam	Controlled by grade-control sills. Local scour D/S of sills	Minor channel bank erosion between grade-control sills	N	L	Large storm could cause some severe bank erosion between grade-control structures
Embudo Dam to Monte Largo Dr.	NE 1	Embudo Dam	UL, 2 soil-cement grade-control structures immediately U/S of Monte Largo which is start of lined channel all the way to NDC	Large active alluvial fan on the north side of arroyo D/S of dam	Degradation due to stormwater runoff from development on south side of arroyo ~ 6-7' of incision	Mass failure of the banks in the incised reach of the valley floor fan	Treads of the grade-control structures are storing sediment	H	Very good example of increased runoff due to development causing channel incision

Table A2
Measured Sediment Concentrations Composite Samples

Location (Source)	Date	Concentration mg/l	Percent Finer 0.0625 mm
Tijeras Canyon [1]	1937-1947	58,000	88
Embudo Arroyo [1]	1953	9,000-29,000	
Manzano Mtns Arroyo [1]		16,000	
North Diversion Channel [2]	1982-1991	300-15,000	70
Tortugas Reservoir [3]	1963-1974	57,800*	
Bernalillo Reservoir [4]	1956-1974	176,700*	

*Calculated from measured outflow and deposition.
[1] USAED Albuquerque 1956.
[2] USGS 1982, 1983.
[3] Funderburg and Roybal 1977.
[4] Funderburg (1977)

Table A3
Measured Sediment Concentrations Upstream from Bernalillo Reservoir[1]

Date	Discharge cfs	Concentration mg/l	Percent Finer 0.0625 mm
1952	20	278,000	53
1957	30	13,400	63
1957	25	4,000	100
1957	-	21,700	86
1957	-	10,800	89
1959	30	66,400	76
1959	10	24,500	91
1963	-	61,400	79
1963	-	65,400	95
1963	-	48,300	91
1964	20	85,800	65
1964	1	85,300	57

[1] Funderburg 1977.

Table A4
Unofficial Sediment Yields by Soil Type (SCS)

Soil Classification	Sediment Yield (acre-ft/acre/yr)	Sediment Yield (acre-ft/square mile/yr
Badland	0.006250	4.00
Rough Broken Land	0.003125	2.00
Bluepoint	0.001063	0.68
Caliza	0.001220	0.78
Wink	0.000648	0.41
Madurez	0.000648	0.41
Caja	0.001328	0.84
Witt	0.000440	0.28
Monzano	0.000500	0.32
Hap	0.000312	0.20
Embudo	0.000462	0.30
Tijeras	0.000358	0.23
Ildefonso	0.000688	0.44
Dean	0.000375	0.24
Laporte	0.000645	0.41
Travessilla	0.000680	0.43
Pajarito	0.000224	0.14
Pino	0.001047	0.67
Wilcoxson	0.000491	0.31
Supervisor	0.000491	0.31
Akela	0.000687	0.44
Alemada	0.000453	0.29
Salas	0.000250	0.16
Scholle	0.000203	0.13
Washoe	0.000203	0.13
Tome	0.000547	0.35
Adelino	0.000547	0.35
Atrisoc	0.000488	0.31
Gila	Irrigated Bottom Land	
Vinton	Irrigated Bottom Land	
Agua	Irrigated Bottom Land	

Table A5
Summary of Hydrologic Computation Results

Location	Concentration Point[1]	Drainage Area (square mile)	Storm Centering	100-Year		50-Year		25-Year		10-Year		5-Year		2-Year	
				QP (cfs)	Vw (acre-ft)	QP (cfs)	Vw (acre-ft)	QP (cfs)	Vw (acre-ft)	Qp (cfs)	Vw acre-ft	Qp (cfs)	Vw (acre-ft)	Qp (cfs)	Vw (acre-ft)
North La Cueva upstream Coronado Airport	2a	5.91	3	1,407	244	679	125	477	92	269	57	154	37	112	27
South La Cueva upstream Coronado Airport	2b	0.53	3	422	22	206	11	141	8	74	5	37	3	26	2
Domingo Baca at NDC	3a	11.55	3	2,575	256	2,109	451	1,598	350	1,000	231	590	146	193	63
South Domingo Baca at Holbrook	3b	5.49	3	869	53	720	44	559	34	352	23	216	15	73	7
North Pino at NDC	4a	2.7	2	1,817	169	1,510	144	1,181	116	793	84	526	59	241	33
North Pino at Holbrook	4b	0.80	2	771	49	655	41	527	32	380	24	232	15	86	7
South Pino at Wyoming	5a	5.98	2	1,098	66	946	56	776	46	552	34	385	25	180	14
South Pino at NDC	5b	9.33	2	2,276	380	1,935	318	1,554	249	992	166	748	115	402	68
Bear at NDC	6	15.51	2	1,750	794	1,493	665	1,197	485	855	353	607	221	354	126
Embudito	9e	0.82	4	1,489	67	1,293	58	1,074	49	815	39	568	29	315	20
North Glenwood Hills	9a	0.90	4	777	51	652	42	521	33	366	23	220	14	69	6
South Glenwood Hills Tributary	9c	0.19	4	361	16	315	14	267	12	205	10	146	7	80	5
Piedra Lisa upstream Tramway Boulevard	9d	0.63	4	59	32	53	26	51	20	44	12	36	7	9	1
Embudo upstream Monte Largo	9f	3.72	4	280	160	260	131	229	96	191	56	144	31	24	4

[1]See Plate A-1 for location.

Table A6
Summary of K Values Used in MUSLE Computations

Soil Type	K	Percent Silt/Clay (<0.074 mm)	
		Minimum	Maximum
Bluepoint-Kokan Association, hilly (BKD)	0.12	3	20
Embudo, gravelly fine sandy loam, 0.5% slopes (Emb)	0.15	25	50
Embudo-Tijeras complex, 0-9% slopes (EtC)	0.21	28	54
Tijeras gravelly fine sandy loam, 1-5% slopes (TgB)	0.19	35	65
Wink-Embudo complex, 0-5% slopes (WeB)	0.27	28	43
Cut and fill land (Cu)	0.40	26	47
Madurez-Wink Association, gently sloping (MWA)	0.27	36	52

Table A7
Summary of Soil Type Distribution and MUSLE Computations

Basin Designation	Soil Type (square miles)								Total	Weighted K	CP	Avg Slope Length (ft)	Avg Slope (ft/ft)	n	LS
	BKD	EmB	EtC	TgB	WeB	Cu	MWA	(Upland) Other							
CA1	0.077	0.057	0.652	0.000	0.000	0.000	0.000	0.000	0.786	0.197	0.4	250	0.025	0.3	0.318
CA2	0.000	0.446	2.626	0.020	0.000	0.000	0.000	1.843	4.935	0.126	0.4	150	0.04	0.4	0.469
LC1	0.091	0.444	0.599	0.000	0.168	0.000	0.000	0.000	1.302	0.191	0.4	250	0.02	0.3	0.263
LC2	0.000	1.383	1.776	0.081	0.000	0.000	0.000	3.201	6.440	0.092	0.4	200	0.05	0.4	0.682
DB1	0.000	0.624	0.005	0.000	0.080	0.000	0.000	0.000	0.709	0.164	0.4	250	0.02	0.3	0.263
DB2	0.000	1.252	2.875	0.542	0.000	0.000	0.000	0.000	4.669	0.192	0.4	200	0.03	0.4	0.390
DB4	0.000	0.121	0.670	0.128	0.000	0.000	0.000	0.631	1.551	0.118	0.4	300	0.05	0.4	0.802
DB3	0.000	0.153	0.485	0.206	0.000	0.000	0.000	3.725	4.569	0.036	0.4	300	0.05	0.4	0.802
DB3	0.000	0.409	0.000	0.000	0.000	0.000	0.000	0.000	0.443	0.139	0.4	150	0.02	0.3	0.226
DB3	0.000	0.332	0.608	0.203	0.000	0.000	0.000	0.000	1.144	0.189	0.4	200	0.03	0.4	0.390
DB3	0.000	0.193	0.674	0.224	0.000	0.000	0.000	0.000	1.091	0.195	0.4	275	0.035	0.4	0.517
SP3	0.000	0.256	0.417	0.067	0.000	0.000	0.000	4.221	4.960	0.028	0.4	300	0.06	0.5	1.162
SP1	0.000	0.888	0.999	0.353	0.044	0.000	0.000	0.000	2.284	0.185	0.1	200	0.03	0.4	0.390
SP2	0.000	0.383	0.450	0.073	0.000	0.000	0.000	0.000	0.905	0.183	0.4	250	0.04	0.4	0.575
BA4	0.000	0.134	0.074	0.165	0.000	0.000	0.000	0.722	1.095	0.061	0.4	300	0.04	0.4	0.618
BA1	0.000	0.879	0.690	0.149	0.000	0.000	0.000	0.000	1.718	0.178	0.1	250	0.02	0.3	0.263
BA2	0.000	0.817	1.951	0.613	0.000	0.000	0.000	0.030	3.411	0.190	0.25	250	0.03	0.4	0.426
BA3	0.000	0.619	0.573	0.227	0.000	0.000	0.000	5.894	7.312	0.035	0.4	300	0.04	0.4	0.618

(Continued)

Table A7 (Concluded)

Basin Designation	Soil Type (square miles)								Total	Weighted K	CP	Avg Slope Length (ft)	Avg Slope (ft/ft)	n	LS
	BKD	EmB	EtC	TgB	WeB	Cu	MWA	(Upland) Other							
EA8	0.000	0.181	0.104	0.000	0.000	0.000	0.000	2.783	3.068	0.016	0.4	400	0.06	0.5	1.341
EA7	0.000	0.007	0.000	0.000	0.000	0.000	0.000	0.141	0.148	0.007	0.4	400	0.15	0.5	5.184
EA6	0.000	0.006	0.000	0.000	0.000	0.000	0.000	0.182	0.188	0.005	0.4	400	0.15	0.5	5.184
PL	0.000	0.000	0.002	0.000	0.000	0.000	0.000	0.514	0.516	0.001	0.4	400	0.15	0.5	5.184
EA4	0.000	0.940	3.064	0.573	0.000	0.000	0.000	1.759	6.336	0.141	0.2	275	0.04	0.4	0.597
EA5	0.000	0.076	0.000	0.000	0.000	0.000	0.000	3.252	3.329	0.003	0.4	400	0.15	0.5	5.184
2A	0.000	1.266	1.627	0.075	0.000	0.000	0.000	2.933	5.900	0.092	0.4	200	0.05	0.4	0.682
2B	0.000	0.509	0.027	0.000	0.000	0.000	0.000	0.000	0.536	0.153	0.4	200	0.03	0.4	0.390
3B	0.000	0.450	0.466	0.113	0.000	0.000	0.000	0.000	1.028	0.182	0.4	250	0.04	0.4	0.575
4B	0	0.191	0.453	0.156	0.000	0.000	0.000	0.000	0.800	0.192	0.4	200	0.03	0.4	0.390
9A	0.000	0.150	0.014	0.000	0.000	0.000	0.000	0.734	0.899	0.028	0.4	200	0.04	0.4	0.526
9C	0.000	0.044	0.028	0.000	0.000	0.000	0.000	0.117	0.189	0.066	0.2	200	0.04	0.4	0.526
9E	0.000	0.172	0.631	0.000	0.000	0.000	0.000	0.020	0.823	0.192	0.1	50	0.02	0.3	0.163

Table A8
Summary of Fine Sediment Concentrations

Basin	Storm Centering	2-Year Average Fine Sediment Conc., Cf (Total basin to this point)	5-Year Average Fine Sediment Conc., Cf (Total basin to this point)	10-Year Average Fine Sediment Conc., Cf (Total basin to this point)	25-Year Average Fine Sediment Conc., Cf (Total basin to this point)	50-Year Average Fine Sediment Conc., Cf (Total basin to this point)	100-Year Average Fine Sediment Conc., Cf (Total basin to this point)
CA1	3	6743	8877	9928	10804	11242	11554
CA2	3	6317	8384	9325	10122	10550	10844
LC1	3	6560	8098	8922	9736	10153	10420
LC2	3	6339	7591	8353	9097	9500	9788
DB1	3	7004	8779	9585	10303	10706	10959
DB2	3	7041	8818	9598	10306	10700	10961
DB4	3	9177	10786	11593	12271	12714	13002
DB3	3	2640	3389	3694	3952	4115	4221
NP1	2	11312	13390	14277	15238	15690	20394
NP2	2	12528	14912	15832	16861	17310	22929
NP3	2	15483	18983	20116	21368	21943	33124
SP3	2	2819	3307	3830	4197	4419	4549
SP1	2	4152	4859	5354	5787	6009	6135
SP2	2	4856	5718	6357	6849	7116	7263
BA4	2	4283	5818	6313	6591	6833	6938
BA1	2	3214	3868	4192	4502	4672	4781
BA2	2	3460	4180	4534	4870	5057	5175
BA3	2	1863	2358	2663	2897	3037	3121
EA8	4	0	652	2628	2877	3005	3095
EA7	4	0	6657	6596	6305	6545	6657
EA6	4	0	4259	4209	4538	4619	4617
PL	4	774	809	861	891	919	931
EA4	4	0	3256	3975	4229	4361	4469
EA5	4	1847	2415	2597	2756	2850	2919
2A	3	6187	6436	7266	8104	8625	9653
2B	3	7679	7826	9201	10717	11509	12660
3B	3	4797	6218	6771	7312	7561	7745
4B	2	10688	13285	14227	15041	15230	15424
9A	4	2161	2848	3043	3164	3226	3267
9C	4	2101	2536	2621	2805	2875	2926
9E	4	1149	1357	1458	1539	1585	1610

Table A9
Fine Sediment Yield Calculations for the 2-year Storm

Basin Designation	Qp (cfs)	Vw (ac-ft)	Percent Impervious	Sediment Yield (tons)	Unit Sediment Yield tons/acre	% Soils <0.074		Minimum			Maximum			Average Fine Sediment Concentration Cf (ppm)	Weighted Average Fine Sediment Concentration[1] Cf (ppm)
						min	max	Fine Sediment Yield (tons)	Cf (ppm)	Unit Fine Sediment Yield tons/acre	Fine Sediment Yield ton(s)	Cf (ppm)	Unit Fine Sediment Yield tons/acre		
CA1	59	4	10	137	0.27	25.3%	50.4%	35	6,329	0.07	69	12,509	0.14	9,419	6,743
CA2	72	15	5	320	0.10	27.6%	53.5%	88	4,313	0.03	171	8,321	0.05	6,317	6,317
LC1	107	8	10	226	0.27	25.2%	48.8%	57	5,228	0.07	111	10,071	0.13	7,650	6,560
LC2	153	38	10	830	0.20	26.9%	52.6%	223	4,303	0.05	436	8,375	0.11	6,339	6,339
DB1	59	4	10	94	0.21	25.4%	49.2%	24	4,389	0.05	47	8,486	0.10	6,437	7,004
DB2	225	30	10	1,068	0.36	28.0%	54.2%	299	7,281	0.10	579	13,995	0.19	10,638	7,041
DB4	60	14	10	422	0.43	28.6%	55.0%	121	5,300	0.12	232	12,055	0.23	9,177	9,177
DB3	50	15	5	127	0.04	29.2%	56.0%	37	1,811	0.01	71	3,469	0.02	2,640	2,640
NP1	44	3	10	57	0.20	25.2%	49.5%	14	3,505	0.05	28	6,849	0.10	5,177	11,312
NP2	218	20	30	641	0.88	28.4%	54.8%	182	6,651	0.25	351	12,765	0.48	9,708	12,528
NP3	104	10	10	507	0.73	28.9%	55.6%	147	10,667	0.21	282	20,299	0.40	15,483	15,483
SP3	44	13	5	123	0.04	27.6%	53.6%	34	1,918	0.01	66	3,720	0.02	2,819	2,819
SP1	381	41	30	320	0.22	27.9%	53.9%	89	1,602	0.06	173	3,090	0.12	2,346	4,152
SP2	180	14	20	771	1.33	27.3%	53.2%	210	10,936	0.36	410	21,094	0.71	16,015	4,856
BA4	13	2	0	27	0.04	30.0%	57.4%	8	2,946	0.01	15	5,621	0.02	4,283	4,283
BA1	332	33	30	171	0.16	27.1%	52.9%	46	1,029	0.04	90	2,009	0.08	1,519	3,214

(Continued)

[1]Includes all fine sediment and runoff volume for upstream watersheds.

Table A9 (Concluded)

Basin Designation	Qp (cfs)	Vw (ac-ft)	Percent Impervious	Sediment Yield (tons)	Unit Sediment Yield tons/acre	% Soils <0.074		Minimum			Maximum			Average Fine Sediment Concentration Cf (ppm)	Weighted Average Fine Sediment Concentration Cf (ppm)
						min	max	Fine Sediment Yield (tons)	Cf (ppm)	Unit Fine Sediment Yield tons/acre	Fine Sediment Yield ton(s)	Cf (ppm)	Unit Fine Sediment Yield tons/acre		
BA2	579	72	30	1,562	0.72	28.5%	55.0%	446	4,535	0.20	859	8,705	0.39	6,620	3,460
BA3	62	21	5	130	0.03	27.8%	54.0%	36	1,267	0.01	70	2,458	0.02	1,863	1,863
EA8	0	0	0	0	0.00	26.1%	51.5%	0	0	0.00	0	0	0.00	0	0
EA7	5	0	0	0	0.00	25.0%	50.0%	0	0	0.00	0	0	0.00	0	0
EA6	6	0	0	0	0.00	25.0%	50.0%	0	0	0.00	0	0	0.00	0	0
PL	15	1	0	3	0.01	28.0%	54.0%	1	529	0.00	1	1,019	0.00	774	774
EA4	741	153	35	2,112	0.52	28.3%	54.6%	597	2,862	0.15	1,152	5,511	0.28	4,186	2,625
EA5	25	4	0	27	0.01	25.0%	50.0%	7	1,232	0.00	13	2,461	0.01	1,847	1,847
2A	112	27	10	575	0.15	26.9%	52.6%	155	4,200	0.04	302	8,175	0.08	6,187	6,187
2B	26	2	10	56	0.16	25.1%	50.2%	14	5,143	0.04	28	10,214	0.08	7,679	7,679
3B	70	7	10	344	0.52	27.5%	53.5%	94	9,823	0.14	184	18,949	0.28	14,386	4,797
4B	86	7	20	245	0.48	28.7%	55.2%	70	7,337	0.14	135	14,039	0.26	10,688	10,688
9A	69	6	6	47	0.08	25.3%	50.3%	12	1,446	0.02	24	2,877	0.04	2,161	2,161
9C	80	5	35	37	0.30	26.2%	51.6%	10	1,416	0.08	19	2,786	0.16	2,101	2,101
9E	315	20	35	78	0.15	27.4%	53.1%	21	781	0.04	41	1,517	0.08	1,149	1,149

Table A10
Fine Sediment Yield Calculations for the 5-year Storm

Basin Designation	Qp (cfs)	Vw (ac-ft)	Percent Impervious	Sediment Yield (tons)	Unit Sediment Yield tons/acre	% Soils <0.074		Minimum			Maximum			Average Fine Sediment Concentration Cf (ppm)	Weighted Average Fine Sediment Concentration[1] Cf (ppm)
						min	max	Fine Sediment Yield (tons)	Cf (ppm)	Unit Fine Sediment Yield tons/acre	Fine Sediment Yield ton(s)	Cf (ppm)	Unit Fine Sediment Yield tons/acre		
CA1	157	8	10	349	0.69	25.3%	50.4%	88	8,056	0.18	176	15,897	0.35	11,976	8,877
CA2	259	40	5	1,134	0.36	27.6%	53.5%	313	5,728	0.10	607	11,039	0.19	8,384	8,384
LC1	316	15	10	591	0.71	25.2%	48.8%	149	7,256	0.18	288	13,952	0.35	10,604	8,098
LC2	342	70	10	1,833	0.44	26.9%	52.6%	493	5,155	0.12	964	10,027	0.23	7,591	7,591
DB1	157	8	10	241	0.53	25.4%	49.2%	61	5,589	0.13	119	10,796	0.26	8,193	8,779
DB2	626	64	10	2,894	0.97	28.0%	54.2%	811	9,234	0.27	1,569	17,718	0.53	13,476	8,818
DB4	150	31	10	1,100	1.11	28.6%	55.0%	315	7,410	0.32	605	14,163	0.61	10,786	10,786
DB3	179	43	5	467	0.16	29.2%	56.0%	136	2,326	0.05	261	4,453	0.09	3,389	3,389
NP1	115	5	10	113	0.40	25.2%	46.2%	26	3,817	0.09	52	7,604	0.18	5,711	13,390
NP2	397	32	30	1,167	1.59	28.4%	54.8%	331	7,559	0.45	640	14,495	0.87	11,027	14,912
NP3	280	22	10	1,373	1.97	28.9%	55.6%	397	13,097	0.57	763	24,869	1.09	18,983	18,983
SP3	107	28	5	311	0.10	27.6%	53.6%	86	2,250	0.03	167	4,363	0.05	3,307	3,307
SP1	656	62	30	547	0.37	27.9%	53.9%	153	1,810	0.10	295	3,491	0.20	2,650	4,859
SP2	385	25	20	1,632	2.82	27.3%	53.2%	446	12,945	0.77	868	29,921	1.50	18,933	5,718
BA4	86	11	0	200	0.29	30.0%	57.4%	60	4,004	0.09	115	7,632	0.16	5,818	5,818
BA1	582	51	30	298	0.27	27.1%	52.9%	81	1,164	0.07	158	2,271	0.14	1,717	3,868

(Continued)

[1]Includes all fine sediment and runoff volume for upstream watesheds.

Table A10 (Concluded)

Basin Designation	Qp (cfs)	Vw (ac-ft)	Percent Impervious	Sediment Yield (tons)	Unit Sediment Yield tons/acre	% Soils <0.074		Minimum			Maximum			Average Fine Sediment Concentration Cf (ppm)	Weighted Average Fine Sediment Concentration Cf (ppm)
						min	max	Fine Sediment Yield (tons)	Cf (ppm)	Unit Fine Sediment Yield tons/acre	Fine Sediment Yield ton(s)	Cf (ppm)	Unit Fine Sediment Yield tons/acre		
BA2	1,033	111	30	2,752	1.26	28.5%	55.0%	786	5,180	0.36	1,514	9,939	0.69	7,559	4,180
BA3	187	50	5	393	0.08	27.8%	54.0%	109	1,605	0.02	212	3,112	0.05	2,358	2,358
EA8	5	9	0	21	0.01	26.1%	51.5%	5	439	0.00	11	865	0.01	652	652
EA7	23	1	0	24	0.26	25.0%	50.0%	6	4,451	0.06	12	8,863	0.13	6,657	6,657
EA6	32	2	0	31	0.26	25.0%	50.0%	8	2,845	0.06	16	5,674	0.13	4,259	4,259
PL	75	7	0	19	0.06	28.0%	54.0%	5	553	0.02	10	1,066	0.03	809	809
EA4	1,208	229	35	3,480	0.86	28.3%	54.6%	984	3,150	0.24	1,899	6,064	0.47	4,607	3,256
EA5	202	31	0	272	0.13	25.0%	50.0%	68	1,612	0.03	136	3,218	0.06	2,415	2,415
2A	154	37	10	820	0.22	26.9%	52.6%	221	4,369	0.06	431	8,504	0.11	6,436	6,436
2B	37	3	10	85	0.25	25.1%	50.2%	21	5,242	0.06	43	10,410	0.13	7,826	7,826
3B	207	15	10	967	1.47	27.5%	53.5%	265	12,851	0.40	517	24,722	0.79	18,787	6,218
4B	232	15	20	656	1.28	28.7%	55.2%	188	9,130	0.37	362	17,440	0.71	13,285	13,285
9A	220	14	6	144	0.25	25.3%	50.3%	36	1,905	0.06	72	3,790	0.13	2,848	2,848
9C	146	7	35	62	0.51	26.2%	51.6%	16	1,710	0.13	32	3,363	0.27	2,536	2,536
9E	568	29	35	133	0.25	27.4%	53.1%	36	923	0.07	71	1,791	0.13	1,357	1,357

Table A11
Fine Sediment Yield Calculations for the 10-year Storm

Basin Designation	Qp (cfs)	Vw (ac-ft)	Percent Impervious	Sediment Yield (tons)	Unit Sediment Yield tons/acre	% Soils <0.074		Minimum			Maximum			Average Fine Sediment Concentration Cf (ppm)	Weighted Average Fine Sediment Concentration[1] Cf (ppm)
						min	max	Fine Sediment Yield (tons)	Cf (ppm)	Unit Fine Sediment Yield tons/acre	Fine Sediment Yield ton(s)	Cf (ppm)	Unit Fine Sediment Yield tons/acre		
CA1	294	13	10	650	1.29	25.3%	50.4%	165	9,235	0.33	328	18,200	0.65	13,717	9,928
CA2	498	72	5	2,273	0.72	27.6%	53.5%	628	6,374	0.20	1,216	12,276	0.39	9,325	9,325
LC1	567	25	10	1,091	1.31	25.2%	48.8%	275	8,034	0.33	533	15,437	0.64	11,735	8,922
LC2	596	114	10	3,287	0.80	26.9%	52.6%	884	5,674	0.21	1,728	11,031	0.42	8,353	8,353
DB1	294	13	10	449	0.99	25.4%	49.2%	114	6,409	0.25	221	12,369	0.49	9,389	9,585
DB2	1,026	98	10	4,846	1.62	28.0%	54.2%	1,357	10,087	0.45	2,627	19,339	0.88	14,713	9,598
DB4	233	46	10	1,756	1.77	28.6%	55.0%	502	7,966	0.51	966	15,219	0.97	11,593	11,593
DB3	320	74	5	877	0.30	29.2%	56.0%	256	2,535	0.09	490	4,853	0.17	3,694	3,694
NP1	226	9	10	229	0.81	25.2%	46.2%	53	4,300	0.19	106	8,563	0.37	6,432	14,277
NP2	551	42	30	1,633	2.23	28.4%	54.8%	463	8,053	0.63	895	15,437	1.22	11,745	15,832
NP3	428	33	10	2,185	3.13	28.9%	55.6%	632	13,885	0.90	1,214	26,346	1.74	20,116	20,116
SP3	240	56	5	721	0.23	27.6%	53.6%	199	2,807	0.06	386	5,052	0.12	3,830	3,830
SP1	837	76	30	703	0.48	27.9%	53.9%	196	1,897	0.13	379	3,658	0.26	2,777	5,354
SP2	552	34	20	2,373	4.09	27.3%	53.2%	648	13,822	1.12	1,262	26,589	2.18	20,206	6,357
BA4	153	19	0	375	0.54	30.0%	57.4%	113	4,345	0.16	216	8,280	0.31	6,313	6,313
BA1	825	68	30	426	0.39	27.1%	52.9%	115	1,246	0.10	225	2,433	0.21	1,840	4,192

(Continued)

[1]Includes all fine sediment and runoff volume for upstream watesheds.

Table A11 (Concluded)

Basin Designation	Qp (cfs)	Vw (ac-ft)	Percent Impervious	Sediment Yield (tons)	Unit Sediment Yield tons/acre	% Soils <0.074		Minimum			Maximum			Average Fine Sediment Concentration Cf (ppm)	Weighted Average Fine Sediment Concentration Cf (ppm)
						min	max	Fine Sediment Yield (tons)	Cf (ppm)	Unit Fine Sediment Yield tons/acre	Fine Sediment Yield ton(s)	Cf (ppm)	Unit Fine Sediment Yield tons/acre		
BA2	1,410	146	30	3,819	1.75	28.5%	55.0%	1,090	5,464	0.50	2,102	10,481	0.96	7,972	4,534
BA3	385	95	5	843	0.18	27.8%	54.0%	234	1,813	0.05	455	3,514	0.10	2,663	2,663
EA8	135	25	0	231	0.12	26.1%	51.5%	60	1,770	0.03	119	3,485	0.06	2,628	2,628
EA7	39	2	0	48	0.51	25.0%	50.0%	12	4,410	0.13	24	8,782	0.25	6,596	6,596
EA6	54	4	0	61	0.51	25.0%	50.0%	15	2,811	0.13	31	5,607	0.25	4,209	4,209
PL	128	12	0	34	0.10	28.0%	54.0%	10	588	0.03	19	1,134	0.06	861	861
EA4	1,619	301	35	4,779	1.18	28.3%	54.6%	1,351	3,291	0.33	2,607	6,333	0.64	4,812	3,975
EA5	366	56	0	529	0.25	25.0%	50.0%	132	1,733	0.06	264	3,460	0.12	2,597	2,597
2A	269	57	10	1,428	0.38	26.9%	52.6%	384	4,934	0.10	751	9,596	0.20	7,266	7,266
2B	74	5	10	168	0.49	25.1%	50.2%	42	6,167	0.12	84	12,235	0.25	9,201	9,201
3B	338	23	10	1,616	2.46	27.5%	53.5%	444	13,996	0.67	864	26,895	1.31	20,446	6,771
4B	380	24	20	1,124	2.20	28.7%	55.2%	322	9,781	0.63	621	18,673	1.21	14,227	14,227
9A	366	23	6	252	0.44	25.3%	50.3%	64	2,036	0.11	127	4,050	0.22	3,043	3,043
9C	205	10	35	92	0.76	26.2%	51.6%	24	1,767	0.20	47	3,476	0.39	2,621	2,621
9E	815	39	35	192	0.36	27.4%	53.1%	53	992	0.10	102	1,924	0.19	1,458	1,458

Table A12
Fine Sediment Yield Calculations for the 25-year Storm

Basin Designation	Qp (cfs)	Vw (ac-ft)	Percent Impervious	Sediment Yield (tons)	Unit Sediment Yield tons/acre	% Soils <0.074		Minimum			Maximum			Average Fine Sediment Concentration Cf (ppm)	Weighted Average Fine Sediment Concentration[1] Cf (ppm)
						min	max	Fine Sediment Yield (tons)	Cf (ppm)	Unit Fine Sediment Yield tons/acre	Fine Sediment Yield ton(s)	Cf (ppm)	Unit Fine Sediment Yield tons/acre		
CA1	490	20	10	1,102	2.19	25.3%	50.4%	279	10,161	0.55	555	20,006	1.10	15,084	10,804
CA2	840	116	5	3,979	1.26	27.6%	53.5%	1,099	6,922	0.35	2,129	13,323	0.67	10,122	10,122
LC1	915	37	10	1,776	2.13	25.2%	48.8%	448	8,832	0.54	867	16,957	1.04	12,894	9,736
LC2	956	171	10	5,375	1.30	26.9%	52.6%	1,446	6,182	0.35	2,826	12,012	0.69	9,097	9,097
DB1	483	20	10	755	1.67	25.4%	49.2%	192	6,998	0.42	372	13,498	0.82	10,248	10,303
DB2	1,602	145	10	7,745	2.59	28.0%	54.2%	2,169	10,887	0.73	4,196	20,858	1.40	15,872	10,306
DB4	347	67	10	2,710	2.73	28.6%	55.0%	775	8,434	0.78	1,491	16,107	1.50	12,271	12,271
DB3	521	118	5	1,496	0.51	29.2%	56.0%	436	2,712	0.15	837	5,191	0.29	3,952	3,952
NP1	377	14	10	390	1.38	25.2%	46.2%	90	4,713	0.32	180	9,382	0.64	7,048	15,238
NP2	769	55	30	2,289	3.13	28.4%	54.8%	650	8,615	0.89	1,254	16,506	1.71	12,561	16,861
NP3	631	47	10	3,310	4.74	28.9%	55.6%	957	14,757	1.37	1,839	27,978	2.63	21,368	21,368
SP3	425	94	5	1,327	0.42	27.6%	53.6%	366	2,858	0.12	711	5,537	0.22	4,197	4,197
SP1	1,322	109	30	1,111	0.76	27.9%	53.9%	310	2,090	0.21	599	4,030	0.41	3,060	5,787
SP2	776	46	20	3,401	5.87	27.3%	53.2%	928	14,632	1.60	1,809	28,125	3.12	21,378	6,849
BA4	249	32	0	660	0.94	30.0%	57.4%	198	4,537	0.28	379	8,644	0.54	3,591	6,591
BA1	1,157	89	30	599	0.54	27.1%	52.9%	163	1,338	0.15	317	2,311	0.29	1,975	4,502

(Continued)

[1]Includes all fine sediment and runoff volume for upstream watesheds.

Table A12 (Concluded)

Basin Designation	Qp (cfs)	Vw (ac-ft)	Percent Impervious	Sediment Yield (tons)	Unit Sediment Yield tons/acre	% Soils <0.074		Minimum			Maximum			Average Fine Sediment Concentration Cf (ppm)	Weighted Average Fine Sediment Concentration Cf (ppm)
						min	max	Fine Sediment Yield (tons)	Cf (ppm)	Unit Fine Sediment Yield tons/acre	Fine Sediment Yield ton(s)	Cf (ppm)	Unit Fine Sediment Yield tons/acre		
BA2	1974	191	30	5,360	2.46	28.5%	55.0%	1,530	5,859	0.70	2,949	11,234	1.35	8,547	4,870
BA3	664	157	5	1,516	0.32	27.8%	54.0%	421	1,971	0.09	819	3,822	0.17	2,897	2,897
EA8	285	48	0	486	0.25	26.1%	51.5%	127	1,938	0.06	250	3,815	0.13	2,877	2,877
EA7	62	4	0	92	0.97	25.0%	50.0%	23	4,215	0.24	46	8,395	0.48	6,305	6,305
EA6	85	6	0	99	0.82	25.0%	50.0%	25	3,031	0.21	50	6,044	0.41	4,538	4,538
PL	203	20	0	59	0.18	28.0%	54.0%	17	608	0.05	32	1,173	0.10	891	891
EA4	2,166	382	35	6,428	1.59	28.3%	54.6%	1,817	3,487	0.45	3,507	6,710	0.86	5,098	4,229
EA5	622	96	0	962	0.45	25.0%	50.0%	240	1,840	0.11	481	3,673	0.23	2,756	2,756
2A	477	92	10	2,573	0.68	26.9%	52.6%	692	5,505	0.18	1,353	10,704	0.36	8,104	8,104
2B	141	8	10	313	0.91	25.1%	50.2%	79	7,188	0.23	157	14,246	0.46	10,717	10,717
3B	536	34	10	2,604	3.96	27.5%	53.5%	715	15,238	1.09	1,392	29,247	2.12	22,242	7,312
4B	527	32	20	1,587	3.10	28.7%	55.2%	455	10,344	0.89	876	19,738	1.71	15,041	15,041
9A	521	33	6	377	0.65	25.3%	50.3%	95	2,117	0.17	190	4,210	0.33	3,164	3,164
9C	267	12	35	118	0.98	26.2%	51.6%	31	1,891	0.26	61	3,718	0.50	2,805	2,805
9E	1,074	49	35	255	0.48	27.4%	53.1%	70	1,047	0.13	136	2,031	0.26	1,539	1,539

Table A13
Fine Sediment Yield Calculations for the 50-year Storm

Basin Designation	Qp (cfs)	Vw (ac-ft)	Percent Impervious	Sediment Yield (tons)	Unit Sediment Yield tons/acre	% Soils <0.074		Minimum			Maximum			Average Fine Sediment Concentration Cf (ppm)	Weighted Average Fine Sediment Concentration[1] Cf (ppm)
						min	max	Fine Sediment Yield (tons)	Cf (ppm)	Unit Fine Sediment Yield tons/acre	Fine Sediment Yield ton(s)	Cf (ppm)	Unit Fine Sediment Yield tons/acre		
CA1	658	27	10	1,537	3.06	25.3%	50.4%	389	10,499	0.77	774	20,666	1.54	15,582	11,242
CA2	1,154	158	5	5,652	1.79	27.6%	53.5%	1,561	7,216	0.49	3,024	13,885	0.96	10,550	10,550
LC1	1,220	49	10	2,442	2.93	25.2%	48.8%	616	9,166	0.74	1,193	17,594	1.43	13,380	10,153
LC2	1,287	226	10	7,422	1.80	26.9%	52.6%	1,096	6,457	0.48	3,902	12,543	0.95	9,500	9,500
DB1	651	26	10	1,034	2.28	25.4%	49.2%	262	7,367	0.58	509	14,204	1.12	10,785	10,706
DB2	2,085	186	10	10,319	3.45	28.0%	54.2%	2,890	11,304	0.97	5,593	21,648	1.87	16,476	10,700
DB4	442	84	10	3,522	3.55	28.6%	55.0%	1,007	8,741	1.01	1,937	16,688	1.95	12,714	12,714
DB3	694	155	5	2,046	0.70	29.2%	56.0%	597	2,824	0.20	1,145	5,405	0.39	4,115	4,115
NP1	516	18	10	536	1.89	25.2%	46.2%	124	5,029	0.44	247	10,008	0.87	7,518	15,690
NP2	941	67	30	2,863	3.91	28.4%	54.8%	812	8,842	1.11	1,569	16,936	2.14	12,889	17,310
NP3	792	59	10	4,269	6.11	28.9%	55.6%	1,234	15,158	1.77	2,372	28,728	3.40	21,943	21,943
SP3	605	131	5	1,947	0.61	27.6%	53.6%	537	3,009	0.17	1,044	5,829	0.33	4,419	4,419
SP1	1,624	131	30	1,382	0.95	27.9%	53.9%	386	2,163	0.26	746	4,170	0.51	3,166	6,009
SP2	946	56	20	4,242	7.32	27.3%	53.2%	1,158	14,988	2.00	2,257	28,799	3.90	21,893	7,116
BA4	329	42	0	899	1.28	30.0%	57.4%	270	4,704	0.38	516	8,961	0.74	6,833	6,833
BA1	1,407	108	30	744	0.68	27.1%	52.9%	201	1,371	0.18	394	2,676	0.36	2,023	4,672

(Continued)

[1]Includes all fine sediment and runoff volume for upstream watesheds.

Table A13 (Concluded)

Basin Designation	Qp (cfs)	Vw (ac-ft)	Percent Impervious	Sediment Yield (tons)	Unit Sediment Yield tons/acre	% Soils <0.074		Minimum			Maximum			Average Fine Sediment Concentration Cf (ppm)	Weighted Average Fine Sediment Concentration Cf (ppm)
						min	max	Fine Sediment Yield (tons)	Cf (ppm)	Unit Fine Sediment Yield tons/acre	Fine Sediment Yield ton(s)	Cf (ppm)	Unit Fine Sediment Yield tons/acre		
BA2	2,408	229	30	6,631	3.04	28.5%	55.0%	1,693	6,045	0.87	3,649	11,589	1.67	8,817	5,057
BA3	922	214	5	2,166	0.46	27.8%	54.0%	602	2,067	0.13	1,170	4,007	0.25	3,037	3,037
EA8	394	72	0	761	0.39	26.1%	51.5%	10		0.10	391	3,985	0.20	3,005	3,005
EA7	79	5	0	119	1.26	25.0%	50.0%	80	4,376	0.31	60	8,714	0.63	6,545	6,545
EA6	110	8	0	135	1.12	25.0%	50.0%	34	3,086	0.28	67	6,152	0.56	4,619	4,619
PL	264	26	0	79	0.24	28.0%	54.0%	22	628	0.07	43	1,211	0.13	919	919
EA4	2,615	456	35	7,888	1.95	28.3%	54.6%	2,229	3,584	0.55	4,303	6,896	1.06	5,240	4,361
EA5	843	131	0	1,357	0.64	25.0%	50.0%	339	1,902	0.16	679	3,797	0.32	2,850	2,850
2A	679	125	10	3,723	0.99	26.9%	52.6%	1,001	5,860	0.27	1,957	11,390	0.52	8,625	8,825
2B	206	11	10	463	1.35	25.1%	50.2%	116	7,722	0.34	232	16,296	0.68	11,509	11,509
3B	691	44	10	3,469	5.27	27.5%	53.5%	952	15,676	1.45	1,854	30,075	2.82	22,876	7,561
4B	655	41	20	2,059	4.02	28.7%	55.2%	590	10,475	1.15	1,136	19,985	2.22	15,230	15,230
9A	652	42	6	489	0.85	25.3%	50.3%	123	2,158	0.21	246	4,293	0.43	3,226	3,226
9C	315	14	35	141	1.17	26.2%	51.6%	37	1,938	0.31	73	3,811	0.60	2,875	2,875
9E	1,293	58	35	311	0.59	27.4%	53.1%	85	1,078	0.16	165	2,092	0.31	1,585	1,585

Table A14
Fine Sediment Yield Calculations for the 100-year Storm

Basin Designation	Qp (cfs)	Vw (ac-ft)	Percent Impervious	Sediment Yield (tons)	Unit Sediment Yield tons/acre	% Soils <0.074		Minimum			Maximum			Average Fine Sediment Concentration Cf (ppm)	Weighted Average Fine Sediment Concentration[1] Cf (ppm)
						min	max	Fine Sediment Yield (tons)	Cf (ppm)	Unit Fine Sediment Yield tons/acre	Fine Sediment Yield ton(s)	Cf (ppm)	Unit Fine Sediment Yield tons/acre		
CA1	790	32	10	1,873	3.72	25.3%	50.4%	474	10,790	0.94	943	21,233	1.88	16,011	11,554
CA2	1,425	194	5	7,136	2.26	27.6%	53.5%	1,970	7,416	0.62	3,817	14,271	1.21	10,844	10,844
LC1	1,445	59	10	2,978	3.57	25.2%	48.8%	751	9,282	0.90	1,454	17,814	1.74	13,548	10,420
LC2	1,571	272	10	9,206	2.23	26.9%	52.6%	2,476	6,653	0.60	4,839	12,922	1.17	9,788	9,788
DB1	785	32	10	1,290	2.04	25.4%	49.2%	327	7,466	0.72	635	14,394	1.40	10,930	10,959
DB2	2,521	224	10	12,736	4.26	28.0%	54.2%	3,567	11,582	1.19	6,904	22,174	2.31	16,878	10,961
DB4	532	101	10	4,332	4.37	28.6%	55.0%	1,238	8,940	1.25	2,383	17,064	2.40	13,002	13,002
DB3	849	189	5	2,559	0.88	29.2%	56.0%	746	2,897	0.26	1,432	5,544	0.49	4,221	4,221
NP1	616	22	10	662	2.33	25.2%	46.2%	153	5,084	0.54	306	10,116	1.08	7,600	20,394
NP2	1,096	77	30	3,371	4.61	28.4%	54.8%	956	9,057	1.31	1,847	17,344	2.52	13,200	22,929
NP3	933	70	10	7,743	11.09	28.9%	55.6%	2,238	22,988	3.20	4,302	43,260	6.16	33,124	33,124
SP3	753	162	5	2,479	0.78	27.6%	53.6%	684	3,097	0.22	1,329	6,000	0.42	4,549	4,549
SP1	1,901	152	30	1,641	1.12	27.9%	53.9%	458	2,212	0.31	885	4,266	0.61	3,239	6,135
SP2	1,098	66	20	5,056	8.73	27.3%	53.2%	1,380	15,153	2.38	2,690	29,112	4.64	22,133	7,263
BA4	400	52	0	1,130	1.61	30.0%	57.4%	339	4,777	0.48	649	9,100	0.93	6,938	6,938
BA1	1,647	125	30	882	0.80	27.1%	52.9%	239	1,404	0.22	467	2,740	0.42	2,072	4,781

(Continued)

[1]Includes all fine sediment and runoff volume for upstream watesheds.

Table A14 (Concluded)

Basin Designation	Qp (cfs)	Vw (ac-ft)	Percent Impervious	Sediment Yield (tons)	Unit Sediment Yield tons/acre	% Soils <0.074		Minimum			Maximum			Average Fine Sediment Concentration Cf (ppm)	Weighted Average Fine Sediment Concentration Cf (ppm)
						min	max	Fine Sediment Yield (tons)	Cf (ppm)	Unit Fine Sediment Yield tons/acre	Fine Sediment Yield ton(s)	Cf (ppm)	Unit Fine Sediment Yield tons/acre		
BA2	2,809	265	30	7,845	3.59	28.5%	55.0%	2,239	6,179	1.03	4,317	11,844	1.98	9,011	5,175
BA3	1,135	262	5	2,726	0.58	27.8%	54.0%	758	2,124	0.16	1,472	4,118	0.31	3,121	3,121
EA8	495	90	0	980	0.50	26.1%	51.5%	256	2,085	0.13	504	4,104	0.26	3,095	3,095
EA7	94	6	0	146	1.54	25.0%	50.0%	36	4,451	0.38	73	8,863	0.77	6,657	6,657
EA6	131	10	0	168	1.40	25.0%	50.0%	42	3,085	0.35	84	6,150	0.70	4,617	4,617
PL	318	32	0	99	0.30	28.0%	54.0%	20	636	0.08	53	1,226	0.16	931	931
EA4	2,967	521	35	9,233	2.28	28.3%	54.6%	2,609	3,672	0.64	5,037	7,064	1.24	5,368	4,469
EA5	1,030	160	0	1,698	0.80	25.0%	50.0%	425	1,949	0.20	849	3,890	0.40	2,919	2,919
2A	1,407	244	10	8,143	2.16	26.9%	52.6%	2,190	6,561	0.58	4,281	12,745	1.13	9,653	9,653
2B	422	22	10	1,019	2.97	25.1%	50.2%	256	8,499	0.75	512	16,821	1.49	12,660	12,660
3B	834	53	10	4,278	6.50	27.5%	53.5%	1,174	16,042	1.78	2,287	30,767	3.47	23,404	7,745
4B	771	49	20	2,492	4.87	28.7%	55.2%	714	10,610	1.39	1,376	20,239	2.69	15,424	15,424
9A	777	51	6	601	1.05	25.3%	50.3%	152	2,186	0.26	303	4,348	0.53	3,267	3,267
9C	361	16	35	164	1.36	26.2%	51.6%	43	1,972	0.36	85	3,879	0.70	2,926	2,926
9E	1,489	67	35	365	0.69	27.4%	53.1%	100	1,095	0.19	194	2,125	0.37	1,610	1,610

Table A15
Summary of Average Annual Total Sediment Yield for the Study Area

Location	Site Number	Reach	Drainage Area square miles	Runoff (in.)	Unit Sediment Yield			Sediment Yield		
					Bed Material (tons/acre)	Wash Load (tons/acre)	Total (tons/acre)	Bed Material (tons)	Wash Load (tons)	Total (tons)
North La Cueva upstream Coronado Airport	2a		5.91	0.10	1.62	0.08	1.70	6,110	315	6,424
South La Cueva upstream Coronado Airport*	2b		0.53	0.10	0.61	0.11	0.72	209	35	244
Domingo Baca at NDC	3a	Upstream arroyo	11.55	0.17	0.67	0.17	0.84	4,954	1,255	6,208
Domingo Baca at NDC	3a	Silt basin output	11.55	0.17	0.03	0.17	0.20	199	1,255	1,454
South Domingo Baca at Holbrook Street	3b	Upstream arroyo	5.49	0.14	2.05	0.10	2.15	7,197	358	7,555
South Domingo Baca at Holbrook Street	3b	Silt basin output	5.49	0.14	0.73	0.10	0.83	2,566	358	2,924
North Pino at NDC	4a	Silt basin output	2.70	0.27	0.01	0.44	0.45	18	761	779
North Pino at Holbrook Street	4b		0.80	0.25	2.14	0.71	2.85	769	191	959
South Pino at Wyoming	5a	Upstream arroyo	5.98	0.11	0.34	0.04	0.41	1,555	279	1,834
South Pino at Wyoming	5a	Silt basin output	5.98	0.11	0.00	0.06	0.06	0	279	279
South Pino at NDC	5b	Silt basin output	9.33	0.09	0.00	0.09	0.09	11	522	533
Bear at NDC	6	Upstream arroyo	15.51	0.19	0.25	0.08	0.33	2,457	846	3,304
Bear at NDC	6	Silt basin output	15.51	0.19	0.00	0.08	0.09	6	846	853
Embudito	9e		0.82	0.47	4.52	0.07	4.59	2,371	38	2,408
North Glenwood Hills	9a		0.90	0.20	3.07	0.07	3.13	1,765	37	1,802
South Glenwood Hills Tributary	9c		0.19	0.50	2.43	0.28	2.71	296	34	330
Piedra Lisa	9d		0.63	0.14	0.21	0.01	0.22	83	5	88
Embudo	9f (right)		3.72	0.10	2.98	0.03	3.00	7,080	69	7,149
Embudo			3.72	0.10	1.36	0.03	1.39	3,232	72	3,304

Table A16
Summary of 100-year Storm Total Sediment Yield for the Study Area

Location	Site Number	Reach	Drainage Area square miles	Runoff (in.)	Unit Sediment Yield			Sediment Yield		
					Bed Material (tons/acre)	Wash Load (tons/acre)	Total (tons/acre)	Bed Material (tons)	Wash Load (tons)	Total (tons)
North La Cueva upstream Coronado Airport	2a		5.91	0.77	32.16	0.85	33.02	121,654	3,231	124,886
South La Cueva*	2b		0.53	0.77	19.65	1.12	20.77	6,664	381	7,045
Domingo Baca at NDC	3a	Upstream arroyo	11.55	0.88	8.65	1.11	9.76	63,974	8,198	72,173
Domingo Baca at NDC	3a	Silt basin output	11.55	0.88	0.16	1.11	1.26	1,149	8,198	9,348
South Domingo Baca at Holbrook Street	3b	Upstream arroyo	5.49	0.83	19.66	0.73	20.39	69,075	2,564	71,639
South Domingo Baca at Holbrook Street	3b	Silt basin output	5.49	0.83	6.88	0.73	7.61	24,162	2,564	26,726
North Pino at NDC	4a	Silt basin output	2.70	1.12	0.02	2.73	2.75	32	4,711	4,743
North Pino at Holbrook Street	4b		0.80	1.14	18.17	2.01	20.20	9,308	1,033	10,340
South Pino at Wyoming	5a	Upstream arroyo	5.98	0.65	4.46	0.53	5.00	17,085	2,045	19,130
South Pino at Wyoming	5a	Silt basin output	5.98	0.65	0.00	0.53	0.53	0	2,045	2,045
South Pino at NDC	5b	Silt basin output	9.33	0.31	0.01	0.50	0.50	41	2,972	3,013
Bear at NDC	6	Upstream arroyo	15.51	0.89	1.83	0.49	2.31	18,112	4,813	22,924
Bear at NDC	6	Silt basin output	15.51	0.89	0.00	0.49	0.49	20	4,813	4,832
Embudito	9e		0.82	1.52	31.92	0.28	32.20	16,750	146	16,896
North Glenwood Hills	9a		0.90	1.06	35.77	0.39	36.16	20,603	226	20,829
South Glenwood Hills Tributary	9c		0.19	1.61	20.35	1.07	21.42	2,475	130	2,605
Piedra Lisa	9d		0.63	0.94	1.85	0.10	0.22	745	40	785
Embudo	9f (right)		3.72	0.76	31.81	0.25	32.06	75,735	603	76,338
Embudo	9f (left)		3.72	0.81	16.99	0.27	17.26	40,459	638	41,097

Table A17
Tatum Method Input Parameters

Location	Drainage Area square mile	Slope ft/mile	Drainage Density mile/square mile	Hypso-metric Index	Maximum 3-hr Rain in.
Embudo Dam	3.39	870	1.84	0.37	1.98
Piedra Lisa Dam	0.56	1255	2.54	0.36	2.28
Glenwood Basins	0.20	1709	4.27	0.32	2.28
Hidden Valley Basin	0.12	1490	3.88	0.48	2.28
J.B. Robert Dam	10.19	503	1.92	0.48	1.82
Pino Dam	6.02	599	2.43	0.31	1.92
South Domingo Baca	4.49	779	2.73	0.27	1.96
North Domingo Baca	1.59	654	3.34	0.14	2.17
Downstream from Embudo Dam	0.57	1148	2.56	0.29	2.28
South Glenwood Hills Trib.	0.13	1817	4.03	0.32	2.28
North Glenwood Hills	0.67	1259	1.65	0.50	2.28

Table A18
Los Angeles District Method Input Parameters

Location	Drainage Area acres	Relief Ratio ft/mile	One-hour Rainfall 100*in.	Unit Peak Discharge cfs/square mile
Embudo Dam	2,169	870		206.5
Piedra Lisa Dam	358	1,255	202	
Glenwood Basins	125	1,709	202	
Hidden Valley Basin	74	1,490	202	
John B. Robert Dam	6,524	503		157.0
Pino Dam	3,852	599		166.2
South Domingo Baca	2,876	779		178.0
North Domingo Baca	1,020	654		313.7
Downstream from Embudo Dam	362	1,148	202	
South Glenwood Hills Trib.	85	1,817	202	
North Glenwood Hills	432	1,259	202	

Appendix B
Description of TABS-1 Computer Program

The computer program TABS-1 calculates water-surface profiles and changes in the streambed profile. Water velocity, water depth, energy slope, sediment load, gradation of the sediment load, and gradation of the bed surface are also computed. Water-surface profile and sediment movement calculations are fully coupled using an explicit computation scheme. First, the conservation of energy equation is solved to determine the water-surface profile and pertinent hydraulic parameters (velocity, depth, width, and slope) at each cross section along the study reach:

$$\frac{\partial H}{\partial X} + \frac{\partial \left(\alpha \frac{V^2}{2g} \right)}{\partial X} = S \qquad \text{(B1)}$$

where

H = water-surface elevation
X = direction of flow
α = coefficient for the horizontal distribution of velocity
V = average flow velocity
g = acceleration due to gravity
S = slope of energy line

In addition, the continuity of sediment material is expressed by

$$\frac{\partial G}{\partial X} + B \cdot \frac{\partial y_s}{\partial t} = q_s \qquad \text{(B2)}$$

where

G = rate of sediment movement, cu ft/day
X = distance in direction of flow, ft
B = width of movable bed, ft
y_s = change in bed surface elevation, ft
t = time, days
q_s = lateral inflow of sediment, cu ft/ft/day

The third equation relates the rate of sediment movement to hydraulic parameters as follows:

$$G = f(V,y,B,S,T,d_{eff},d_{si},P_i) \tag{B3}$$

where

y = effective depth of flow
T = water temperature
d_{eff} = effective grain size of sediment mixture
d_{si} = geometric mean of class interval
P_i = percentage of i^{th} size class in the bed

The numerical technique used to solve Equation B1 is commonly called the Standard Step Method. Equation B2 has both time and space domains. An explicit form of a six-point finite difference scheme is utilized. Several equations of the form of Equation B3 are available. These transport capacity equations are empirical and G is determined analytically.

Equation B2 is the only explicit equation, but it controls the entire analysis by imposing stability constraints. Several different computation schemes were tested, and the six-point scheme proved the most stable. No stability criteria have been developed for this scheme. The rule of thumb is to observe the amount of bed change during a single computation interval and reduce the computation time until that bed change is tolerable.

Oscillation in the bed elevation is a key factor in selecting a suitable computation interval. The computation time interval must be made short enough to eliminate oscillation. On the other hand, computer time increases as the computation interval decreases. The proper value to use is determined by successive approximations, running test cases, and observing the amount of bed change.

Several supporting equations are required in transforming the field data for the computer analysis. The Manning equation is used to evaluate friction loss. Average geometric properties are combined, using an average end area approach, into an average conveyance for the reach. Manning's roughness coefficients are entered for the channel and both overbanks and may be

changed with distance along the channel, discharge, or stage. Contraction and expansion losses are calculated as "other" losses by multiplying a coefficient times the change in velocity head. All geometric properties are calculated from cross-section coordinates.

Only subcritical flow may be analyzed in the computer program; however, zones of critical or supercritical flow may occur within the study reach. The program treats supercritical zones as "critical" for determination of water-surface elevation, but calculates hydraulic parameters for sediment transport based on normal depth. Critical depth in a section with both channel and overbank is defined as the minimum specific energy for that section assuming a level water surface. Starting water-surface elevations can be input as a rating curve with stage and discharge, or stage can be set for each specific time interval. Steady-state conditions are assumed for each time interval, although the discharge may be changed to account for tributary inflow. A hydrograph is simulated by creating a histograph of steady-state discharges, using small time intervals when discharge variations are great and longer time intervals when changes in water and sediment discharges are small.

In some cases the temperature of water can be an important parameter in sediment transport and, consequently, may be prescribed with each water discharge in the hydrograph. Flexibility of input permits a value to be entered as needed to change from a previous entry.

Geometry is input into the numerical model as a series of cross sections similar to the widely used HEC-2 backwater program (U.S. Army Engineer Hydrologic Engineering Center 1990[1]). A portion of the cross section is designated as movable and a dredging template may also be specified. Spacing of cross sections is somewhat more critical for TABS-1 than it is for HEC-2 because of numerical stability problems. Long reach lengths are desirable because reach length and computation interval are related. Very short time intervals may be required if excessive bed changes occur within a specific reach. No special provisions are available to calculate head losses at bridges. The contracted opening may be modeled such that scour and deposition are simulated during the passing of a flood event, but calculated results must be interpreted with the aid of a great deal of engineering judgment and sensitivity analysis.

Four different sediment properties are required: (a) the total concentration of suspended and bed loads, (b) grain-size distribution for the total concentration, (c) grain-size distribution for sediment in the streambed, and (d) unit weight of deposits. A wide range of sediment material may be accommodated in the transport calculations (0.004 mm to 64 mm).

The usefulness of a calculation technique depends a great deal upon the coefficients which must be supplied. As in HEC-2, Manning's n values,

---

[1] References cited in this appendix are included in the References at the end of the main text.

contraction coefficients, and expansion coefficients must be provided to accomplish the water-surface profile calculations. Several other coefficients are required for sediment calculations as follows:

a. The specific gravity and shape of sediment particles must be specified.

b. The bed shear stress at which silt or clay particles begin to move and deposit are required coefficients.

c. The unit weight of silt, clay, and sand deposits is somewhat like a coefficient because of the difficulty in measuring. Also, the density changes with time.

All of the sediment-related coefficients have default values because sediment data seem to be much more scarce than hydraulic data. There are fewer sources for generalized coefficients. All of the default values should be replaced by field data where possible, and the input data are structured for such a process.

REPORT DOCUMENTATION PAGE

Form Approved
OMB No. 0704-0188

1. AGENCY USE ONLY (Leave blank)	2. REPORT DATE	3. REPORT TYPE AND DATES COVERED
	March 1995	Final report

4. TITLE AND SUBTITLE

Albuquerque Arroyos Sedimentation Study;
Numerical Model Investigation

5. FUNDING NUMBERS

6. AUTHOR(S)

Ronald R. Copeland

7. PERFORMING ORGANIZATION NAME(S) AND ADDRESS(ES)

U.S. Army Engineer Waterways Experiment Station
3909 Halls Ferry Road, Vicksburg, MS 39180-6199

8. PERFORMING ORGANIZATION REPORT NUMBER

Technical Report
HL-95-2

9. SPONSORING/MONITORING AGENCY NAME(S) AND ADDRESS(ES)

U.S. Army Engineer District, Albuquerque
P.O. Box 1580
Albuquerque, NM 87103-1580

10. SPONSORING/MONITORING AGENCY REPORT NUMBER

11. SUPPLEMENTARY NOTES

Available from National Technical Information Service, 5285 Port Royal Road, Springfield, VA 22161.

12a. DISTRIBUTION/AVAILABILITY STATEMENT

Approved for public release; distribution is unlimited.

12b. DISTRIBUTION CODE

13. ABSTRACT *(Maximum 200 words)*

The sedimentation study for the Albuquerque Arroyos Flood Control Project was conducted to determine if deposition in the concrete-lined North Diversion and Embudo Arroyo Channels would cause overtopping during the 100-year-frequency flood. The project was originally designed and constructed by the U.S. Army Corps of Engineers for the Standard Project Flood, but the effects of sediment deposition in the channel were ignored. A recent flood deposited significant quantities of sediment in the Embudo Arroyo Channel, raising concerns about the channel's ability to carry larger flood discharges.

The sedimentation study included a geomorphic assessment conducted under contract by Resource Consultants and Engineers of Fort Collins, CO. The geomorphic study assessed the stability of arroyos that drain into the North Diversion Channel and identified primary sediment sources in the watershed.

The sedimentation study also included determination of sediment yield for each watershed that drains into the North Diversion Channel. Since there is no generally accepted method for calculating sediment yield, several different methods were used to calculate yield and compared with limited measured data.

(Continued)

14. SUBJECT TERMS		15. NUMBER OF PAGES
Albuquerque Arroyos	Flood control	153
Bed Forms	Numerical Model	16. PRICE CODE
Channel Roughness	Sedimentation	

17. SECURITY CLASSIFICATION OF REPORT	18. SECURITY CLASSIFICATION OF THIS PAGE	19. SECURITY CLASSIFICATION OF ABSTRACT	20. LIMITATION OF ABSTRACT
UNCLASSIFIED	UNCLASSIFIED		

Abstract (Concluded).

Trap efficiencies for flood detention reservoirs and sediment traps were estimated. The detention basins had trap efficiencies between 88 and 96 percent. In the larger basins almost all of the sand and greater sediment sizes were trapped. The sediment traps effectively remove between 62 and 74 percent of the sand and greater size sediment.

The TABS-1 numerical sedimentation model was used to predict deposition in the concrete-lined channels. The effect of sediment deposits on boundary roughness was determined using analytical techniques. Calculated roughnesses were incorporated into the numerical model and an iterative procedure was used to determine the effect of deposited sediment on conveyance and roughness. The numerical model was circumstantiated using data from a historical flood where significant deposition occurred in the Embudo Arroyo Channel. Sediment inflow to the numerical model was determined using results of the sediment yield and trap efficiency studies. It was determined that the primary source of sediment was the unlined channels upstream from the concrete-lined channels. Considerable uncertainty exists relative to the quantity of sediment delivered by the 100-year-frequency flood. Sensitivity studies were conducted to assess the impact of different sediment loadings.

The study concluded that, while channel roughness was increased in certain reaches of the concrete-lined channel, the increase in roughness was insufficient to result in overtopping of the existing channel during the 100-year-frequency flood. The study also concluded that sediment deposition problems in the North Diversion Channel and Embudo Arroyo are decreasing due to continuing channel improvement projects.